The geochemistry of fossil termite nests in Calitzdorp, Western Cape, South Africa

by

Rabia Jacobs

Supervisor: Dr. Miengah Abrahams

Co-Supervisor: Professor Chris Harris

A thesis presented for the degree of Master of Science in Geology, submitted to the University of Cape Town.

November 2024

Table of contents

Declaration

1. I know that plagiarism is wrong. Plagiarism is using another's work and pretending it is one's own.

2. I have used the South African Journal of Geology convention for citation and referencing. Each contribution to, and quotation in, this project from the work(s) of other people has been attributed and has been cited and referenced.

3. This thesis is my work in its entirety.

4. I have not allowed, and will not allow, anyone to copy my work to pass it off as their work.

Signature: Signed by candidate

Date: _____ 15 November 2024_____

Abstract

Termites alter soil profiles by gathering nutrient-rich materials to construct their nests, known as termitaria. Certain termite species also fortify their termitaria using a combination of saliva and excrement (frass), resulting in geochemically distinct termitaria relative to the host soils. The enrichment of exchangeable bases derived from organic matter, including termite frass, and upward groundwater movement frequently leads to post-construction carbonate precipitation within termitaria. Fossil termitaria near Calitzdorp, Western Cape, South Africa, were described nearly two decades ago, but no detailed work has been performed on them until now. Here, these calcretised Quaternary features, which are largely composed of calcite and dolomite, are investigated to 1) determine whether there is evidence of nutrient mining or preferential nutrient enrichment in the fossil termitaria compared to their host palaeosols and 2) assess the palaeoenvironmental conditions at the time of carbonate precipitation. The fossil termitaria are distinct from their host palaeosols, being enriched in CaO, MgO, MnO, and P_2O_5 and depleted in Al_2O_3, Cu, Fe_2O_3, K_2O, and Zn, suggesting that the termites enriched their termitaria by depositing organic matter. However, there is no evidence of termites selectively mining materials, as observed in modern termitaria. The termitaria's unique geochemical signature is attributed to post-construction carbonate precipitation facilitated by termite activity. The enrichment of CaO and MgO can be linked to the termites' localised deposition of organic matter, rich in exchangeable base cations (Ca^{2+}, Mg^{2+}, K^+, Na^+). While calcite is present in other termitaria, the dolomite found in the termitaria in this study is distinctive and likely resulted from secondary carbonate precipitation aided by magnesium-rich organic matter. This exchangeable base enrichment, enhanced by termite activity, likely led to the preferential calcretisation of the termitaria, setting them apart from their host palaeosols. The pedogenic carbonate within the termitaria and some palaeosols indicates an arid environment at the time of carbonate formation. The $\delta^{13}C$ values of the termitaria range from 0 to -8‰, indicating a mixed C_3-C_4 vegetation matrix, with a more pronounced C_4 signature at the northern ichnosite and a stronger C_3 signature in the southern ichnosite. This mixture suggests a close association with year-round rainfall, with a higher proportion of arid-adapted vegetation in the north and a lower proportion in the south. Furthermore, the $\delta^{18}O$ values indicate a similar water source between the two ichnosites and reflect palaeotemperatures ranging from ~20 to 35 °C.

Acknowledgements

First and foremost, I express my deepest gratitude to God for granting me the strength and opportunity to complete this thesis. To my parents, Nadeema and Rudewaan Jacobs, and my sisters, Kauthar Conrad and Saarah Jacobs, thank you for your unwavering love, support, and inspiration.

I sincerely thank my supervisors, Dr. Miengah Abrahams and Professor Chris Harris, for their guidance and invaluable feedback throughout this project. Special thanks to Chris Harris and Joshua Munro in the Department of Geological Sciences at UCT and Julie Luyt in the Department of Archaeology for their assistance with carbon and oxygen isotope analyses. Appreciation is also extended to Jonathan Van Rooyen and Rene Van de Merwe for their help in sample preparation for XRF analysis and to Phil Janney for conducting the XRF analyses. A special thank you to Megan Welman Purchase from the University of the Free State for conducting the XRD analyses. I gratefully acknowledge the support of my funding bodies: Genus, the NRF (National Research Foundation), SEPM, IAS, and IIA societies, which supported me financially from (2022–2024). This research was also supported by grants obtained by Dr. Miengah Abrahams: DSI-NRF Centre of Excellence in Palaeosciences Grant 86073; NRF Thuthuka Grant 138151; DST-NRF Research Development Grant for New Generation of Academics Programme Grant 19694; Palaeontological Scientific Trust 2021.

I want to extend my sincere thanks to Cape Nature, with special appreciation to Tom, Cornelius, and Willem for their assistance in granting access to the Groenefontein Nature Reserve. I am also grateful to Robert Muir, Senate Marakabei, and Nkazimulo Zuma for their invaluable support in the fieldwork and sample collection. Thank you to the Geological Sciences Department at UCT for fostering a supportive environment and to Mapaseka Mashego for being my constant support. I also appreciate the Biological Sciences Department for welcoming me on their annual field trip.

Lastly, to my nieces and nephew, your curiosity and wonder remind me why I pursued science in the first place. Thank you for being my inspiration.

1. Introduction

Termites are renowned as ecosystem engineers, known for altering soil profiles through the construction of their termite nests (i.e., termitaria; e.g., Lock, 2013; Seymour et al., 2014; Kandasami et al., 2016; Muvengwi et al., 2018; Mills and Sirami, 2018; Bera et al., 2020). These intricate termitaria are typically biogeochemically different from the adjacent soils, particularly in nutrient-poor environments, where termites selectively mine nutrient-rich materials throughout the soil profile. During the termitarium's construction, organic matter—comprising termite excrement, saliva, and plant material—and fine-grained sediments (e.g., sands and muds) are deposited. This combination, along with groundwater infiltration, enriches nutrients, exchangeable bases, and carbonates within the termitaria relative to the adjacent soils (Brune and Kühl, 1996; Hopkins et al., 1998; Holt and Lepage, 2000; Jouquet et al., 2004; Singh et al., 2017). As a result, the nutrient availability in termitaria is higher than that of the surrounding soils.

In the geological record, termite body fossils are rare (Stevens, 1980; Peterson, 2006). However, the more robust structure of fossil termitaria gives them a much higher preservation potential, and they are more frequently recorded in the literature (e.g., Moore and Picker, 1991; Hasiotis and Dubiel, 1995; Genise, 1997; Duringer et al., 2007). Fossil termitaria are typically preserved as distinct, cylindrical structures that stand out from the surrounding soils (Crossley, 1984; Hasiotis and Dubiel, 1995; Duringer et al., 2007; Francis and Poch, 2019). These formations often display horizontal shelving and may contain pedogenic carbonates, which are typically associated with semi-arid to arid environments and contribute significantly to the preservation of the formations. Pedogenic carbonates form when inorganic carbon, commonly in the form of calcium carbonate ($CaCO_3$), dissolves and migrates through the soil, eventually re-precipitating in situ (Retallack and Wright, 1990; Srivastava et al., 2016). The precipitation of carbonates is complex and may extend over thousands of years after the initial development of the soil, depending on various factors such as the composition of the soil, climate and other environmental conditions (Machette, 1985; Durand et al., 2006). This potential temporal lag implies that the carbonates within a soil horizon may not be contemporaneous with the primary soil, thereby necessitating careful interpretation and implying an inherent limitation when using them as palaeoclimate proxies. These carbonates

usually precipitate under warm and dry conditions, where evaporation exceeds precipitation, and are marked by significant dissolution-reprecipitation during climate fluctuations. The carbon isotope composition of pedogenic carbonates is closely linked to the types of vegetation which were present in the primary soil, while their oxygen isotope composition can offer insights into temperature and rainfall patterns at the time of carbonate precipitation (Goudie, 1973, 1983; Lintern et al., 2006; Potts et al., 2009; Candy and Black, 2009; Alonso-Zarza and Wright, 2010; Tanner, 2010). While constraining the precise sequence of carbonate is beyond the scope of this study, there are methods of dating the carbonates, such as uranium-thorium (U-Th) and radiocarbon dating, that provide an estimated geological age. Consequently, the carbon and oxygen isotope composition of pedogenic carbonates in fossil termitaria serves as a proxy for ancient climate and vegetation, providing valuable insights into palaeoenvironmental conditions.

To date, fossil termitaria studies focus on morphology, termite evolution and fungus farming, and, although some studies have investigated the palaeoclimate potential of fossil termitaria, different proxies have been used, which cannot be easily compared (e.g., Thorne et al., 2000; Genise et al., 2000; Pickford, 2006; Duringer et al., 2007; Hasiotis and Dubiel, 2008; Bordy et al., 2009; Roberts et al., 2016; Genise, 2017; Backwell et al., 2020). While it is well-documented that termites act as nutrient cyclers in modern environments, enriching nutrients in termitaria compared to surrounding soils, limited research has been conducted on nutrient cycling within fossil termitaria (Coaton, 1981; Moore and Picker, 1991; Bordy et al., 2009; Backwell et al., 2020). Locally, stable isotope analysis of carbonates from ~30 ka Heuweltjies (subaerial mounds thought to be termite-constructed) has successfully demonstrated their use as a palaeoclimate proxy (Potts et al., 2009). The age of the Heuweltjies has been constrained through radiocarbon dating (Midgley et al., 2002). However, these mounds differ significantly in morphology and potentially in their tracemaker from the subterranean fossil termitaria examined in this study. Fossil termitaria in South Africa are scarce, with most reports providing only brief descriptions based on fragmentary material (Coaton, 1981; Moore and Picker, 1991; Bordy et al., 2009). As a result, local fossil termitaria warrant further investigation, as they hold the potential to offer valuable insights into past climates and ancient termite activity, which could enhance our understanding of termite evolution in the region.

Here, we explore two fossil termitaria locations in Calitzdorp, Western Cape (South Africa), that John Almond briefly reported on in a Palaeontological Impact Assessment (Almond, 2005), which was subsequently worked on and expanded by the UCT Continental Trace Studies Group (Hadebe, 2021; Abrahams et al., 2022; Muir et al., 2022). Modern termitaria samples from Bainskloof, Western Cape, were also analysed to add a contemporary comparison for interpreting the fossil data. This study, focused on six fossil termitaria, aims to:

1. Assess the mineral composition of the host palaeosol and fossil termitaria using XRD analysis.
2. Investigate the major and trace element composition of both the host palaeosol and fossil termitaria to determine if the nutrient content is higher relative to the host palaeosol.
3. Examine the stable isotope composition of the host palaeosol (where applicable) and fossil termitaria to infer past climate and vegetation.

This research offers valuable insights into the palaeoclimate record of the southern Cape during the Quaternary, a period of notable climate fluctuations for which local data remains limited (Petit et al., 1999; Elias, 2013; Ehlers et al., 2018; Strobel et al., 2022). Additionally, the evidence of active nutrient cycling by termites, followed by mineral precipitation within the fossil termitaria, could help to reveal more about ancient termite behaviour. Overall, these findings will contribute to refining reconstructions of the local palaeoenvironment during the Quaternary.

2. Background

Quaternary, calcretised fossilised termitaria have been reported along the Gamka Valley 12 km south of Calitzdorp (Fig. 2.1; Western Cape, South Africa; Almond, 2005; Abrahams et al., 2022). The investigation of these termitaria forms part of a larger ongoing project, and many more fossil termitaria are likely preserved in the greater Oudtshoorn region. The fossilised termitaria are large (up to ~1.5 m tall), cylindrical, shelved features and are interpreted to be subterranean termitaria constructed by ancient termites (Abrahams et al., 2022). After construction, carbonates precipitated within the termitaria, i.e., they underwent calcretisation and subsequent dolomitisation, aiding their preservation. The timing of these diagenetic processes relative to the construction of the termitaria is unknown, as it has not been explored in this study.

2.1 Geological context

Two study localities, herein referred to as the Calitzdorp and Groenefontein ichnosites, have been identified along the Gamka Valley, south of the main Calitzdorp town (Fig. 2.1 B). The dominant geology of the Calitzdorp area comprises the 510 Ma Cape Supergroup (southern study area) and 183 Ma Uitenhage Group (northern study area), where the Gamka River has incised the Uitenhage Group and Cape Supergroup (Rogers, 1903; Dingle, 1973; Dingle et al., 1983; Tinker et al., 2008; Weckmann et al., 2012; Muir et al., 2017; Martin and Croukamp, 2021; Green et al., 2022). Quaternary alluvial deposits have developed above these older units (Hadebe, 2021).

At the Calitzdorp ichnosite (see Table 3.1 for coordinates), the fossil termitaria are preserved within calcretised Quaternary sands, which are overlain by nodular to hardpan calcretes and underlain by gravels (Hadebe, 2021). This type of carbonate succession is common in pedogenic soil profiles (Netterberg, 1980; Wright and Tucker, 2009). The age of the fossil termitaria at Calitzdorp has been tentatively assigned to ~300 ka based on preliminary U-Th dating of the pedogenic carbonates within the termitaria (Muir et al., 2022). The U-Th dating was conducted on the carbonates above the termitaria, yielding U-Th ages of 319.3 ± 8.6 ka and 322.2 ± 8.3 ka, which provide a minimum age constraint of ~320 ka, placing these fossil termitaria in the Middle Pleistocene. The dating process utilised Laser Ablation Inductively

Coupled Plasma Mass Spectrometry (LA-ICP-MS) and multi-collector ICP-MS (MC-ICP-MS) techniques, which ensured a high degree of precision in the age determination. At the Groenefontein ichnosite (see Table 3.1 for coordinates), the fossil termitaria are preserved within shallow, sandy and muddy regolith of the Devonian Bokkeveld Group (Cape Supergroup).

Although both sites preserve termitaria with similar morphological features, they are hosted in different lithologies, reflecting variability in the local sedimentary environments rather than indicating differences in age or tracemaker. While the age of the Calitzdorp termitaria has been tentatively assigned, the age of the Groenefontein termitaria remains to be refined by the research group.

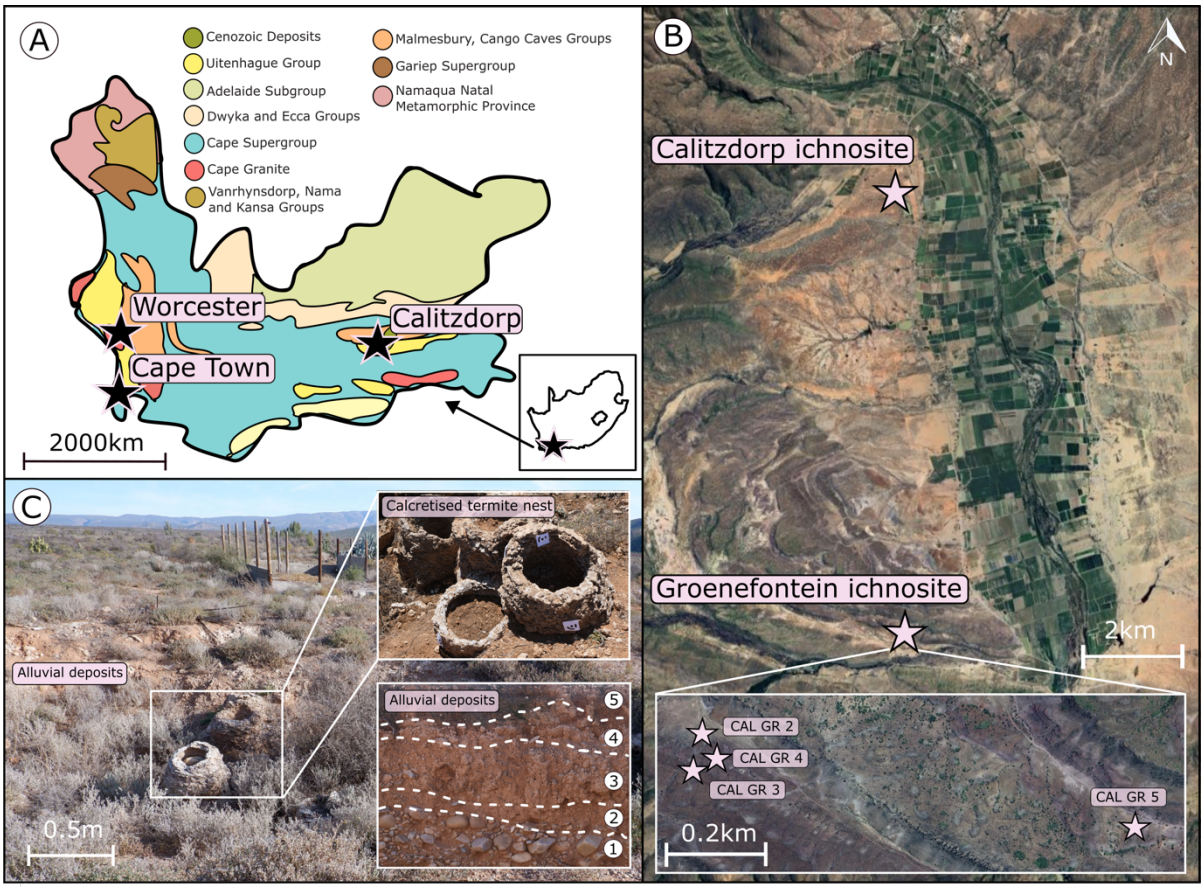

Figure 2.1. Overview of the fossilised termitaria ichnosites. A) Geological map of the Western Cape (South Africa) including the location of the Heuweltjies (Potts et al., 2009) B) Google Earth image of the Gamka Valley with ichnosite locations C) Fossil termitaria at the Calitzdorp ichnosite, which are preserved within calcretised alluvial deposits: 1) polymictic gravels, 2) fine-grained calcretised sand, 3) nodular calcrete, 4) hardpan layer, and 5) unconsolidated modern soil.

2.2 Fossil termitaria

Termites are soft-bodied invertebrates with a low preservation potential in the geological record (Stevens, 1980; Peterson, 2006). They first appear in the body fossil record during the Early Cretaceous (~127 Ma) and are geographically widespread, with body fossils reported from Asia, Europe, North America, and Russia (Rohr et al., 1986; Korb, 2008; Bezerra et al., 2021). The large termitaria, which have a higher preservation potential than the soft-bodied termites, are more commonly reported in the geological records from Asia, Europe, North America, and South America (Bown and Laza, 1990; Genise, 1997; Thorne et al., 2000; Pickford, 2006; Duringer et al., 2007; Roberts et al., 2016). Tentative fossil termitaria date to the Late Triassic and Early Jurassic, but the termite origin of these features is highly debated and would shift the timing of the origin of termites based on the body fossils by 110 million years (Hasiotis and Dubiel, 1995; Bordy et al., 2004; Genise et al., 2005).

Termites are found on all continents except Antarctica, with a greater prevalence in warm climate regions, primarily between 45 degrees north and south of the equator (Wood, 1988). They exhibit the highest diversity near the equator, where humidity levels are elevated (Abe et al., 2000; Turner et al., 2006). Through intricate architectural designs, termites create stable, humid microclimates within their termitaria, effectively buffering against extreme temperatures, water scarcity, and other unfavourable conditions characteristic of semi-arid to arid regions (Lüscher, 1961; Wood, 1988; King et al., 2015; Joseph et al., 2016; Jouquet et al., 2016; Ocko et al., 2017; Katariya et al., 2018). The termitaria may be below-ground, above-ground, or tree-hosted, depending on the environmental conditions and available resources (Noirot and Darlington, 2000). In warmer, wetter environments, tree-hosted termitaria are more prevalent, whereas below-ground termitaria dominate in drier conditions (Wilson, 1971; Specht, 1981; Whitford et al., 1992; Grube and Rudolph, 1995; Turner et al., 2006; Wijas et al., 2022). Subterranean termitaria, built deep within the soil profile, protect it from harsh surface conditions such as extreme temperatures and aridity (Jones and Oldroyd, 2006; Korb, 2008; Gouttefarde et al., 2017). Within these structures, intricate networks of galleries and storage chambers are designed to optimise temperature, ventilation, and humidity.

Termites engineer resilient termitaria by combining strategic material selection with effective moisture management, optimising nutrient availability, structural stability, and longevity in their termitaria (De Bruyn & Conacher, 1990; Turner, 2001; Su & Puche, 2003; Lock, 2013; Ocko et al., 2017; Seymour et al., 2014; Kandasami et al., 2016; Mills & Sirami, 2018; Muvengwi et al., 2018; Bera et al., 2020). They primarily use two types of building materials: exogenous materials such as soil and plant matter, which are transported in their mandibles, and faecal matter, deposited through excretion (Lee and Wood, 1971; Pomeroy, 1983). Additionally, termites preferentially excavate fine-grained sediments, like clay and silt, from deep within the soil profile and mix these with saliva to form a cohesive building agent (De Bruyn and Conacher, 1990; Holt and Lepage, 2000; Jouquet et al., 2016; Oberst et al., 2020). The faecal matter serves as a cementing agent, waterproofing and reinforcing the termitarium's structure (Wood, 1988; Holt and Lepage, 2000; Brauman, 2000). Due to the alkaline nature of the termite digestive tract, the faeces, and consequently the reinforced termitaria, are enriched in exchangeable base cations, including Ca^{2+}, Mg^{2+}, K^{+}, Na^{+}, and Al^{+} (e.g., Midgley and Musil, 1990; Brune and Kühl, 1996; Hopkins et al., 1998; Mahaney et al., 1999; Jouquet et al., 2004; Seymour et al., 2014; Singh et al., 2017; Mills and Sirami, 2018; Souza et al., 2020; Chen et al., 2021; Koné et al., 2022). Furthermore, termitaria exhibit enrichment in micronutrients such as Co, Cu, Fe, Mn, and Zn, which is facilitated by behaviours such as fungus culturing and a preference for clays, known to be richer in micronutrients compared to sand (Mills et al., 2009; Stewart et al., 2012; Wang and Henderson, 2013; Janzow and Judd, 2015; Baig et al., 2018).

In both modern (Black and Okwakol, 1997; Mujinya et al., 2011; Singh et al., 2017) and fossil termitaria (Watson, 1974; Coaton, 1981; Moore and Picker, 1991; Liu et al., 2007; Potts et al., 2009; Francis and Poch, 2019), local accumulation of carbonates is observed, even in regions characterised by non-calcareous soils. Importantly, not all fossilised termitaria contain carbonates, likely due to the specific conditions required for carbonate precipitation within the termitaria (e.g., Badawy, 2018; Ngoy et al., 2023). Several models have been proposed to explain the observed carbonate enrichment in termitaria, but the precise mechanism is not fully understood and likely involves a combination of these models (Milne, 1947; Lee and Wood, 1971; Watson, 1974; Mujinya et al., 2011; Francis and Poch, 2019). The two primary models for carbonate mineralisation in termitaria are biogenic and abiogenic processes.

Biogenic mineralisation is attributed to living organisms like termites or bacteria, which can involve the biomineralisation or the foraging of $CaCO_3$ and organic matter from the soil, thus enriching the termitaria in calcium ions or carbonates directly. In contrast, abiogenic carbonate mineralisation occurs through physical processes, such as the upward movement and evaporation of groundwater, which enrich the termitaria with Ca^{2+} and HCO_3^- that react to produce calcium carbonate. Carbonate precipitation can occur within a living termitarium or after its construction (producing overprinting), due to one or both biogenic and abiogenic processes (Lee & Wood, 1971; Mujinya et al., 2011; Francis & Poch, 2019). However, distinguishing between biogenic and abiogenic contributions is generally reported to be complex.

2.3 Pedogenic carbonates

Pedogenic carbonates are accumulations that replace terrestrial sediments within the soil profile (De Bruyn and Conacher, 1990; Turner, 2001; Su and Puche, 2003; Ocko et al., 2017) and have been present in the geological record since the Precambrian (e.g., Potts et al., 2009; Wright and Tucker, 2009; Alonso-Zarza and Wright, 2010; Elidrissi et al., 2018). These carbonate accumulations primarily consist of calcite ($CaCO_3$) but may also include dolomite (($CaMg(CO_3)_2$); Whipkey et al., 2002; Wright and Tucker, 2009; Kearsey et al., 2011). While calcite is typically the dominant carbonate phase, dolomite can occur as a replacement mineral or, more rarely, precipitate directly under specific conditions. Dolomitisation may be facilitated by magnesium-enriched porewaters or the leaching of calcium, though distinguishing primary from secondary dolomite can be challenging, particularly in fine-grained (or micritic) carbonates (Bustillo and Alonso-Zarza, 2007; Podwojewski, 1995; Alonso-Zarza and Wright, 2010). The presence of dolomite complicates the interpretation of stable isotope data, especially $\delta^{18}O$, due to differences in isotopic fractionation and the potential for later fluid interactions. The precipitation of pedogenic carbonates occurs across a wide range of climatic conditions, extending from arid to sub-humid (Goudie, 1973, 1983; Lintern et al., 2006; Candy and Black, 2009; Wright and Tucker, 2009 Gocke et al., 2012). However, warmer, drier climates favour their formation.

Pedogenic carbonates serve as valuable proxies for palaeoclimatic conditions (e.g., Dubbin, 2001; Potts et al., 2009; Tanner, 2010). The carbon and oxygen isotope composition of the carbonates reflects that of the soils in which they precipitate and provides valuable information on environmental conditions, carbon cycling, and ecosystem processes at the time of soil formation (Sharp, 2017).

The carbon in the soil profile originates from CO_2 derived from the atmosphere, groundwater, plant material, and microbial activity. The two main photosynthetic pathways, C_3 and C_4, help plants adapt to different climates. Plants with C_3 photosynthetic pathway can thrive in arid and humid environments and typically exhibit $\delta^{13}C$ values ranging from -33 to -23‰, whereas C_4 pathway plants are better adapted to arid conditions, with $\delta^{13}C$ values ranging from -16 to -9‰, which averages approximately 13‰ higher than those of C_3 plants (Sage et al., 1999; Sharp, 2017). Moreover, pure C_3 and C_4 source plants break down in the soil and produce pedogenic carbonates within typical $\delta^{13}C$ ranges of -12 to -9‰ and 1 to 3‰, respectively (Cerling, 1999). A $\delta^{13}C$ value below the range of -9 to 1‰ suggests mixed vegetation, with lower $\delta^{13}C$ values indicating a higher proportion of C_3 plants, while more positively skewed values point to C_4 plant dominance. For example, a $\delta^{13}C$ value of -4‰ would represent a midpoint in this spectrum, indicating a mix of C_3 and C_4 vegetation, where values above this threshold indicate a stronger C_4 signature, and those below suggest a stronger C_3 influence. The isotopic composition of carbonates in vegetated soils is predominantly influenced by the ratio of C_3 to C_4 plants within the local ecosystem (Irwin et al., 1977; Cerling et al., 1989; Mack and Cole, 1991; Quade, 1993; Ghosh et al., 1995; Kuzyakov, 2006; Duvert et al., 2018). Consequently, the $\delta^{13}C$ values of pedogenic carbonates can inform about the dominant photosynthetic pathways of ancient vegetation.

Variations in the $\delta^{18}O$ values of pedogenic carbonates are influenced by the water temperature during carbonate precipitation, making them valuable indicators for reconstructing palaeotemperature changes (e.g., Talma and Netterberg, 1983; Dworkin et al., 2005; Jolivet and Boulvais, 2021). The $\delta^{18}O$ values of the rainwater influence the $\delta^{18}O$ of the soil and, subsequently, the carbonates. During phases where liquid and vapour coexist in the hydrological cycle, water undergoes Rayleigh fractionation, a temperature-dependent process that modifies the $\delta^{18}O$ values of local rainfall. Typically, groundwater reflects the $\delta^{18}O$

value of total local rainfall, which is often determined from the weighted mean of monthly rainfall, providing insights into atmospheric moisture content. However, the interpretation of $\delta^{18}O$ values in groundwater presents certain limitations, including uncertainties associated with ambient rainfall isotopic values and various factors influencing soil water content (Dansgaard, 1964; Koch, 1998). Consequently, changes in moisture availability are generally expressed in relative terms.

2.4 Quaternary Climate

The Quaternary period, comprising the Pleistocene (2580 – 11.7 ka) and Holocene epochs (11.7 ka – present), is characterised by global climate oscillations (Fig. 2.2; e.g., Petit et al., 1999; Elias, 2013; Ehlers et al., 2018). Long periods of glaciation, mainly affecting ice sheet growth in the northern hemisphere, were followed by shorter intervals of warmer global climate, with the Mid-Pleistocene transition (1.2 – 0.8 Ma) marking a shift towards shorter glacial and interglacial cycles, driving global climate change (Pisias and Moore, 1981; Siddall et al., 2010; deMenocal, 2011; Elderfield et al., 2012; Elias, 2013; Detlef et al., 2018; Sutter et al., 2019; Williams, 2023). These climatic variations resulted in the extinction of many species, along with adaptive behavioural changes in those species that survived (Deacon, 1983; Vrba, 1995; Bennett, 1997; Coope et al., 1997; Elias, 2013; Castañeda et al., 2016; Timmermann and Friedrich, 2016; Venter et al., 2020; Stynder and Bishop, 2023).

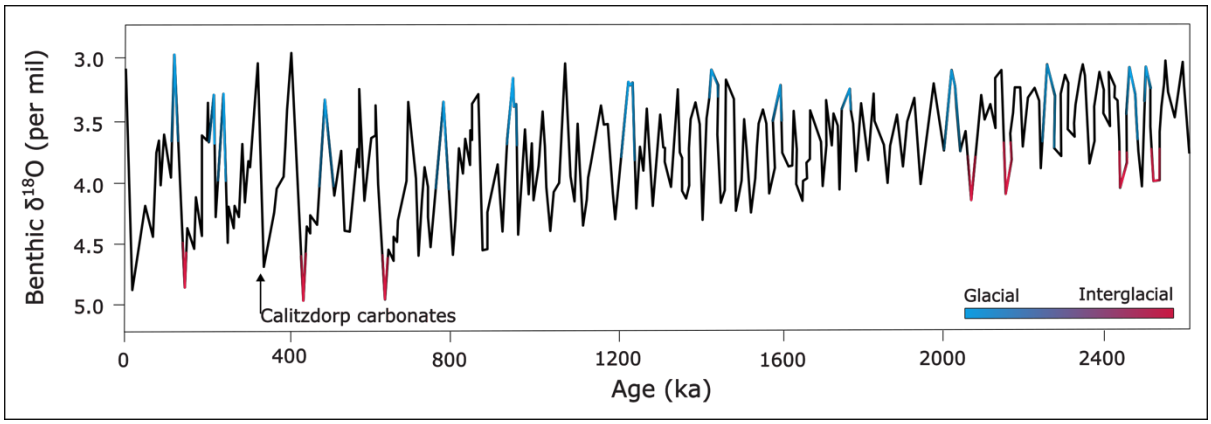

Figure 2.2. The Quaternary global benthic $\delta^{18}O$ oscillation from foraminiferal calcite indicates major global climate fluctuations of the last 2.4 million years (Lisiecki and Raymo, 2005). The carbonates in the termitaria age (determined by U-Th dating) indicated (Muir et al., 2022).

The Quaternary climatic trends in southern Africa are shaped by regional factors such as atmospheric circulation and oceanic currents (warm Eastern Agulhas and cold Western Benguela), which result in nuanced and variable climate dynamics that do not necessarily mirror global climate change observations (Rogers, 1988; Walker, 1990; Hewitt, 2000; Chase and Meadows, 2007; Holzkämper et al., 2009; Bruch et al., 2012; Hare and Sealy, 2013; Strobel et al., 2022). Due to the geographical complexities of South Africa, understanding the Quaternary climate remains challenging. The existing records, spanning approximately 320 ka, are not only scarce but often contradictory. While some studies suggest cooler conditions, others propose that the middle to late Pleistocene was warmer and drier, evidenced by the expansion of C_4 grasses and elevated interglacial sea levels (Henshilwood, 2008; Bar-Matthews et al., 2010; Eze, 2013; Quick et al., 2015; Compton, 2016; Dupont et al., 2022; Strobel et al., 2022). These discrepancies may be attributed to a lack of continuous palaeoclimate proxies over ~320 ka, along with research focus on intervals of high interest, such as the Last Glacial Maximum (LGM) and the Plio-Pleistocene boundary interval; crucial periods for climate change, and faunal and human evolution (e.g., Partridge et al., 1990; Avery, 2001; deMenocal, 2004; Reynolds, 2007; Hopley and Maslin, 2010; Cooper et al., 2018).

Across South Africa, vegetation patterns are closely tied to rainfall regimes and temperature. The western region, especially in the winter rainfall zone (WRZ), tends to support C_3 vegetation, partly due to cooler temperatures and winter precipitation. In contrast, the eastern regions of the country, which are warmer and receive summer rainfall, are dominated by C_4 grasses that are better adapted to high temperatures and seasonal summer rain (Vogel et al., 1978; Cowling, 1983; Chase and Meadows, 2007). Calitzdorp is located in the southern interior and is situated within the year-round rainfall zone (YRZ) and supporting a mix of C_3 and C_4 vegetation.

During the Pleistocene, there was a general shift toward warmer and drier conditions in South Africa (Henshilwood, 2008; Quick et al., 2015; Mohale et al., 2022). The SRZ transitioned from mixed C_3/C_4 vegetation in the Early to Middle Pleistocene with C_4 dominance later in the Pleistocene, reflecting a change from cooler and wetter climatic conditions to drier conditions (Cawthra and Bateman, 2016; Hahn et al., 2017). Terrestrial sediment cores from ~263 ka and

offshore sediment cores from ~300 ka in the southern Cape Coast provide some palaeoclimate context for the Middle Pleistocene in the southern Cape. These cores indicate generally warm and arid conditions, characterised by a cessation of major flood events and reduced rainfall, which predominated during the late Pleistocene (Hahn et al., 2017; Strobel et al., 2022). Additionally, speleothem records from Pinnacle Point (~50 km south of Calitzdorp) suggest a year-round rainfall regime during the Pleistocene (Braun et al., 2019). Given the spatial and temporal variability in climate driven by local factors, extrapolating the palaeoclimatic conditions for the Calitzdorp area back to ~320 ka is problematic.

3. Materials and Methodology

Between 2022 and 2024, numerous field trips to Calitzdorp and Groenefontein were conducted to contextualise the fossil termitaria and collect samples for analysis. To quantitatively assess the geochemistry of the fossil termitaria and their host palaeosols, three analytical methods were employed: X-ray diffraction (XRD), X-ray fluorescence (XRF) and stable isotope analysis.

3.1 Fieldwork: sample collection

3.1.1 Fossil Termitaria

Calitzdorp

At the Calitzdorp ichnosite, eight calcretised fossil termitaria are preserved laterally within 1 m of each other in a palaeosol profile comprising different morphological carbonate forms (Fig. 2.1 B; Hadebe, 2021; Abrahams et al., 2022). These include calcretised sands, calcrete nodules and hardpan calcrete. There is a strong lithological control on the preservation of the fossil termitaria, they are only preserved in the calcretised sands (the physical host palaesol), with their base corresponding to underlying gravel and their observed upper limit in line with the nodular calcrete, though it is possible they originally extended into the hardpan (Hadebe, 2021). Consequently, the four forms of calcrete are considered herein as the "host palaeosols". However, for ease of direct comparison, the host palaeosol in the syntheses and discussion refers specifically to the calcretised sands (PCS) in which the fossil termitaria are predominantly preserved.

In this study, two fossil termitaria and four host palaeosols samples were collected for geochemical analyses (Table 3.1): fossil termitaria (CAL 2.1 and CAL 2.2), calcretised powdery sands (PCS), nodular calcrete (CAL 2.4 and PCN), and hardpan calcrete (CALI H).

Groenefontein

At the Groenefontein ichnosite, a single fossil termitarium was initially reported by Almond (2005), while five more were discovered during the current study (Fig. 2.1 C; Table 3.1). The fossil termitaria are preserved in relative lateral isolation, and individual termitaria are located between 0.05 km–1 km apart and are preserved in fine sands and muds from the

Bokkeveld shale regolith, which have not undergone calcretisation. Therefore, only one host palaeosol sample was collected because the fossil termitaria are preserved in this host palaeosol.

For this study, four fossil termitaria (CAL GR 2, CAL GR 3, CAL GR 4 and CAL GR 5) and a single sample of the muddy sand from the Bokkeveld shale regolith (CAL GR 2-H) were collected for geochemical analyses (Table 3.1).

3.1.2 Modern termitaria

Matjiesriver

During fieldwork in the Gamka Valley, a termitarium was identified ~13 km north of the Calitzdorp study site, with its internal structures exposed (Table 3.1). This termitarium was notable for its distinctly white interior, suggesting potential calcification. A sample was collected for further analysis and comparison with other samples in this study.

Bainskloof

Subaerial termitaria of *Amitermes hastatus* were collected from the Bainskloof area (~230 km east of the Calitzdorp study area), with sample locations spaced 10–100 m apart (Table 3.1). These termitaria are characterised by a distinctive black exterior. These termitaria are situated within sandy soils derived from the erosion of Table Mountain Sandstone. Although not fully exposed, these mounds exhibited horizontal tunnelling similar to that at the Calitzdorp and Groenefontein ichnosites. While they lack carbonates, the Bainskloof mounds were collected as a modern comparison within the Western Cape, providing valuable insight into nutrient enrichment processes in contemporary termitaria relative to fossilised counterparts.

Table 3.1. Details, including sample name, description of analytical techniques performed on the collected sample, and GPS location from which the samples were collected.

Sample name	Description	Analytical technique(s)	# of stable isotope powdered subsamples
Calitzdorp	33°33'18.0"S 21°40'24.0"E		
CAL 2.1	Calcretised fossil termitaria	XRD, XRF, SIA	15
CAL 2.2	Calcretised fossil termitaria	XRD, XRF, SIA	18
CALI H	Hardpan calcrete (HP)	XRD, XRF, SIA	15
CAL 2.4	Nodular calcrete small (HP) ~1cm diameter nodules	XRD, XRF, SIA	1
PCN	Nodular calcrete large (HP) ~8cm diameter nodules	XRD, XRF, SIA	19
PCS	Fossil termitaria bearing calcretised powdery sand (HP)	XRD, XRF, SIA	1
Groenefontein			
CAL GR 2	Calcretised fossil termitaria 33°37'22.3"S, 21°39'13.6"E	XRD, XRF, SIA	13
CAL GR 3	Calcretised fossil termitaria 33°37'24.0"S, 21°39'14.6"E	XRD, XRF, SIA	10
CAL GR 4	Calcretised fossil termitaria 33°38'07.4"S, 21°39'13.6"E	XRD, XRF, SIA	6
CAL GR 5	Calcretised fossil termitaria 33°37'30.2"S 21°39'58.3"E	XRD, XRF, SIA	6
CAL GR 2-H	Fine-grained sand and mud (HP) -33°37'22.3"S, 21°39'13.6"E	XRD, XRF	No carbonate
Matjiesrivier	33°26'05.0"S 21°37'33.7"E		
MAT 1	Modern calcretised termitaria	XRD	1
Bainskloof			
BABL 1	Modern termitaria 33°37'21.9"S 19°05'55.8"E	XRF	1
BABL 2	Modern termitaria 33°37'23.9"S 19°05'53.9"E	XRF	1
BABL 3	Modern termitaria 33°37'23.7"S 19°05'53.7"E	XRF	1

Notes: Abbreviation– XRD- X-ray diffraction, XRF- X-ray fluorescence, SIA- Stable isotope analysis, HP- Host palaeosol.

3.2 Sample preparation and analysis

3.2.1 X-ray Diffraction

Twelve samples were analysed by X-ray diffraction (XRD) to determine the bulk mineral composition of the termitaria and associated palaeosols (Table 3.1).

The samples were crushed to a fine powder (10 µm) using a Sturtevant jaw crusher and rotary mill at the University of Cape Town (UCT). A 10 g portion of each powdered sample was analysed with a PANanalytical Empyrical diffractometer, utilising Cu K-alpha radiation at the University of the Free State (UFS). Mineralogical identification was done using HighScore software, which facilitates profile fitting, phase identification, and pattern analysis. This method, however, is semi-quantitative and can only detect phases with a minimum volume of approximately 1% (Malvern Panalytical, 2024).

3.2.2 X-ray fluorescence

X-ray fluorescence (XRF) analysis was performed on 14 samples to determine the bulk major and trace elemental composition of the termitaria and host palaeosols, utilising two sample preparation methods (Table 3.1). Thirteen samples were analysed at UCT, while one calcretised sand sample (PCS) was analysed at UFS.

For major element analysis, 13 fusion discs were prepared at UCT. Each disc was created from 2 g of powdered sample dried at 110 °C for 4 hours, followed by dehydration at 900 °C for 4 hours. A mixture of 0.7 g dehydrated sample and 6 g Claisse XRF flux was melted in platinum crucibles using the Claisse M4 automated flux. The molten mixture was poured into moulds and cooled for 5 minutes before analysis. At UFS, a 10 g PCS sample underwent similar dehydration at 110 °C and was then heated to 1050 °C to determine ignition loss. A flux—0.2445 g La_2O_3, 0.705 g $Li_2B_4O_7$, 0.5505 g Li_2CO_3, and 0.02g $NaNO_3$—was added to 0.28 g of the sample, heated to 950 °C for 5 minutes in a platinum crucible, poured into a mould, and pressed into a disc.

For trace element analysis, 13 pressed pellets were prepared at UCT by mixing 10 g of powdered sample with 2.5 g of Hoescht wax for 20 minutes, then compressed at 15 tonnes

in a stainless-steel die. At UFS, an 8 g PCS sample was mixed with 3 g of Hoechst wax in a Turbula mixer and pressed at over 395 N/m.

The XRF analysis of 13 samples at UCT utilised a Panalytical Axios wavelength-dispersive XRF spectrometer, focusing on 11 major oxides (Fe, Mn, Ti, Ca, K, S, P, Si, Al, Mg, and Na) and Ni and Cr when concentrations exceeded 2000 ppm (0.2%). Fusion discs were prepared with lithium borate flux to ensure uniformity and trace element concentrations were determined using pressed powder briquettes. Intensity data underwent corrections for mass absorption, enhancement, and spectral interferences to enhance accuracy. Calibration was performed using international rock standards from MINTEK, USGS, and the Geological Survey of Japan, with curves constructed to correlate known concentrations against corrected peak-background intensities. Results were validated through cross-checking with additional geochemical techniques, ensuring the reliability of the chemical composition data. The PCS sample was similarly analysed at UFS using the Rigaku Primus IV WDXRF. However, Cr_2O_3, NiO, and SO_3 could not be quantified at this facility. To maintain consistency in the geochemical comparisons, these oxides were excluded from the comparative graphs (Figs. 4.4, 4.5, 4.9–4.12), but their concentrations are reported in Table 4.2.

Although XRD is useful in identifying the minerals present, it is only semi-quantitative and only identifies minerals present in > 1 wt.%. As the number of minerals in a mixture increases, the likelihood of errors in XRD-derived proportions increases due to the overlapping diffraction peaks and potential interference between minerals. Therefore, the proportions based on XRD data may not correlate well with mineral proportions estimated from XRF data, which provides a more precise measure of chemical composition and can be considered more empirically robust for quantifying elemental concentrations. To cross-check the XRD-derived mineralogy, the estimated mineral proportions were back-calculated from XRF data based on the expected stoichiometry of the common rock-forming mineral (Appendix Table 2; Deer et al., 2009). However, discrepancies may still arise due to the inherent differences between the two techniques in detection limits.

3.2.3 Stable Isotopes

Carbon and oxygen stable isotope analysis was conducted on 108 powdered subsamples from 10 main samples of host palaeosol from Calitzdorp and carbonate-rich fossil termitaria from both ichnosites (Table 3.1). Notably, preliminary XRD results and petrographic analyses indicate the presence of both calcite and dolomite in the termitaria, which are micritic and indistinguishable to the naked eye. To account for this, corrections were applied using the respective fractionation factors for calcite and dolomite, based on their proportions in the samples. Sample preparation and analysis were conducted at UCT.

The host palaeosols appear macroscopically homogenous, while the fossil termitaria exhibit distinct carbonate-rich and sediment-rich horizons (Fig. 3.1), with the carbonate-rich layers corresponding to cream-coloured sections (Muir et al., 2022). A targeted sampling approach was employed for the fossil termitaria, focusing on the carbonate-rich horizons. Samples were drilled at 0.5 to 3 cm intervals to obtain powdered samples weighing 0.18 to 0.24 g. Larger samples were drilled at wider intervals, while smaller samples with fewer laminations required closer intervals. The larger nodular (PCN) and hardpan (CALI H) host palaeosol samples were sliced and drilled, whereas the smaller nodules (CAL 2.4) and calcretised sands were powdered using a rotary mill, also yielding samples between 0.18 and 0.24 g.

Two methods were used for stable isotope analysis. In 2023, six samples were analysed using the offline method in the Department of Geological Sciences (UCT) due to equipment repairs in the Department of Archaeology. Accurately weighed amounts (3–10 mg) of each powdered sample were reacted with 5 ml of 100% H_3PO_4 at 50 °C to extract CO_2. In 2024, six additional samples were analysed using the gas bench method in the Department of Archaeology after repairs were completed.

For the gas bench method, about 0.25 mg of each powdered subsample was reacted with 5 ml of 100% H_3PO_4 at 70 °C for 4 hours to extract CO_2. The extracted CO_2 was analysed for carbon and oxygen isotopes using a Finnegan MAT Delta XP mass spectrometer in dual-inlet mode. Data corrections were made using the CO_2-dolomite and CO_2-calcite fractionation factors of 1.009 and 1.01065, respectively. The isotopic signals produced by both carbonates

(calcite and dolomite) were considered in the corrections, taking into account their proportions in the samples. The resulting data are reported in δ notation, where:

$$\delta = \frac{Rsample}{Rstandard-1} \times 1000 \text{ and R = } {}^{18}O/{}^{16}O \text{ or } {}^{13}C/{}^{12}C$$

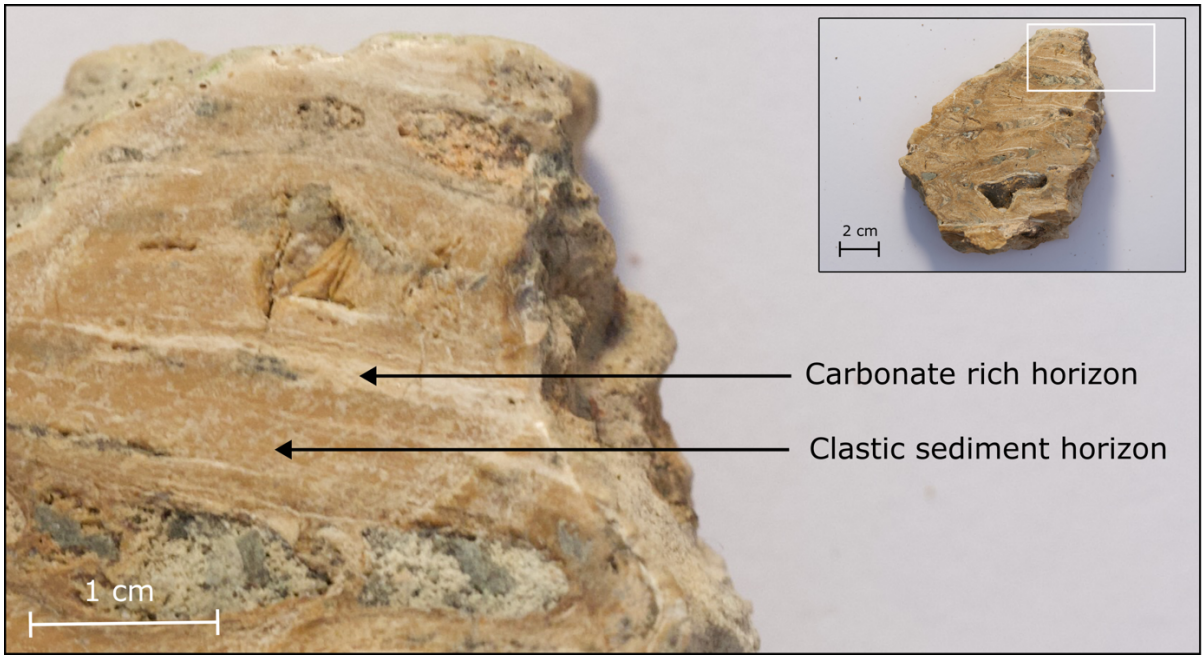

Figure 3.1. A cross-section of fossil termitaria samples CAL GR 3 with carbonate-rich horizons, which were preferentially drilled for SIA and clastic sediment-rich areas.

The Cavendish Marble (CM), Cacara Z (CZ New), and IAEA-CO-08 in-house standards were analysed in duplicate for each set of powdered samples. In the Department of Archaeology, CM, CZ, and IAEA-CO-08 are used to convert raw data to the PDB (Pee Dee Belemnite) and SMOW (Standard Mean Ocean Water) scales. The Department of Geological Sciences uses the NM (NBS-19) standard for these conversions. The PDB standard is primarily used as a reference for carbon isotopes in marine carbonates, while the Standard Mean Ocean Water (SMOW) scale is the preferred reference for carbonates in other rock types as well as for water in isotopic studies. The precision for $\delta^{13}C$ and $\delta^{18}O$ values was better than 0.1‰, as indicated by long-term standard duplication. The analytical method assumed all carbonate is calcite in the acid fractionation correction, resulting in a 1.47‰ overestimation of dolomite. Consequently, dolomite data were adjusted by subtracting 1.47‰. This correction accounted for the mixed isotopic signals from both carbonate minerals. While the Department of

Archaeology follows this method, the Department of Geological Sciences uses the correct acid fractionation equations for dolomite.

The offline method was employed to determine the carbon and oxygen isotopes of six samples (CAL GR 2, CAL GR 3, PCN, CALI H) at the Department of Geological Sciences, UCT. Accurately weighed amounts (3–10 mg) of each powdered sample were reacted with 5 ml of 100% phosphoric acid (H_3PO_4) at 50 °C for 12 hours to extract CO_2 (McCrea, 1950). The extracted CO_2 was analysed to measure the total carbonate content. Given the presence of calcite and dolomite, the dolomite fractionation factor (1.01065) was applied in the correction procedure, along with the CO_2-calcite fractionation factor (1.009). Data were normalised to the SMOW and PDB scales using the internal standard NM95, calibrated against NBS-19 ($\delta^{18}O$ = 25.10‰ and $\delta^{13}C$ = 1.57‰).

While this method effectively dissolves calcite, dolomite reacts more slowly under these conditions (Al-Aasm et al., 1990; Sharma et al., 2002). Although the reaction was allowed to proceed thoroughly, the extent to which all dolomite was dissolved, especially in samples such as CAL 2.2, where it is abundant, cannot be fully confirmed, and may affect the final isotopic signature.

4. Results

The fossil termitaria and their host palaeosols are described for each ichnosite (Calitzdorp and Groenefontein; Table 3.1) to assess differences between the termitaria and the host palaeosols. At both ichnosites, the fossil termitaria exhibit similar morphology and are interpreted to have the same tracemaker (Hadebe, 2021; Muir et al., 2022). Although XRD analysis effectively identified the minerals present, its semi-quantitative nature may result in imprecise estimates of mineral proportions. Nonetheless, its primary purpose here was to confirm mineral presence, particularly within the termitaria, which it achieved successfully. However, it is important to note that XRD has limitations in identifying specific mineral species, such as distinguishing between different types of mica. Furthermore, while U-Th dating indicates the termitaria are approximately 320 ka, the timing between the construction of the termitaria and carbonate precipitation remains uncertain. A detailed analysis of the geological context, trace morphology, and petrography of these ichnosites falls beyond the scope of this study and is being investigated by the broader research group.

4.1 Calitzdorp

4.1.1 Host Palaeosol

The host palaeosol includes samples from different forms of carbonate, including calcretised powdery sands (PCS), nodular calcrete (PCN and CAL 2.4), and hardpan calcrete (CALI H; Table 3.1).

The calcretised powdery sands, PCS, which physically bear the fossil termitaria, are largely composed of quartz (75 wt.%), a moderate proportion of plagioclase (11 wt.%), mica (10 wt.%), and minor amounts of calcite (3 wt.%; Fig. 4.1 A; Table 4.1; Appendix Fig. 1). The major oxide composition is predominantly characterised by very high SiO_2 (66.18 wt.%), followed by Al_2O_3 (7.25 wt.%) and CaO (6.85 wt.%; Table 4.2). The trace elements with the highest concentrations include Ba (417 ppm), Zr (336 ppm), and Sr (238 ppm). The $\delta^{13}C$ and $\delta^{18}O$ SMOW values of a single powdered sample of PCS are -1.74‰ and 32.22‰, respectively (Fig. 4.2; Table 4.3).

Table 4.1. Mineral proportions determined by XRD analysis for host palaeosol and fossil termitaria samples from the Calitzdorp and Groenefontein ichnosites.

Mineral (wt.%)	Calitzdorp						Groenefontein				
	HP				FT		HP	FT			
	CAL 2.4	CALI H	PCN	PCS	CAL 2.1	CAL 2.2	CAL GR 2-H	CAL GR 2	CAL GR 3	CAL GR 4	CAL GR 5
Quartz	25	50	42	75	41	49	45	42	27	20	16
Calcite	65	42	24	3	25	2		20	55	30	54
Dolomite					1	12		33	12	28	24
Plagioclase	10	8	14	11	9	37	21	5	6	10	
Alkali feldspar/rutile			5	1							
Mica			15	10	24		16				3
Kaolinite							18				
Aragonite										12	
Serpentine											3

Notes: Blank data points are either absent or below the detection quantity of 1 wt.%. Abbreviations: HP- Host palaeosol, FT-Fossil termitaria.

The nodular calcrete, PCN and CAL 2.4 mainly comprise calcite (25 and 65 wt.%, respectively), quartz (42 and 25 wt.%, respectively), and plagioclase (14 and 10 wt.%, respectively), while only PCN contains mica (15 wt.%; Fig. 4.1 A; Tables 4.1, 4.2; Appendix Fig. 1). The major element composition is dominated by SiO_2 (37.28 and 30.72 wt.%, respectively), and CaO (24.6 and 29.55 wt.%, respectively). The nodular calcrete is characterised by high concentrations of S (2116 and 2000 ppm, respectively), Ba (2432 and 1203 ppm, respectively) and Sr (817 and 768 ppm, respectively). The $\delta^{13}C$ values of PCN range between -2.69 and -0.29‰, with most of the values below -1.5‰, and the $\delta^{18}O$ values are between 29.93 and 31.31‰ (Fig. 4.2; Table 4.3). The $\delta^{13}C$ of CAL 2.4 is -1.96‰, and the $\delta^{18}O$ is 32.15‰. Relative to PCN, CAL 2.4 has consistent $\delta^{13}C$ and slightly elevated $\delta^{18}O$ (Fig. 4.2; Table 4.3).

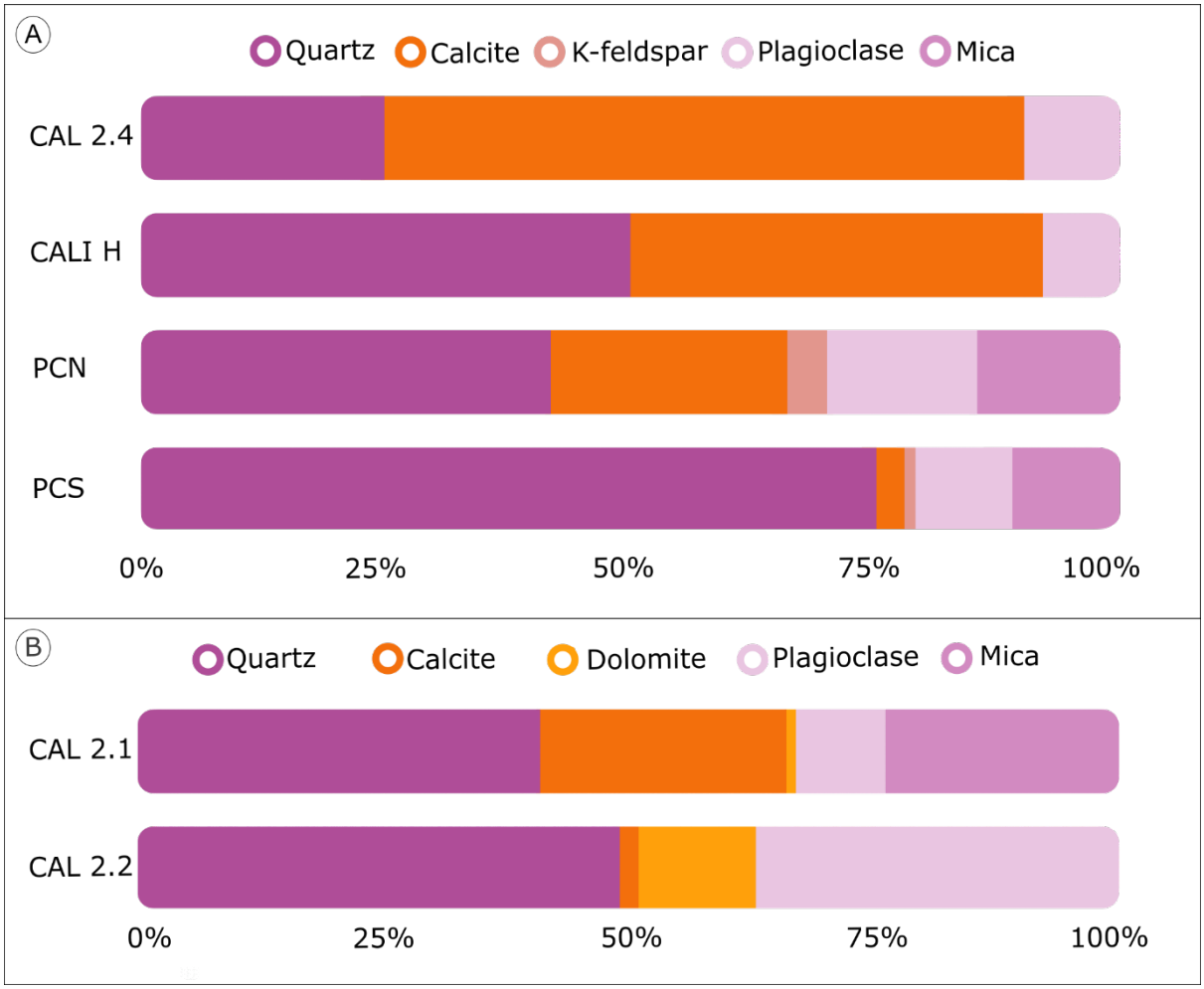

Figure 4.1. Mineral proportions (wt.%) determined by XRD of A) the host palaeosol and B) the fossil termitaria at the Calitzdorp ichnosite. For detailed data, see Table 4.1 and Appendix Figure 1.

The hardpan, CALI H, has a large proportion of quartz (50 wt.%) and calcite (42 wt.%) and a minor proportion of plagioclase (8 wt.%; Fig. 4.1 A; Table 4.1; Appendix Fig. 1). The major oxide composition mainly comprises CaO (30.04 wt.%) and SiO_2 (28.19 wt.%; Table 4.2). The trace elements S (1233 ppm), Ba (834 ppm) and Sr (815 ppm) have the highest proportions. The $\delta^{13}C$ of CALI H ranges between -3.22 to -1.43‰, and the $\delta^{18}O$ ranges from 28.35 – 30.5‰, with a clustering of samples between 28.9 and 29.6‰ (Fig. 4.2; Table 4.3).

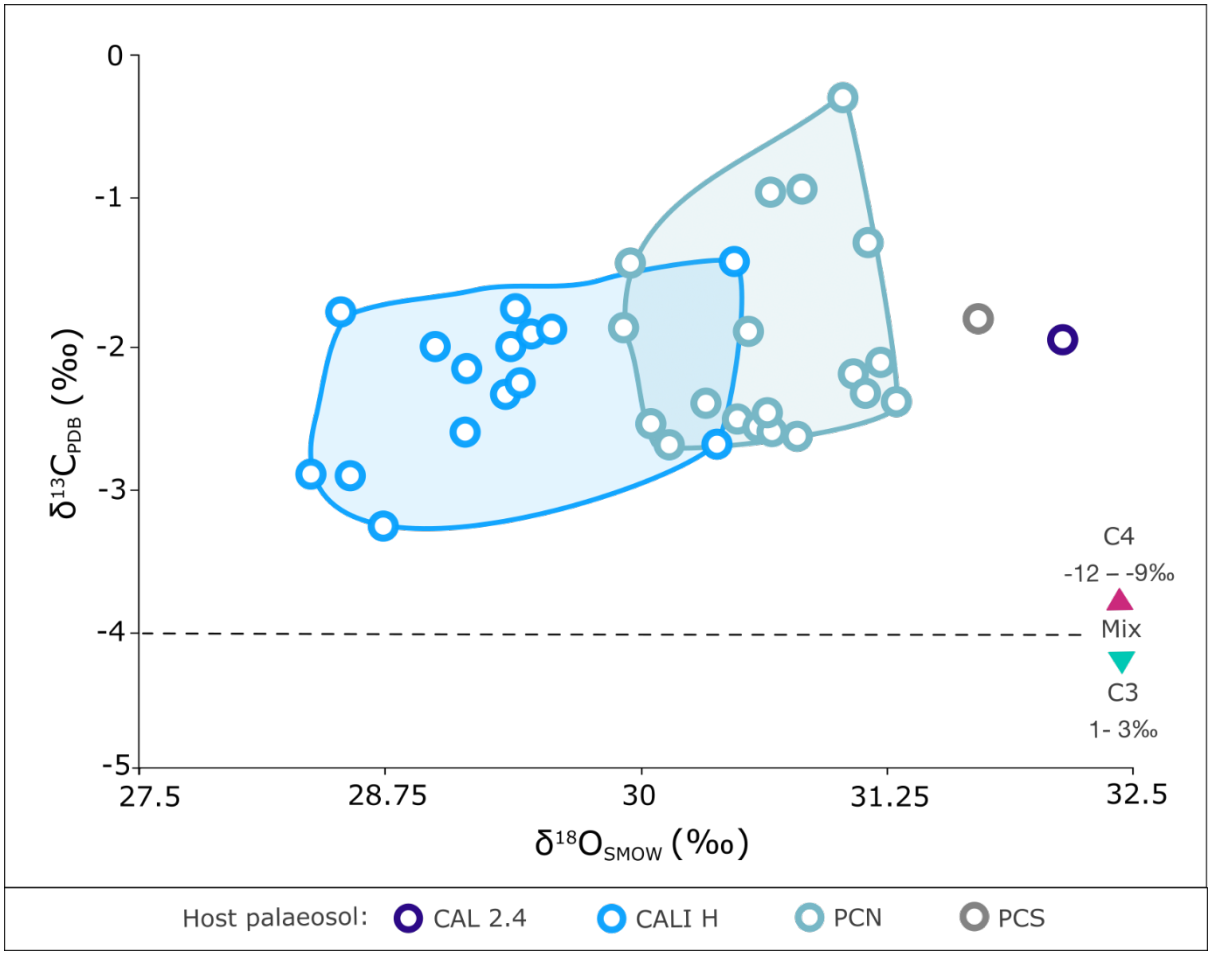

Figure 4.2 The $\delta^{13}C$ vs. $\delta^{18}O$ stable isotope values of the host palaeosols, including the carbonate nodules (CAL 2.4 and PCN), hardpan (CALI H) and the calcretised sands (PCS) at the Calitzdorp ichnosite. For detailed data, see Table 4.3.

Table 4.2. Major oxide and trace element content for samples from the Calitzdorp and Groenefontein ichnosites.

Major oxide (wt.%)	Calitzdorp						Groenefontein				
	HP				FT		HP	FT			
	CAL 2.4	CALI H	PCN	PCS	CAL 2.1	CAL 2.2	CAL GR 2-H	CAL GR 2	CAL GR 3	CAL GR 4	CAL GR
SiO_2	30.72	28.19	37.2	66.18	31.11	32.28	74.07	8.16	5.36	8.51	6.35
TiO_2	0.22	0.24	0.26	0.52	0.21	0.23	0.72	0.08	0.06	0.11	0.07
Al_2O_3	4.65	4.52	5.68	7.25	3.85	3.92	13.93	1.24	1.06	1.67	1.15
Fe_2O_3	1.57	1.50	1.89	3.71	1.24	1.25	4.99	0.50	0.48	0.79	0.62
MnO	0.03	0.05	0.04	0.05	0.04	0.08	0.03	0.10	0.09	0.14	0.10
MgO	2.77	3.74	2.69	2.32	10.35	8.68	1.63	9.55	5.98	15.19	8.73
CaO	29.55	30.04	24.6	6.85	21.56	21.55	0.74	36.8	43.86	71.62	39.2
Na_2O	0.44	0.47	0.50	0.47	0.70	0.54	1.04	0.24	0.09	0.23	0.25
K_2O	0.77	0.76	1.10	2.18	0.83	0.81	2.48	0.20	0.18	0.24	0.20
P_2O_5	0.81	0.60	1.36	0.28	0.48	0.36	0.13	0.20	0.21	0.31	0.26
SO_3	0.28	0.19	0.42	n.a.	0.10	0.09	0.12	0.19	0.16	0.50	0.23
Cr_2O_3	<0.01	<0.01	<0.0	n.a.	<0.01	<0.01	0.01	<0.0	<0.01	b.d.	0.00
NiO	0.04	<0.01	0.01	n.a.	0.03	<0.01	b.d.	0.01	0.01	b.d.	0.01
H_2O	1.72	1.90	b.d.	n.a.	0.64	0.63	5.29	0.70	0.43	3.47	1.26
LOI	25.94	27.52	21.4	n.a.	28.24	28.68	4.41	41.4	41.66	41.65	41.1
Sum	99.41	99.55	99.2	n.a.	99.40	99.12	99.89	99.5	99.46	99.30	99.6
Trace element (ppm)											
Zn	33	37	41	50	31	38	59	26	21	19	31
Cu	25	47	33	6	13	12	24	9	9	8	9
Ni	17	16	17	26	9	11	33	11	3	5	<5
Mo	<5	<5	<5	<1	<5	<5	<5	<5	<5	<5	<5
Nb	12	13	13	10	16	16	7	12	15	17	19
Zr	98	120	122	336	111	143	349	13	<5	<5	<5
Y	<5	6	8	23	8	10	22	<5	<5	5	<5
Sr	768	815	817	238	990	991	71	883	1026	1145	1192
Rb	44	42	53	80	33	33	96	15	14	17	17
U	5	<5	6	<3	<5	<5	<5	<5	<5	5	7
Th	10	9	9	10	8	7	18	8	5	12	13
Pb	34	33	36	18	32	32	43	30	30	31	34
Co	5	25	15	14	<5	<5	7	<5	<5	<5	<5
Mn	341	616	481	n.a.	561	928	248	1330	1220	1216	1415
Cr	59	55	57	33	45	39	78	19	20	14	19
V	64	45	62	80	28	47	98	28	26	23.00	18.0
F	853	701	920	n.a.	681	691	969	799	684	599	545
S	2000	1233	2116	n.a.	717	584	1339	1573	1081	3223	1958
Cl	1959	311	53	n.a.	135	164	5817	949	<10	647	294
Sc	17	16	15	8	14	15	12	18	20	22	21
Ba	1203	834	2432	417	705	430	449	358	156	135	227

Notes: Abbreviations: b.d – below detection limit of ~0.01 wt.% for major oxides, n.a.- not analysed, HP- Host palaeosol and FT- Fossil termitaria.

Table 4.3. The $\delta^{13}C$ and $\delta^{18}O$ values (‰) of the Calitzdorp and Groenefontein host palaeosol and fossil termitaria carbonates.

Calitzdorp

Host palaeosol						Fossil termitaria					
CAL 2.4			PCN			CAL 2.1			CAL 2.2		
#	$\delta^{13}C$	$\delta^{18}O$	#	$\delta^{13}C$	$\delta^{18}O$	#	$\delta^{13}C$	$\delta^{18}O$	#	$\delta^{13}C$	$\delta^{18}O$
1	-1.96	32.15	1	-2.54	30.07	1	-0.69	30.56	1	-2.25	30.60
CALI H			2	-1.88	29.93	2	-3.43	29.70	2	-3.21	30.05
1	-2.27	29.42	3	-2.41	30.34	3	-3.37	29.12	3	-2.77	29.37
2	-2.15	29.14	4	-1.42	29.96	4	-2.73	31.10	4	-2.88	28.67
3	-2.33	29.33	5	-2.69	30.16	5	-2.19	30.67	5	-3.50	30.23
4	-2.01	29.37	6	-0.93	30.66	6	-3.14	30.59	6	-2.22	30.41
5	-1.88	29.57	7	-1.28	31.15	7	-3.00	31.27	7	-1.89	30.66
6	-2.89	28.56	8	-2.50	30.50	8	-2.77	30.66	8	-3.50	29.27
7	-1.92	29.46	9	-0.29	31.03	9	-3.15	30.76	9	-2.31	30.39
8	-2.01	28.98	10	-2.48	30.65	10	-3.45	30.67	10	-2.09	30.22
9	-1.43	30.49	11	-2.10	31.22	11	-0.79	31.93	11	-2.73	29.59
10	-1.76	28.51	12	-2.33	31.15	12	-2.31	30.68	12	-3.35	29.47
11	-1.75	29.38	13	-2.61	30.80	13	-1.49	30.92	13	-1.97	30.32
12	-2.59	29.13	14	-0.91	30.84	14	-2.32	29.09	14	-2.13	30.84
13	-2.89	28.35	15	-1.89	30.55	15	-3.26	30.67	15	-2.91	29.44
14	-3.22	28.72	16	-2.56	30.60				16	-1.02	30.74
15	-2.67	30.40	17	-2.19	31.09				17	-1.55	28.62
PCS			18	-2.61	30.67				18	-3.26	27.10
1	-1.74	32.22	19	-2.40	31.31						

Groenefontein

FT											
CAL GR 2			CAL GR 3			CAL GR 4			CAL GR 5		
1	-3.18	28.72	1	-4.16	30.37	1	-5.98	30.91	1	-7.10	30.76
2	-3.65	28.62	2	-4.39	33.50	2	-6.57	30.42	2	-6.59	31.53
3	-3.47	28.90	3	-4.18	29.88	3	-6.88	30.01	3	-6.90	31.12
4	-3.95	28.12	4	-4.35	30.14	4	-7.12	29.75	4	-6.48	30.93
5	-1.56	29.85	5	-5.25	26.24	5	-6.10	30.98	5	-7.19	30.94
6	-2.70	28.79	6	-4.32	30.74	6	-6.94	29.87	6	-6.25	31.64
7	-3.05	28.98	7	-4.66	30.08						
8	-3.37	28.73	8	-4.13	30.75						
9	-3.27	28.47	9	-4.13	30.75						
10	-3.49	29.12	10	-4.11	30.42						
12	-3.43	28.27									
13	-2.90	28.87									
14	-3.12	28.60									

Notes: The # symbol refers to the sample number.

4.1.2 Fossil Termitaria

The bulk mineralogy of CAL 2.1 comprises quartz (41 wt.%), calcite (25 wt.%), mica (24 wt.%), and plagioclase (9 wt.%) with minor dolomite (1 wt.%; Fig. 4.1 B; Table 4.1; Appendix Fig. 1). The dominant major oxides include SiO_2 (31.11 wt.%), CaO (21.56 wt.%), and MgO (10.35 wt.%; Table 4.2). The most abundant trace elements are Sr (990 ppm), S (717 ppm), and Ba (705 ppm). The $\delta^{13}C$ values for CAL 2.1 range from -3.45 to -0.69‰, with most of the data values <-2‰, and the $\delta^{18}O$ values range between 29.09 to 31.93‰, with most of the data values exceeding 30.5‰ (Fig. 4.3; Table 4.3). The CAL 2.2 fossil termitaria contain a high proportion of quartz (49 wt.%), plagioclase (37 wt.%), and dolomite (12 wt.%), with minor calcite (2 wt.%; Fig. 4.1 B; Table 4.1; Appendix Fig. 1) The most abundant major oxides are SiO_2 (32.2 wt.%), MgO (8.7 wt.%), and CaO (21.5 wt.%; Table 4.2). The sample contains high proportions of Sr (991 ppm), Mn (928 ppm), F (691 ppm), S (584 ppm), and Ba (430 ppm). The $\delta^{13}C$ of CAL 2.2 varies between -3.5‰ and -1.02‰, with clusters around 2‰ and 3‰, and the $\delta^{18}O$ ranges from 27.1 to 30.84‰, with most values above 29‰ (Fig. 4.3; Table 4.3).

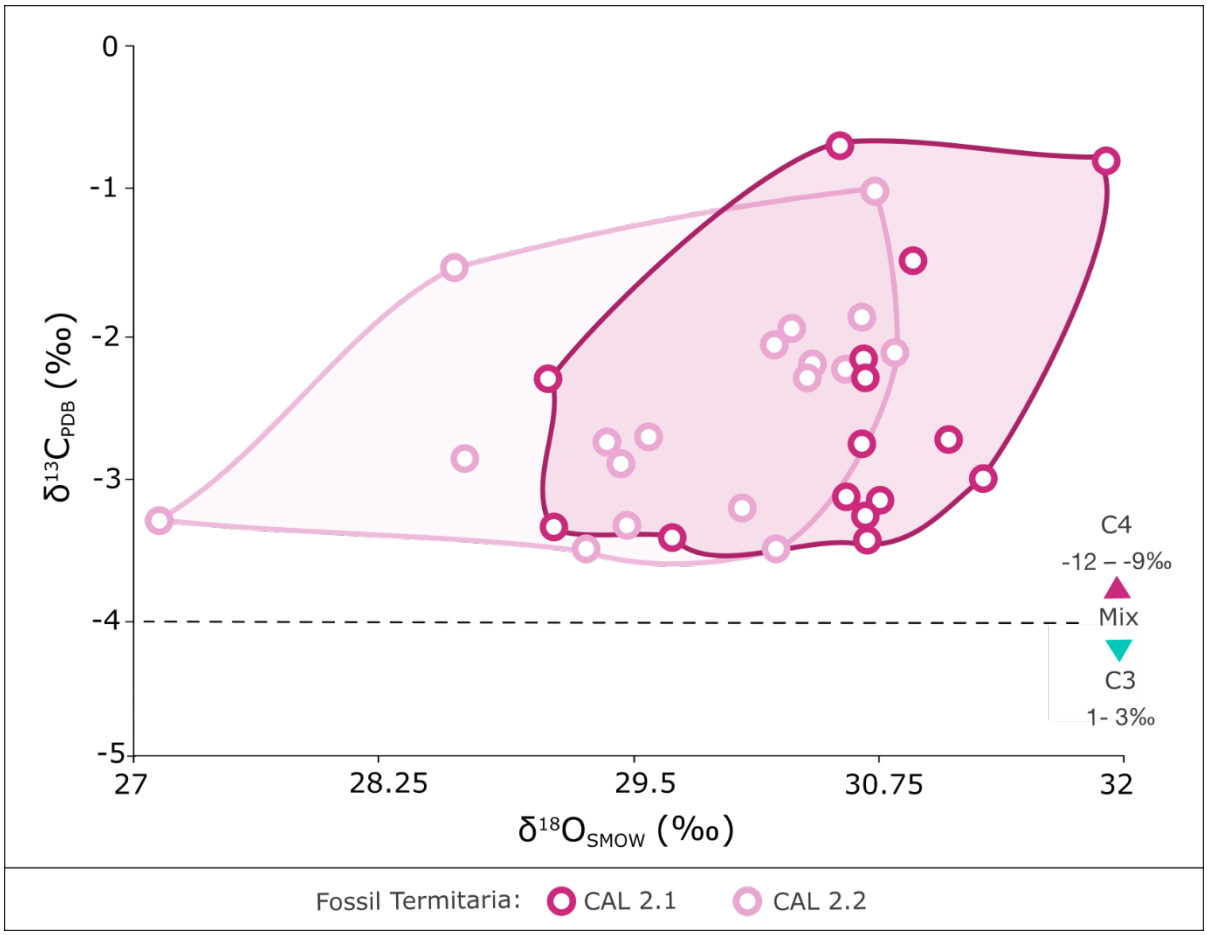

Figure 4.3 The $\delta^{13}C$ PDB vs. $\delta^{18}O$ SMOW stable isotope values of the Calitzdorp fossil termitaria samples (CAL 2.1 and CAL 2.2). For detailed data, see Table 4.3.

4.1.3 Synthesis

The fossil termitaria-bearing host palaeosol, PCS, has the lowest proportion of carbonate minerals (3 wt.%), while the nodular and hardpan calcretes have a higher carbonate content (24– 65 wt.%; Fig. 4.1; Table 4.1). For all host palaeosols, the only carbonate mineral present is calcite. The major oxide composition of PCS is distinctly different from the other host palaeosols, with CAL 2.4 and CALI H exhibiting the most comparable compositions (Fig. 4.4; Table 4.2). The trace element composition of PCS differs from that of the other host palaeosols. Relative to PCS, the fossil termitaria have a higher carbonate content (3 wt.% vs. 13 and 26 wt.%) and while PCS only contains calcite, the termitaria contain both calcite and dolomite. Relative to PCS, the major oxide compositions of fossil termitaria are enriched in CaO, MgO, Na_2O, and P_2O_5 and depleted in Al_2O_3, Fe_2O_3, and K_2O (Figs. 4.4, 4.5). While the major oxide compositions of the termitaria display enrichment in MgO and Na_2O, their trace element proportions are generally comparable to those of the nodules and hardpan. The $\delta^{13}C$ and $\delta^{18}O$ signatures of the host palaeosols and fossil termitaria are largely indistinguishable from each other and exhibit an intermediate C_3/C_4 vegetation signal (Fig. 4.6; Table 4.3).

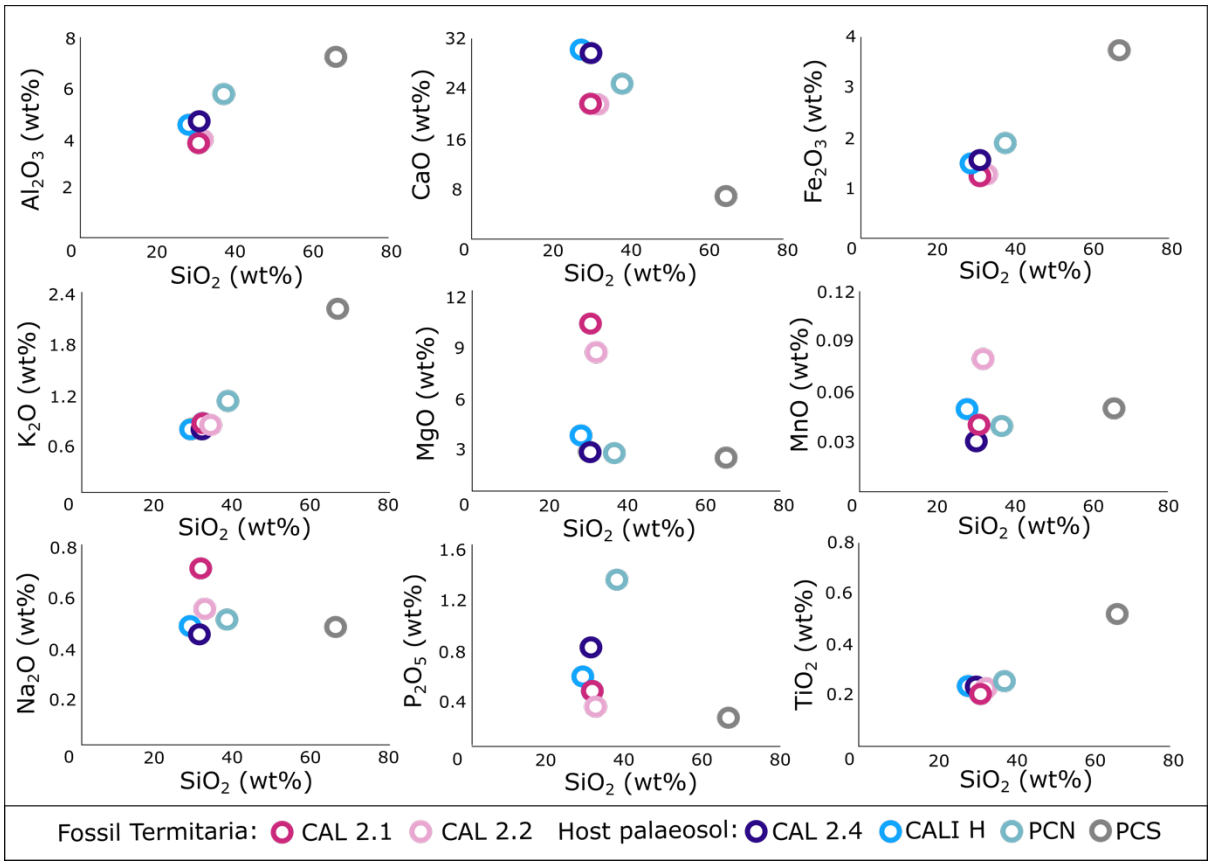

Figure 4.4 The major element oxide composition against SiO_2 for the Calitzdorp host palaeosol and fossil termitaria. For detailed data, see Table 4.2.

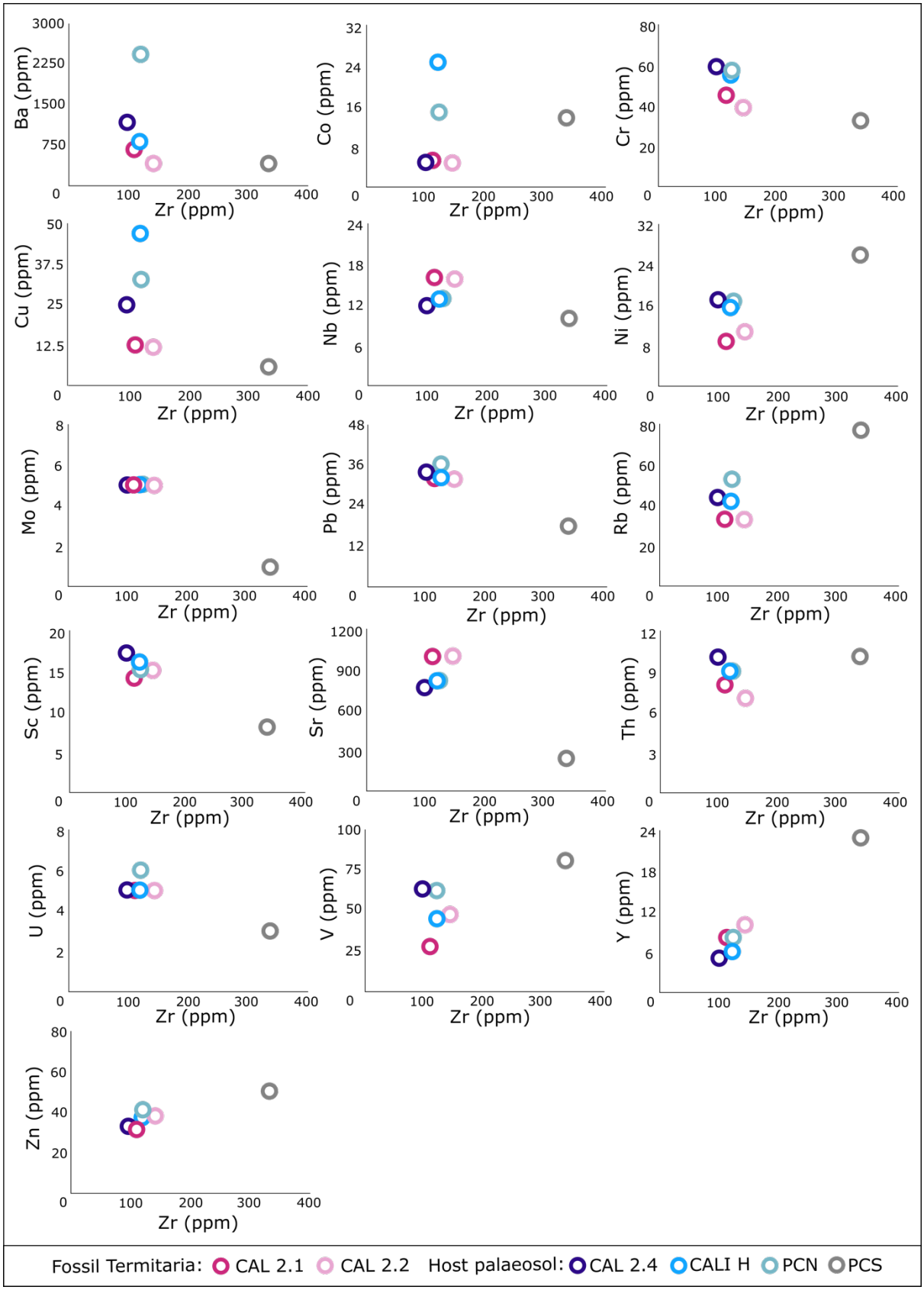

Figure 4.5 The trace element composition against Zr for the Calitzdorp host palaeosol and fossil termitaria. For detailed data, see Table 4.2.

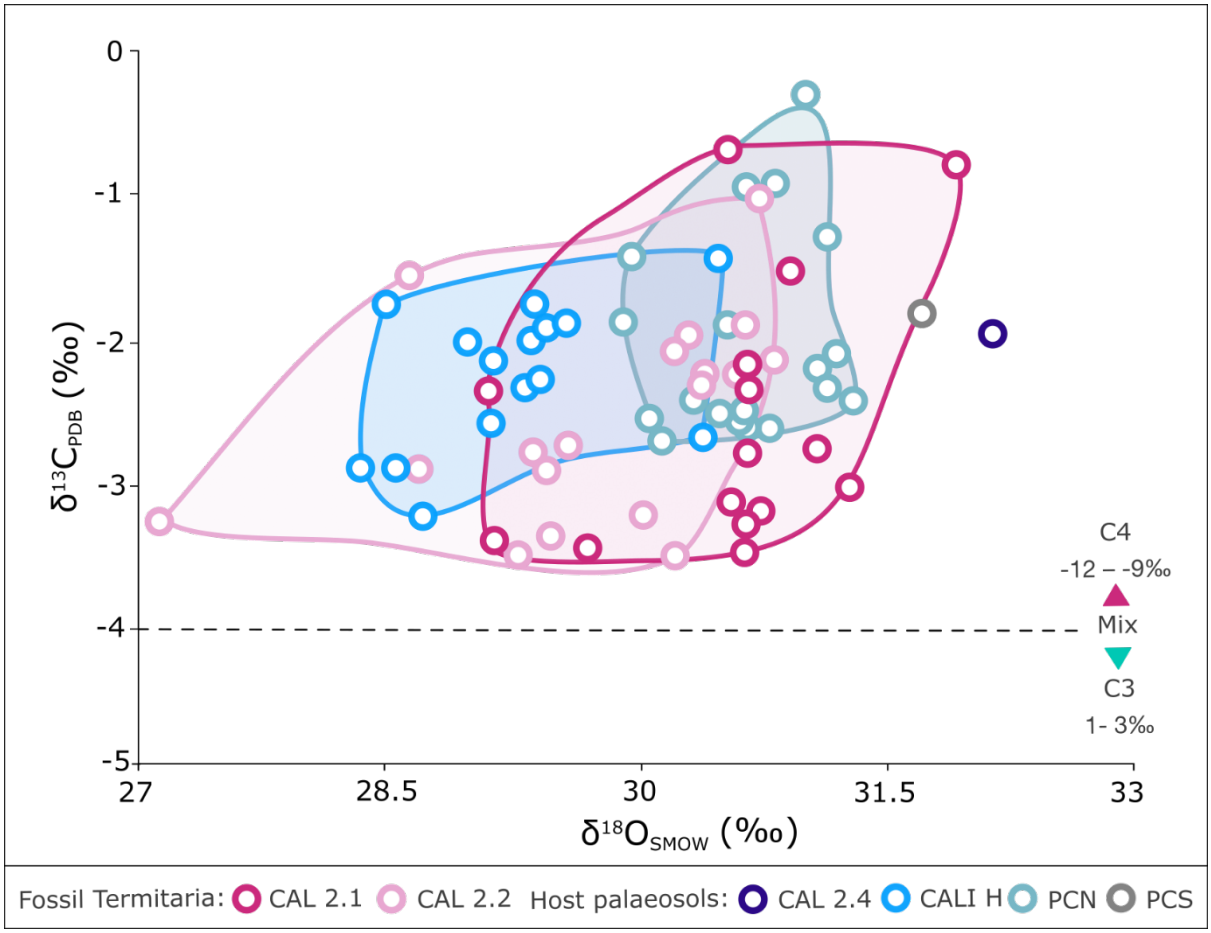

Figure 4.6. The $\delta^{13}C$ vs. $\delta^{18}O$ values of the carbonates in the host palaeosol and fossil termitaria samples at the Calitzdorp ichnosite. For detailed data, see Table 4.3.

4.2 Groenefontein

4.2.1 Host palaeosol

The host palaeosol at the Groenefontein ichnosite, represented by the fine-grained sand and mud of the CAL GR 2-H sample from the Bokkeveld shale, hosts all four termitaria (Table 3.1).

The bulk mineralogy of CAL GR 2-H primarily comprises quartz (45 wt.%) and plagioclase (21 wt.%), with a moderate quantity of mica (16 wt.%) and kaolinite (18 wt.%; Fig. 4.7 A; Table 4.1; Appendix Fig. 1). The most abundant major element is SiO_2 (74.07 wt.%), with a moderate proportion of Al_2O_3 (13.93 wt.%; Table 4.2). The prevalent trace elements include Cl (5817 ppm), S (1339 ppm), and F (969 ppm).

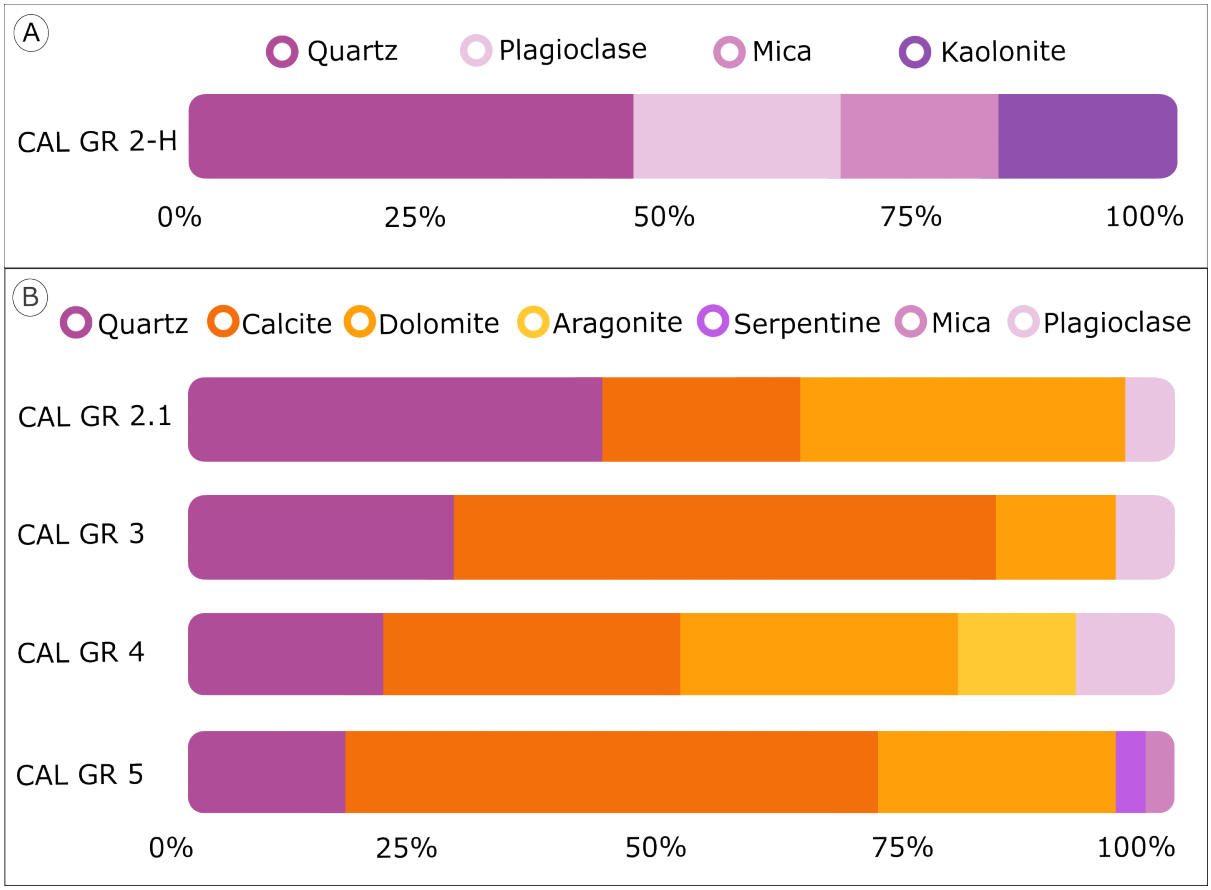

Figure 4.7. Mineral proportions (wt.%), determined by XRD, of A) the host palaeosol and B) the fossil termitaria at the Groenefontein ichnosite. For detailed data, see Table 4.1 and Appendix Figure 2.

4.2.2 Fossil Termitaria

The sample CAL GR 2 is mainly characterised by quartz (42 wt.%), dolomite (33 wt.%), calcite (20 wt.%), and minor plagioclase (5 wt.%; Fig. 4.7 B; Table 4.1; Appendix Fig. 1). The primary major oxide is CaO (36.8 wt.%), with a minor amount of MgO (9.55 wt.%) and SiO_2 (8.16 wt.%), and the prevalent trace elements include S (1573 ppm), Mn (1330 ppm), Cl (949 ppm), and Sr (883 ppm; Table 4.2). The $\delta^{13}C$ and $\delta^{18}O$ values are clustered between -3.95‰ and -2.7‰ and 27.7‰ and 29.4‰, respectively, with a single outlying point at 1.56‰ $\delta^{13}C$ and 29.9‰ $\delta^{18}O$ (Table 4.4; Fig. 4.8).

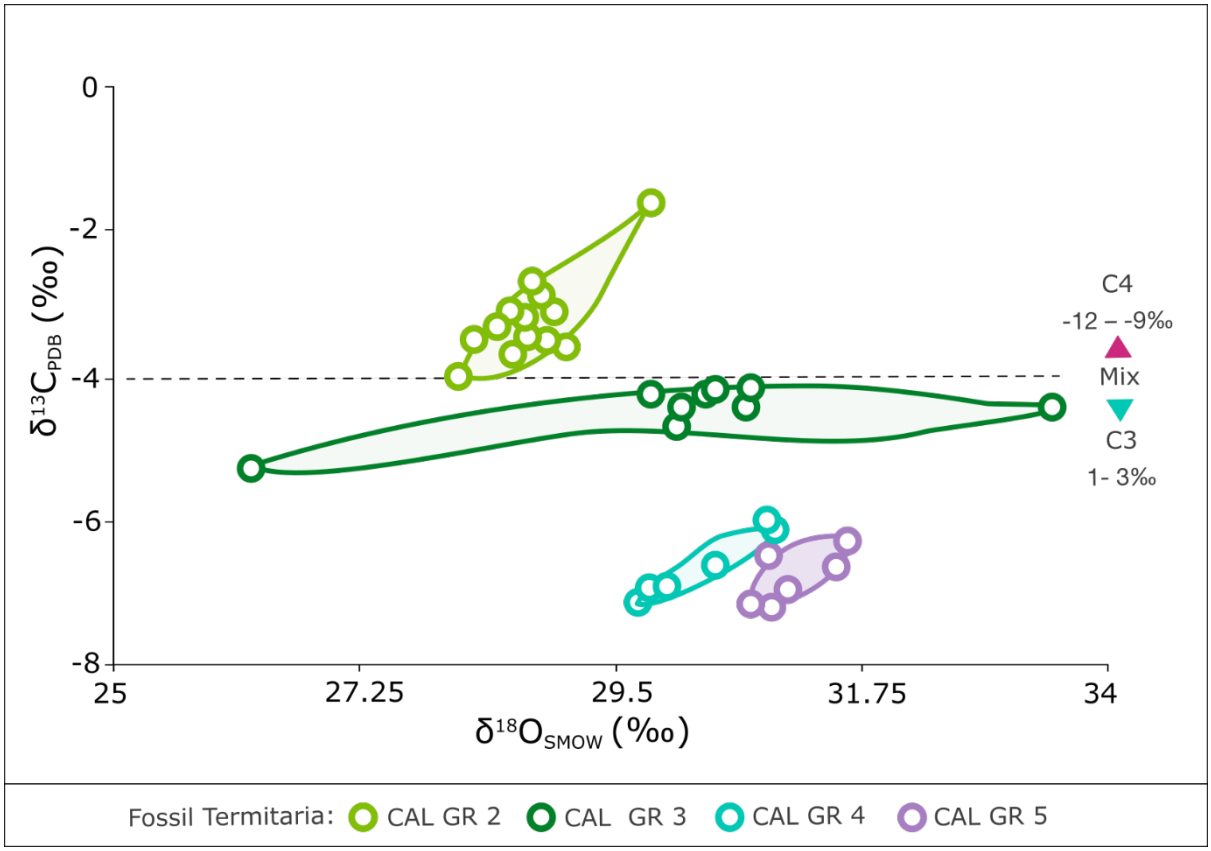

Figure 4.8 The $\delta^{13}C$ vs. $\delta^{18}O$ stable isotope values of the Groenefontein ichnosite fossil termitaria samples. For detailed data, see Table 4.3.

The CAL GR 3 sample contains mostly calcite (55 wt.%), quartz (27 wt.%), and a moderate amount of dolomite (12 wt.%; Fig. 4.7 B; Table 4.1; Appendix Fig. 1). The major oxide composition is dominated by CaO (43.9 wt.%), with minor SiO_2 (5.4 wt.%), and MgO (6 wt.%; Table 4.2). The most abundant trace elements in the sample are Mn (1220 ppm), Sr (1026 ppm), and S (1081 ppm). The $\delta^{13}C$ values are constrained between -5.25 and -4.11‰, while

the $\delta^{18}O$ values range from 26.24 to 33.5‰, although two outliers influence this latter range. Most of the $\delta^{18}O$ values cluster between 29.9 and 30.8‰ (Table 4.4; Fig. 4.8).

Sample CAL GR 4 comprises mainly calcite (30 wt.%), dolomite (28 wt.%), and quartz (20 wt.%), along with moderate aragonite (12 wt.%) and plagioclase (10 wt.%; Fig. 4.7 B; Table 4.1). The primary major oxide is CaO (71.6 wt.%), followed by moderate amounts of MgO (15.2 wt.%) and minor SiO_2 (8.5 wt.%; Table 4.2). The main trace elements in the sample are S (3223 ppm), Mn (1216 ppm), and Sr (1145 ppm). These $\delta^{13}C$ values of CAL GR 4 range between -7.12 to -5.98‰ (Fig. 4.8; Table 4.4). Conversely, the $\delta^{18}O$ values have two discrete clusters of 29.5 – 30‰ and 30.9 – 31‰, respectively.

Calcite (54 wt.%) is the main mineral in CAL GR 5, followed by dolomite (24 wt.%) and quartz (16 wt.%; Fig. 4.7 B; Table 4.1). The primary major oxide is CaO (39.3 wt.%), with minor MgO (8.7 wt.%) and SiO2 (6.3 wt.%; Table 4.2). The sample contains high amounts of S (1958 ppm), Mn (1415 ppm), and Sr (1192 ppm). The $\delta^{13}C$ values are constrained between -7.19 and -6.25‰ (Fig. 4.8; Table 4.4). The $\delta^{18}O$ values are between 30.76 and 31.53‰, with most skewed to below 31.1‰.

4.2.3 Synthesis

The mineral composition of the four fossil termitaria at the Groenefontein ichnosite contains a high proportion of carbonate minerals (calcite and dolomite), whereas the host palaeosol contains kaolinite but no carbonates (Fig. 4.7; Table 4.1; Appendix Fig. 1). Sample CAL GR 4 is anomalous as it includes 12 wt.% aragonite in addition to calcite and dolomite. The major oxide compositions of the fossil termitaria are comparable, apart from elevated proportions of CaO, MnO, and MgO in CAL GR 4 and MgO depletion in CAL GR 3 (Fig. 4.9; Table 4.2). The major oxide composition of the fossil termitaria is distinct from that of the host. Similarly, the trace element compositions of the fossil termitaria are similar to each other but differ from the host palaeosol with relatively higher Sr content and lower Co, Co, Ni, and Zn content (Fig. 4.10; Table 4.2). The stable isotope compositions of the fossil termitaria are distinct, and form 3 groupings based mainly on $\delta^{13}C$ values (Fig. 4.8; Table 4.4): CAL GR 2 is closer to the expected value of a C_4-dominated carbonate, while CAL GR 3, CAL GR 4 and CAL GR 5 are more C_3 in

character. A weaker grouping is apparent for $\delta^{18}O$ values, where CAL GR 2 has the lowest $\delta^{18}O$ values, CAL GR 5 has the highest $\delta^{18}O$ values, and CAL GR 3 and CAL GR 4 are intermediary.

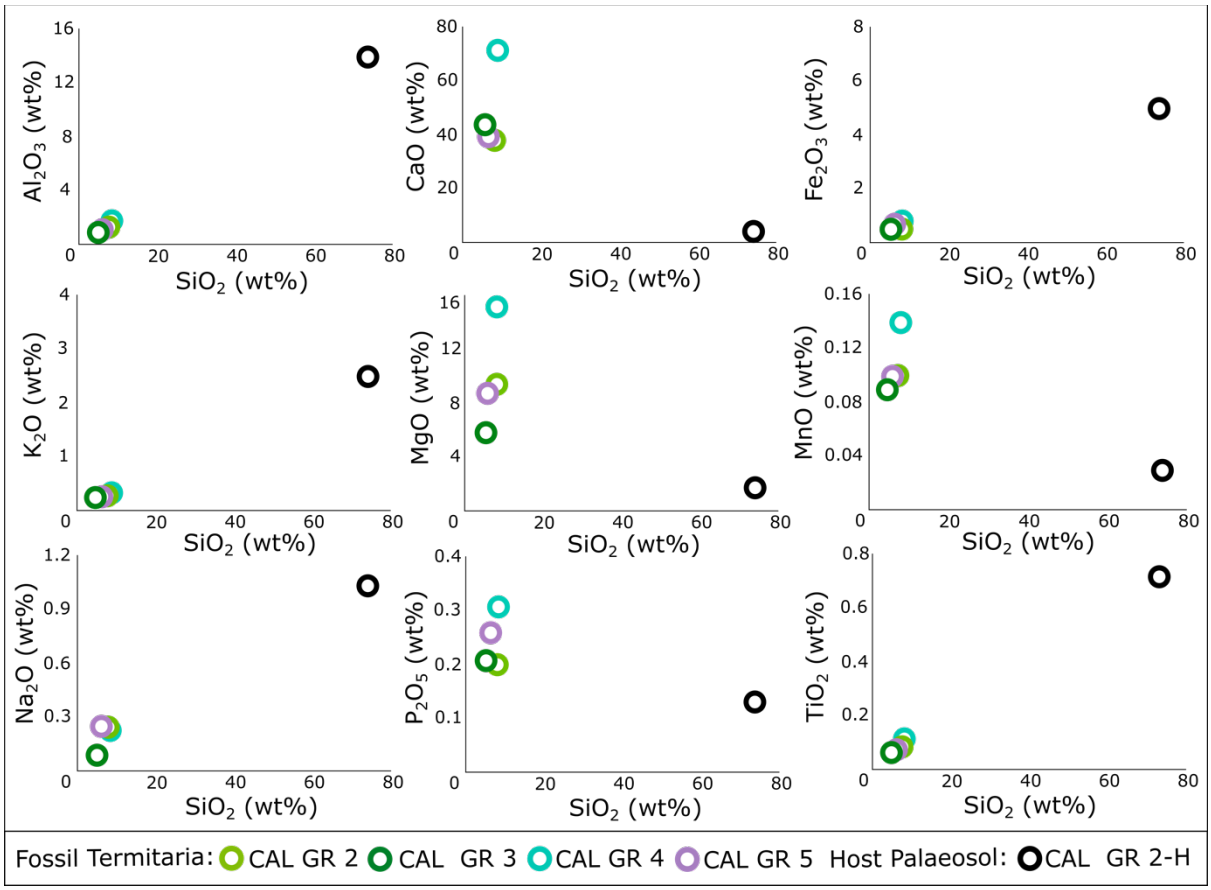

Figure 4.9 The major element oxide composition against SiO_2 of the Groenefontein host palaeosol and fossil termitaria. The dashed line through CAL GR2-H indicates relative major oxide enrichment. For detailed data, see Table 4.2.

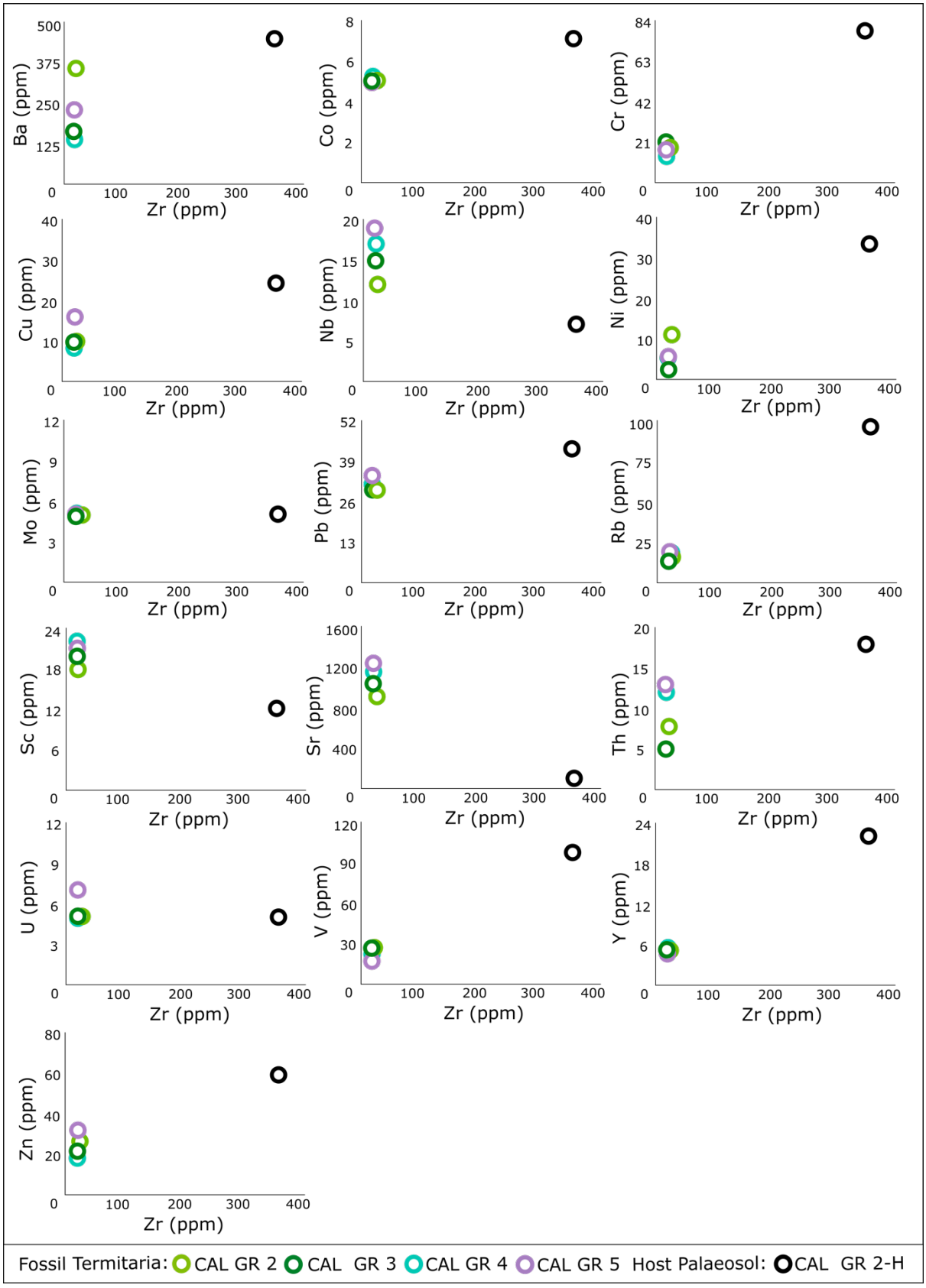

Figure 4.10 The trace element composition against Zr of the Groenefontein host palaeosol and fossil termitaria. For detailed data, see Table 4.2.

4.3 Calitzdorp and Groenefontein Synthesis

The mineral compositions of the fossil termitaria are comparable at both ichnosites, with the fossil termitaria at both locations containing calcite and dolomite (Figs. 4.1, 4.7; Table 4.1; Appendix Figs. 1). Notably, an anomalous fossil termitarium, CAL GR 4, from Groenefontein also contains a moderate proportion of aragonite (12 wt.%; Fig. 4.7; Table 4.1). This carbonate mineralogy (calcite, dolomite and aragonite) is distinct from the host palaeosols, where at Calitzdorp, they exclusively comprise calcite, and at Groenefontein, they contain no carbonate minerals but include a moderate proportion of kaolinite (18 wt.%; a clay-forming mineral). At both ichnosites, relative to the host palaeosols, the fossil termitaria contain greater proportions of carbonate minerals, with the fossil termitaria at Groenefontein containing more carbonate minerals than the fossil termitaria at the Calitzdorp ichnosite (Figs. 4.1, 4.7; Table 4.1).

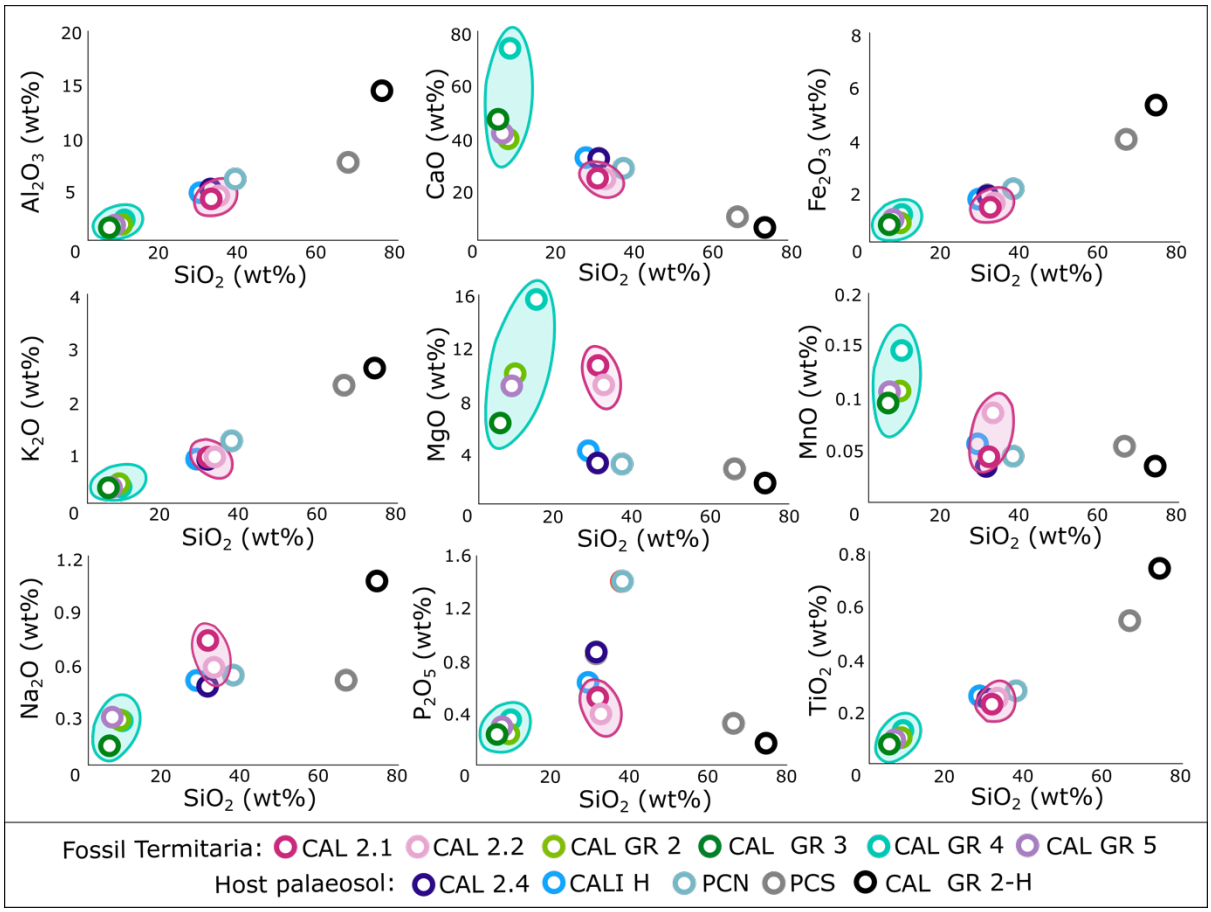

Figure 4.11 The major element oxides composition against SiO_2 of the Calitzdorp and Groenefontein host palaeosols and fossil termitaria. For detailed data, see Table 4.2. The fields encircle the fossil termitaria samples from each ichnosite.

The fossil termitaria are generally comparable when considering major element compositions, with a few exceptions (Fig. 4.11; Table 4.2). While PCS contains a relatively higher CaO (6.85 vs. 0.74 wt.%), MgO (2.32 vs. 1.63 wt.%), MnO (0.05 vs. 0.03 wt.%) and P_2O_5 (0.28 vs. 0.13 wt.%) content than CAL GR 2-H the termitaria at both ichnosites are similarly enriched in these oxides relative to their respective host palaeosols (Figs. 4.11, 4.12; Table 4.2). The host palaeosol at Calitzdorp (PCS) contains a lower SiO_2 (66.18 vs. 74.01 wt.%) and Na_2O (0.47 vs. 1.04 wt.%) contents relative to the Groenefontein host palaeosol (CAL GR 2-H), yet the fossil termitaria at Calitzdorp contain more SiO_2 (~32 wt.% vs. 5–8 wt.%) and Na_2O (~0.5–0.7 wt.% vs. 0.09–0.25 wt.%). Similarly, the CAL GR 2-H contains significantly less CaO than PCS, while the Groenefontein fossil termitaria contain more CaO (37–72 wt.% vs. 22 wt.%). Additionally, CAL GR 4 contains more MgO than all the samples (15 wt.% vs. 9–10 wt.%).

The XRD analysis aided in confirming the presence of calcite, dolomite, and aragonite in termitaria, which differs from the host materials (i.e., PCS, which only contains calcite and CAL GR 2-H, which is carbonate-free). However, XRD's semi-quantitative nature sets limits on its utility, showing a weak correlation between the carbonate (calcite and dolomite) to the 'corresponding' oxides (CaO and MgO; Tables 4.1, 4.2). Although this method is not robust, it was used as an initial check to see if any correlation existed between the XRD and XRF results, helping to avoid unrealistic interpretations based solely on the XRD data.

The major oxide proportions calculated from XRD-derived mineralogy deviated significantly from the actual values obtained through XRF analysis (Appendix Table 2). The CAL 2.1 fossil termitarium was used to exemplify these discrepancies. The SiO_2 content (57.73 wt.%) was overestimated by XRD compared to actual XRF measurements (28.58 wt.%), while CaO (14.29 vs. 22.82 wt.%) and MgO (0.22 vs. 10 wt.%) were significantly underrepresented. This suggests, contrary to the XRD measurements, that quartz (primarily comprising SiO_2) may be less abundant in this termitarium. Since SiO_2 is present in multiple minerals such as quartz, feldspar, and mica, a relative underestimation of total SiO_2 content in XRD results likely reflects a general underestimation of these silicate minerals. In contrast, the relatively higher CaO and MgO content indicates a greater abundance of carbonate phases (e.g., $CaCO_3$ and $CaMg(CO_3)_2$), which comprise a significant proportion of the carbonate composition. Although

XRD successfully identified minerals, its imprecise quantification limits interpretative value in this study.

The trace element composition of the fossil termitaria is indistinguishable between ichnosites, except Cr, which is higher at Calitzdorp (40–45 ppm vs. 14–20 ppm; Fig. 4.12; Table 4.2). The fossil termitaria are distinct from their host palaeosols at both ichnosites and share similar enrichment patterns. While PCS has a lower Ni and higher Sr content than CAL GR 2-H, fossil termitaria from both ichnosites are similarly enriched in Sr and depleted in Ni relative to their host palaeosols (Table 4.2). The PCS palaeosol contains less Cu than CAL GR 2-H (6 ppm vs. 24 ppm), yet the Calitzdorp fossil termitaria are relatively enriched in Cu (12–13 ppm vs. 6 ppm), whereas the Groenefontein fossil termitaria are depleted in Cu (8–9 ppm vs. 24 ppm).

While the Calitzdorp fossil termitaria are indistinguishable from each other in both $\delta^{13}C$ and $\delta^{18}O$ values, the Groenefontein fossil termitaria exhibit three distinct $\delta^{13}C$ groupings, which are indicative of a pronounced C_3 signal. Some overlap is observed in $\delta^{18}O$ values between the ichnosites (Fig. 4.13; Tables 4.3, 4.4). The CAL GR 2 sample is notably indistinguishable from other Calitzdorp samples in terms of $\delta^{13}C$ values. Overall, the $\delta^{13}C$ values of the carbonates in the termitaria at both ichnosites preserve a mixed C_3/C_4 vegetation signal.

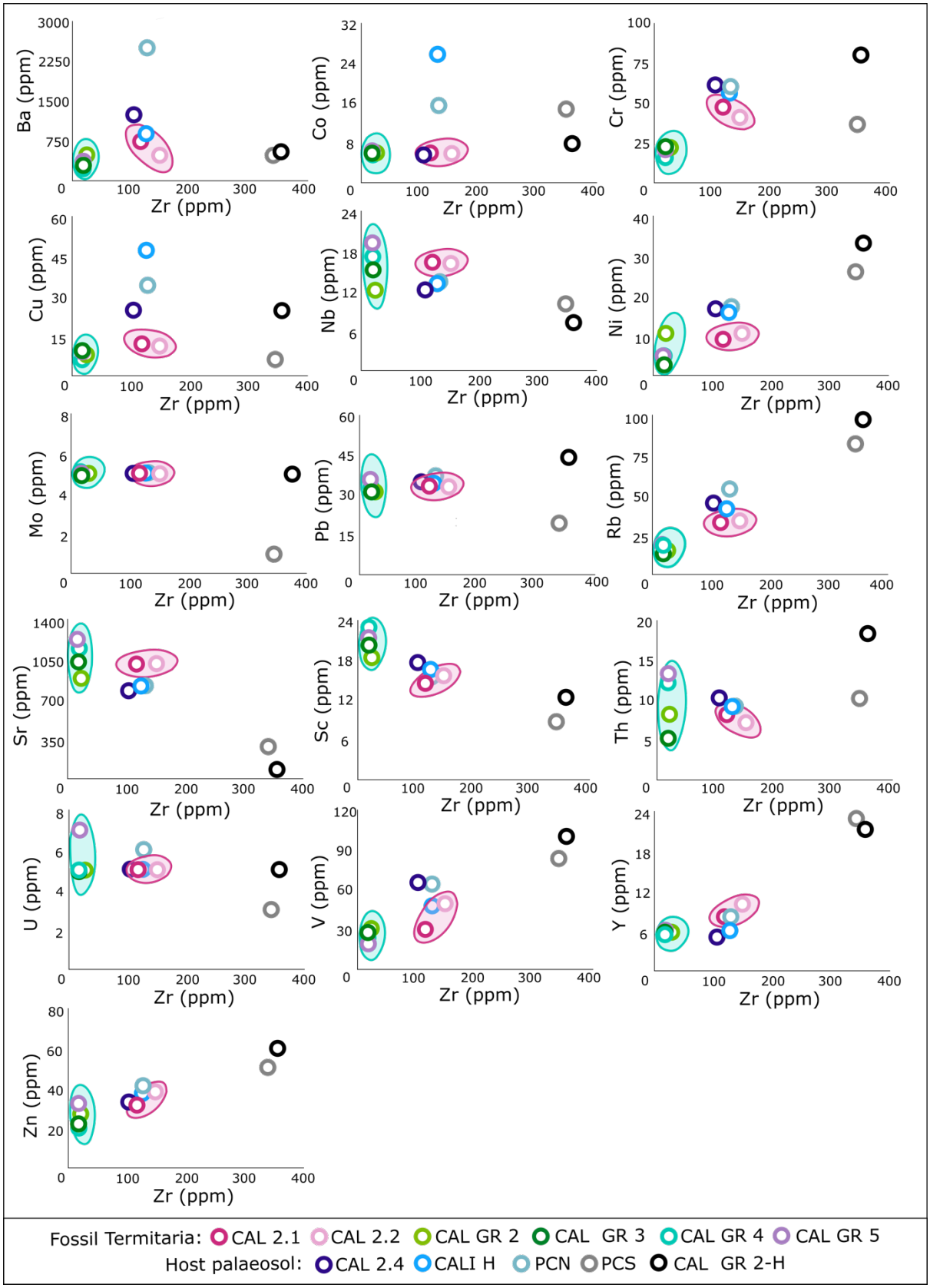

Figure 4.12 The trace element composition against Zr of the Calitzdorp and Groenefontein host palaeosol and fossil termitaria. For detailed data, see Table 4.2. The fields encircle the fossil termitaria samples from each ichnosite.

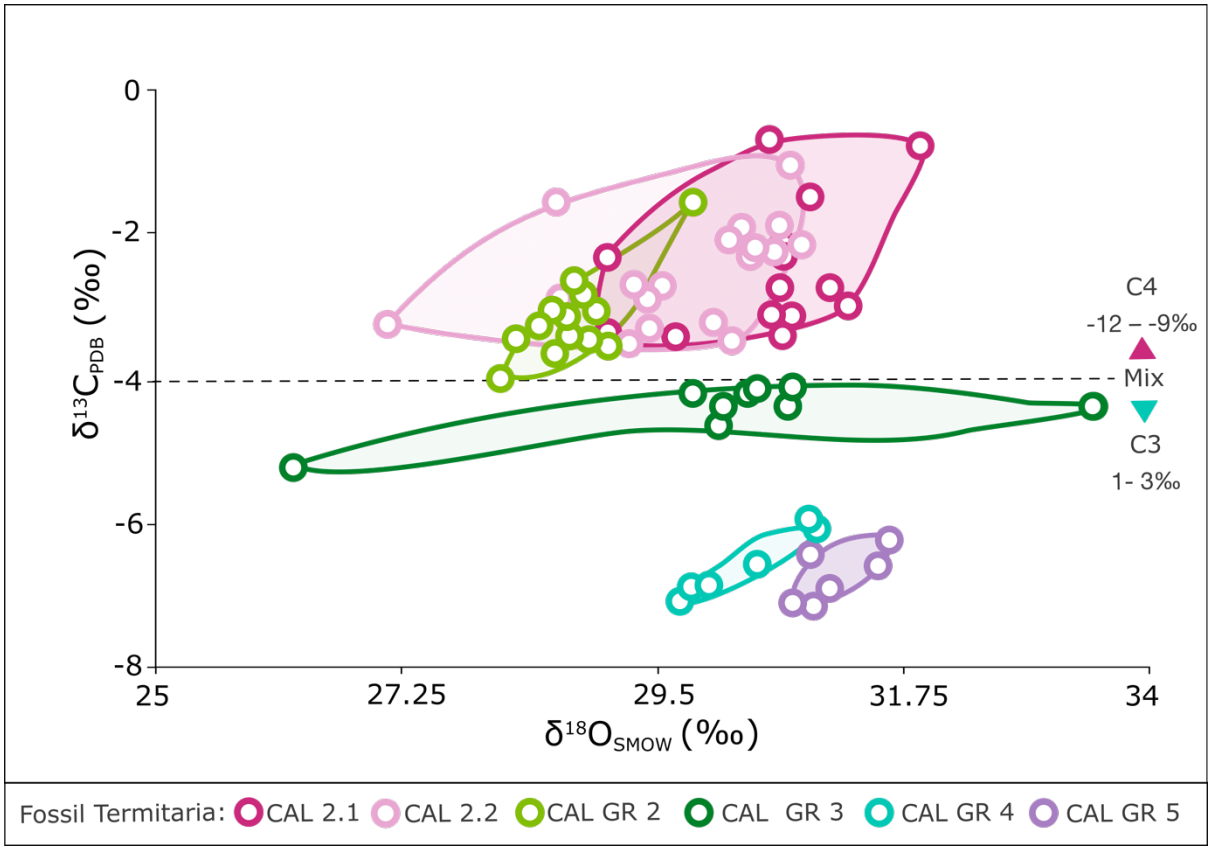

Figure 4.13 The $\delta^{13}C$ vs. $\delta^{18}O$ values of the fossil termitaria from the Calitzdorp and Groenefontein ichnosites.

5. Discussion

5.1 Fossil termitaria preservation

At Calitzdorp and Groenefontein, the fossil termitaria are preserved as carbonate-rich features comprising calcite and dolomite (Figs. 4.1, 4.7; Table 4.1). A single anomalous termitarium at Groenefontein contains minor aragonite (12 wt.%). At Calitzdorp, the termitaria are preserved within a pedogenic carbonate palaeosol, whereas the termitaria at Groenefontein are preserved in a palaeosol with no carbonate content. Interestingly, the host palaeosol at Calitzdorp exclusively contains calcite, i.e., no dolomite is present.

While calcite (CaO_3) is commonly reported to be present in high amounts in both modern and fossil termite structures (e.g., MAT 1; Black and Okwakol, 1997; Mujinya et al., 2011; Singh et al., 2017; Watson, 1974; Coaton, 1981; Moore and Picker, 1991; Liu et al., 2007; Potts et al., 2009), the occurrence of dolomite ($CaMg(CO_3)_2$) is not reported (Lee and Wood, 1971; Arshad, 1981; Moore and Picker, 1991; Asawalam et al., 1999; Mujinya et al., 2011; Francis and Poch, 2019). The exact mechanism behind carbonate precipitation in termitaria remains unclear; it is generally attributed to two main factors:

1) *Biogenic processes:* Carbonate minerals are attributed to the termite activity. Carbonate minerals can be transported by the termites from the soil into their termitaria, or in the organic matter that they deposit, along with saliva and faeces, which breaks down and releases exchangeable bases like Ca and Mg, which promotes carbonate precipitation (Milne, 1947; Watson, 1974; Liu et al., 2007; Mujinya et al., 2011; Hervé et al., 2018; McAuliffe et al., 2019; Francis and Poch, 2019).
2) *Abiogenic (physical) processes*: As water evaporates at the soil's surface, ions in the groundwater, including Ca^{2+} and HCO^{3-} and CO_2 from the soils, are introduced into the termitaria (Hesse, 1955; Weir, 1973; Watson, 1974; Cerling, 1984; Cerling et al., 1989). Once Ca^{2+} and HCO^{3-} become saturated in the termitaria soils, they begin to evaporate. Although these processes can result in carbonate precipitation in both the soil and termitaria, they are often preferentially preserved in the termitaria (e.g., Milne, 1947; Lee and Wood, 1971; Liu et al., 2007; Mujinya et al., 2011; Francis and Poch, 2019; Hadebe, 2021; Muir et al., 2022). For example, the calcium ions can be retained in the

termitaria as water evaporates from the surface of the subaerial mound. Alternatively, under arid conditions, substantial amounts of calcium carbonate can be retained in the termitaria, as limited rainfall reduces the likelihood of chemical leaching (Booi, 2011; Francis and Poch, 2019; Francis et al., 2022).

The two processes are not mutually exclusive, and in some cases, both biogenic and abiogenic processes promote carbonate precipitation within the termitaria. For example, termite bioturbation increases soil capillary networks, allowing calcium-saturated groundwater to evaporate at the surface, resulting in carbonate accumulation in the termitaria from both biogenic and abiogenic processes (Yanes et al., 2008; Mujinya et al., 2011). At the Calitzdorp ichnosite, carbonate minerals are preserved within the host palaeosol and fossil termitaria (Fig. 4.1; Table 4.1). This indicates that at least one phase of abiogenic carbonate precipitation (i.e., unrelated to the ancient termites) occurred at Calitzdorp, affecting both the host palaeosol and the fossil termitaria; the calcretisation of the palaeosol post-dates the termitaria as they are capped by the impenetrable hardpan, and its calcretisation may have been independent of the termitaria. In contrast, at Groenefontein, carbonates are only found within the fossil termitaria, suggesting localised chemical or physical properties linked to the termitaria and termite activity promoted carbonate precipitation (Fig. 4.7; Table 4.1). Dolomite occurs exclusively within the fossil termitaria at both ichnosites. Its precise origin remains uncertain, further complicated by the micritic textures and evidence of overprinting observed in the carbonates. Dolomite typically forms as a secondary replacement of calcite (Bustillo and Alonso-Zarza, 2007), although under certain conditions, such as calcium-leached groundwater or magnesium-rich bedrock, primary dolomite precipitation may occur (Podwojewski, 1995; Alonso-Zarza and Wright, 2010). However, these mechanisms seem unlikely here, as the surrounding carbonates in the palaeosols would also have been affected by such processes, yet are devoid of dolomite. While a full diagenetic reconstruction was beyond the scope of this study, the mineralogical complexity was taken into account during the interpretation of the stable isotope data. The presence of dolomite in the termitaria at both ichnosites is more likely to have been facilitated by high magnesium content in organic matter introduced through biogenic termite activity, including the deposition of organic material (i.e., plant material and termite frass), which is rich in exchangeable base cations (e.g., Ca^{2+}, Mg^{2+}, K^{+}, Na^{+}; Sarcinelli et al., 2009; Abe et al., 2011; Muvengwi et al., 2016; Mills

and Sirami, 2018; Pina et al., 2022; Roberts, 2024). This biogenic magnesium, combined with an influx of groundwater and subsequent ion saturation, likely promoted the carbonate precipitation of the magnesium-rich carbonate, dolomite. The dolomite present in the termitaria is of secondary origin, as evidenced by its co-occurrence with calcite and aragonite ($CaCO_3$), indicating a diagenetic or post-depositional formation process (Mehmood, 2018). This is distinct from primary dolomite ($CaMg(CO_3)_2$), which would typically occur as a pure mineral phase. The Calitzdorp and Groenefontein ichnosites demonstrated that biogenic and abiogenic carbonate precipitation processes were intertwined, with termite-mediated geochemical alterations and groundwater flux combining to produce the observed dolomite-rich carbonate assemblages.

Similarly, local Heuweltjies (Fig. 2.1 A), which are potentially of termite origin, are commonly preserved as carbonate-rich features within non-calcareous soils, where carbonate accumulation is often attributed to termite-mediated mineralisation processes (McAuliffe et al., 2014, 2019; Francis and Poch, 2019; Francis et al., 2022). Unlike the termitaria examined in this study, which contain both calcite and dolomite, Heuweltjies only contain calcite. This disparity suggests variations in carbonate precipitation processes. Notably, Heuweltjies, preserved as subaerial structures, may still contain carbonates linked to termite activity, warranting further investigation (e.g., termite-mediated biomineralisation; Potts et al., 2009; Francis and Poch, 2019) but differ from the subterranean termitaria in age, morphology, and preservation. Their subaerial preservation likely reduces the influence of groundwater on carbonate chemistry. Although exploring these differences is beyond this study's scope, the dolomite enrichment in the termitaria is unique and warrants further investigation.

The origin of the carbonates within the Calitzdorp area's fossil termitaria remains poorly understood but likely results from a complex interplay between abiogenic and biogenic processes. The carbonate-rich composition of these fossil structures aids in their hardness and resistance to weathering, thereby facilitating their preservation within the geological record.

5.2 Nutrient enrichment in the fossil termitaria

The fossil termitaria at both Calitzdorp and Groenefontein are geochemically different to their respective host palaeosols (PCS and CAL GR 2-H; Figs. 4.11, 4.12). The fossil termitaria exhibit enrichment in CaO, MgO, MnO, and P_2O_5 and depletion in Al_2O_3, Co, Cu, Fe_2O_3, K_2O, and Zn (Figs. 4.12, 4.13; Table 4.2). These enrichment patterns are consistent with observations in modern termitaria, where termitaria are often enriched in exchangeable base cations such as Ca^{2+}, Mg^{2+}, K^+, Na^+, and essential nutrients, including Mn and P, relative to the surrounding soils (e.g., Midgley and Musil, 1990; Brune and Kühl, 1996; Hopkins et al., 1998; Mahaney et al., 1999; Jouquet et al., 2004; Seymour et al., 2014; Singh et al., 2017; Mills and Sirami, 2018; Souza et al., 2020; Chen et al., 2021; Koné et al., 2022). The observed differences between the termitaria and PCS may suggest that termites played a biogeochemical role, potentially through the selective use of clays or fungus cultivation. However, the similarity in enrichment patterns across other carbonate-rich palaeosols, which the termitaria are not directly situated in (CAL 2.4, CALI H, and PCN), suggests that physical processes, such as groundwater movement, may also have contributed to the observed geochemical signatures.

Globally, modern and fossil termitaria exhibit significant variability in nutrient enrichment compared to their host soil (e.g., Mujinya et al., 2011; Singh et al., 2017). However, there are consistent geochemical trends across studies, such as high exchangeable base content, that offer valuable insights into termite behaviour and broader environmental dynamics, such as groundwater movement and nutrient cycling within these structures (Watson, 1974; Brune and Kühl, 1996; Hopkins et al., 1998; Holt and Lepage, 2000; Jouquet et al., 2004; Mujinya et al., 2013; Seymour et al., 2014; Singh et al., 2017; Mills and Sirami, 2018; Francis et al., 2022). The geochemistry of the fossil termitaria at Calitzdorp and Groenefontein shows notable similarities with modern termitaria from India and Tanzania, as they are all enriched in CaO, MgO, MnO, and P_2O_5 and depleted in Na_2O and SiO_2 (Fig. 5.1; Mahaney et al., 1999; Singh et al., 2017). However, the fossil termitaria in this study also deviate geochemically from modern termitaria around the world, including local *Amitermes hastatus* termitaria from Bainskloof. These modern termitaria are enriched in Al, Fe, K, Na and Ti (and corresponding oxides), while the fossil termitaria in this study are generally depleted in these elements, apart from minor Na_2O enrichment in the Calitzdorp termitaria.

The most significant distinction between our fossil termitaria and their respective host palaeosols is the pronounced enrichment in CaO (~20–72 wt.% vs. ~1–7 wt.%) and MgO (~9–15 wt.% vs. ~2 wt.%). This is due to the greater carbonate mineral proportion in the fossil termitaria relative to the host palaeosols (Figs. 4.1, 4.7; Table 4.1). A relatively high Ca and Mg content is also observed in local Heuweltjies (in Worcester; Fig. 2.1 A) and worldwide in modern termitaria (Figs. 5.1, 5.2; e.g., Midgley and Musil, 1990; Mahaney et al., 1999; Seymour et al., 2014) due to the high carbonate content in the features, contrasting their siliciclastic host palaeosols (Fig. 4.11; Table 4.2). In addition to the enrichment of CaO and MgO in all the termitaria, the Calitzdorp termitaria are also enriched in Na_2O. While the enrichment of CaO and MgO in the fossil termitaria is likely associated with the presence of carbonates that precipitate after the construction of the termitaria, the enrichment of CaO, MgO and Na_2O may also be directly linked to termite activity as termites typically enrich their termitaria with exchangeable bases from organic matter and frass (Lee and Wood, 1971; Watson, 1977; Lopez-Hernandez et al., 1986; Black and Okwakol, 1997; Brossard et al., 2007; Traoré and Jouquet, 2020). Termitaria are also generally enriched in Al, K and Ti (Singh et al., 2017). In modern termitaria, elevated Al and K are attributed to high clay content, while elevated amounts of Ti are associated with low silica content. In this study, however, the fossil termitaria have a marked depletion in Al_2O_3 and K_2O, enrichment in TiO_2, and an absence of identifiable clay or micaceous minerals. This pattern is unusual, given that termites generally concentrate fine-grained materials such as clays within their termitaria (e.g., Mills et al., 2009; Wang and Henderson, 2013; Janzow and Judd, 2015; Baig et al., 2018). However, it is important to differentiate between particle size and mineralogical composition: termites generally prefer fine-grained materials for construction, but these may not always be composed of clay minerals, and could instead reflect the local lithology. While the absence of clay minerals may be expected in the Calitzdorp termitaria, aligning with the sandy nature of the palaeosol, it is particularly surprising at Groenefontein, where kaolinite, a clay-forming mineral, is readily available in the host palaeosol (Figs. 4.1, 4.7; Table 4.2; Holt and Lepage, 2000; Jouquet et al., 2016; Oberst et al., 2020). In modern termitaria, elevated P is linked to a high pH and organic matter, suggesting a more alkaline environment and organic-rich termitaria (Wood, 1988; Brauman, 2000; Chen et al., 2021). There is a minor enrichment of P_2O_5 in the Calitzdorp and Groenefontein fossil termitaria compared to the palaeosol (~0.2–0.5 wt.% vs. 0.1–0.3 wt.%; Fig. 5.1), which may also reflect the chemistry of organic materials

in the active termitaria that were subsequently preserved. Enrichment of Mn within fossil termitaria is often linked to frass, decomposition of the termites themselves and organic matter, which may include fungi (Mills et al., 2009; Muwawa et al., 2014; Koné et al., 2022). Though Fe and trace elements are often enriched by deep-soil mining (Mills et al., 2009; Sako et al., 2009; Stewart et al., 2012; Singh et al., 2017; Eze et al., 2020; Ngoy et al., 2023), they are not significantly enriched within the Calitzdorp and Groenefontein fossil termitaria, suggesting nonselective material use by ancient termites or geochemical alteration.

While the Calitzdorp and Groenefontein fossil termitaria share similar geochemical compositions relative to their host palaeosols, they exhibit subtle differences in nutrient enrichment and depletion, with the Groenefontein fossil termitaria having more pronounced enrichment or depletion (Figs. 4.11, 4.12). This may be due to:

1) *Mineral composition:* The difference in mineralogy between the host palaeosol and fossil termitaria. At the Calitzdorp ichnosite, both the fossil termitaria and host palaeosols contain carbonate minerals (13–26 wt.% vs 3–65 wt.%), with the fossil termitaria containing both dolomite and calcite carbonates, whereas the palaeosol only contains calcite. Contrastingly, at the Groenefontein ichnosite, the fossil termitaria comprise between 53–75 wt.% total carbonate (20–55 wt.% calcite, 12–33 wt.% dolomite, and 12 wt.% aragonite), while the host palaeosol contains no carbonate (Fig. 4.7; Table 4.1).
2) *Duration of inhabitation:* Termitaria, which are inhabited for longer, tend to show higher nutrient content relative to host soils due to extended periods of nutrient cycling (Seymour et al., 2014). The greater nutrient enrichment in the fossil termitaria at Groenefontein may potentially indicate that the original termitaria remained active for longer than those at Calitzdorp. Unfortunately, it is not possible to determine the duration of inhabitation within the termitaria for fossil material. Investigations into the morphology and clustering of fossil termitaria can provide insights into this, but are beyond the scope of this project. Furthermore, factors related to preservation can warp these interpretations.

While geochemical studies of modern termitaria can definitively demonstrate nutrient differences between the soils and termitaria, there are limitations to interpreting these differences for fossil termitaria. These limitations include:

1) *Impact of post-construction calcretisation:* The fossil termitaria contain high proportions of carbonate minerals, which have aided their preservation. These carbonate minerals likely precipitated long after the construction of the termitaria. This post-construction alteration to the mineralogy of the termitaria, in turn, affected their original geochemical signature.
2) *Unspecified termite species:* the species of the tracemaker can be informative about certain behaviours (like fungus culturing), in addition to the geochemical data (like marked Mn enrichment), which would help refine the interpretations made here; however, there are presently no body fossils or fungus culturing evidence preserved.

The fossil termitaria at Calitzdorp and Groenefontein exhibit enrichment and depletion patterns relative to their host palaeosols that are consistent with modern termitaria (Fig. 4.12; Table 4.2; e.g., Midgley and Musil, 1990; Mahaney et al., 1999; Seymour et al., 2014; Singh et al., 2017). However, there are deviations. The post-construction carbonate mineral precipitation within the fossil termitaria influences the geochemical signatures of the fossil termitaria, but tentative interpretations may be made: the enrichment of MnO and P_2O_5 at both ichnosites and Na_2O enrichment at the Calitzdorp ichnosite can be linked to the active role of termites in termitaria construction.

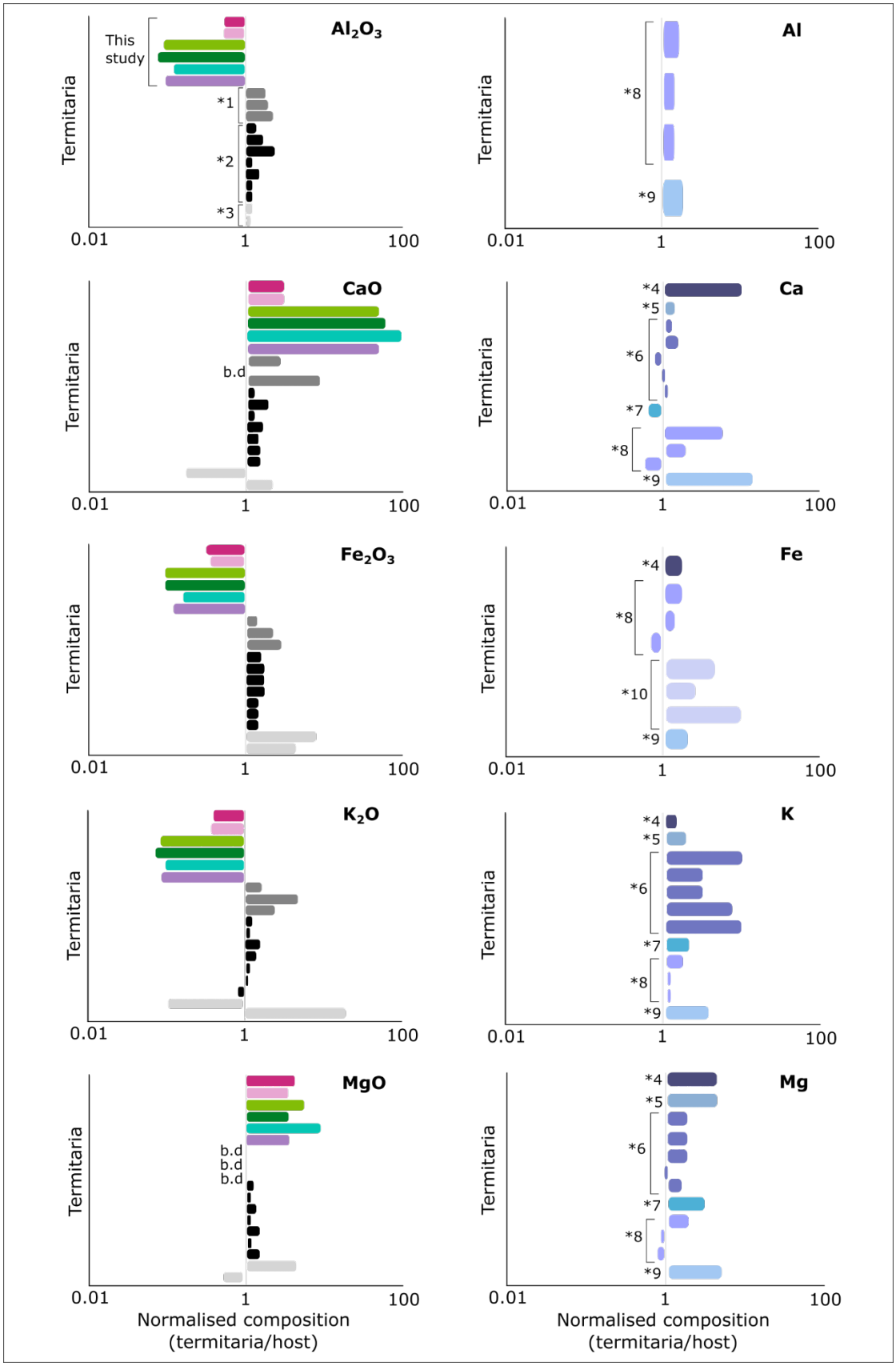
Al2O3
This study
*1
*2
*3
Al
*8
*9
CaO
b.d
Ca
*4
*5
*6
*7
*8
*9
Fe2O3
Fe
*10
K2O
K
MgO
Mg
Termitaria
0.01
1
100
Normalised composition
(termitaria/host)

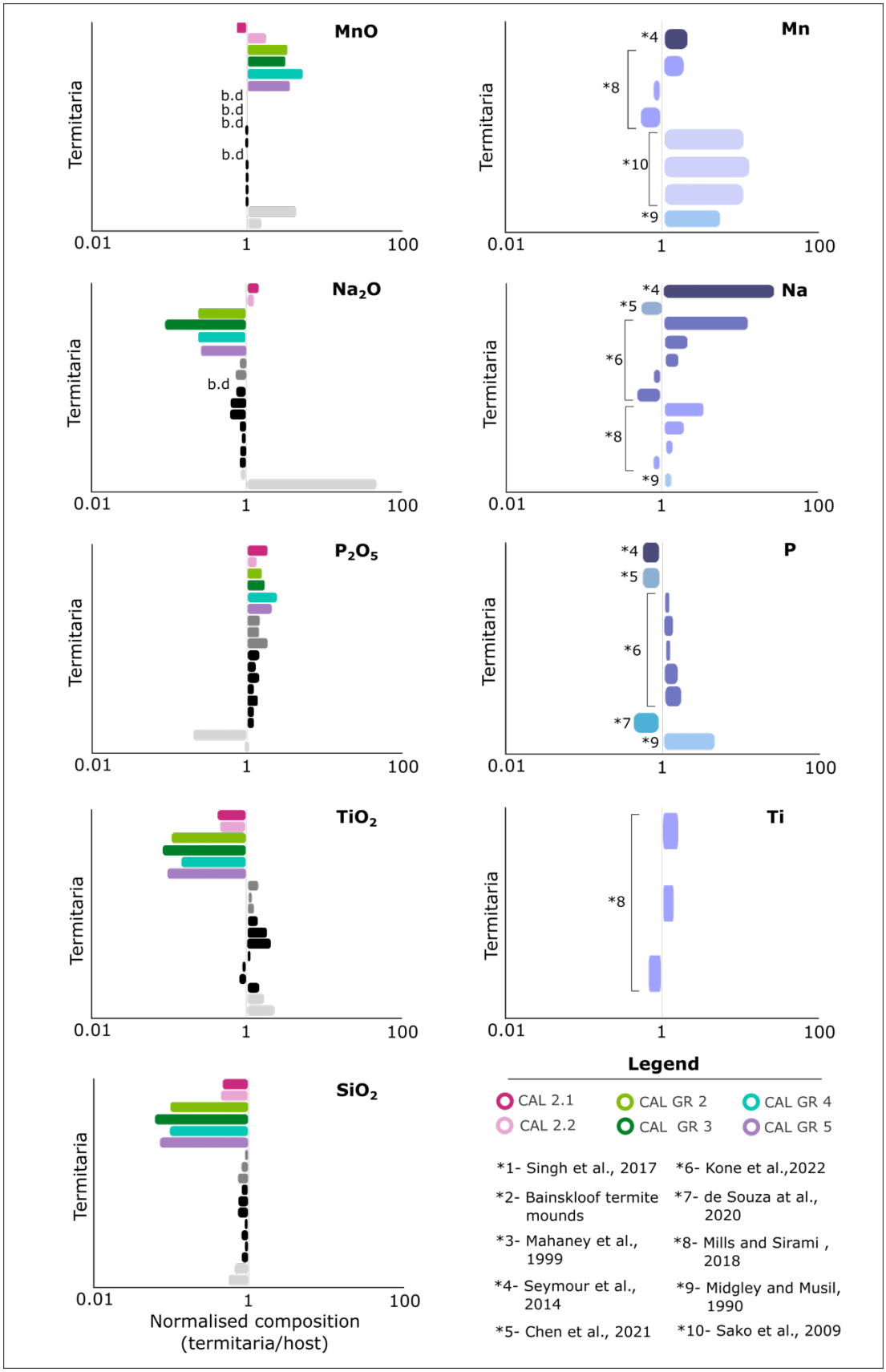

Figure 5.1 Major element proportions of fossil and modern termitaria relative to their host palaeosol or soils. Values <1 indicate depletion in the termitaria, and values >1 indicate enrichment.

5.3 Palaeoclimate

The fossil termitaria from the Calitzdorp area provide a unique record of palaeoclimatic conditions in the southern Cape during the Quaternary, offering insights into both the prevailing vegetation and climate through their carbonate mineral composition and isotopic signatures. This discussion explores termite mounds as palaeoclimate indicators by analysing their mineral composition and stable isotope data to infer past vegetation, temperature, and precipitation conditions in the Calitzdorp region.

The fossil termitaria in the Calitzdorp area are characterised by a high proportion of carbonate minerals within their structure (Fig. 4.1; Table 4.1), providing a valuable proxy for reconstructing palaeoclimatic conditions. These carbonates are pedogenic in origin, particularly evident at the Calitzdorp ichnosite, which preserves a range of morphological forms of pedogenic carbonates within the host palaeosol (Fig. 2.1 C; Hadebe, 2021). The occurrence of pedogenic carbonates in both the fossil termitaria and the surrounding palaeosols indicates semi-arid to arid environmental conditions (Wright and Tucker, 2009; Alonso-Zarza, 2003; Candy and Black, 2009; Gocke and Kuzyakov, 2011). The $\delta^{13}C$ values of the carbonates in the fossil termitaria range from -0.69‰ to 7.19‰ and indicate the presence of both C_3 and C_4 vegetation on the palaeolandscape. This mixed C_3/C_4 signal indicates that the climate was suitable for maintaining vegetation with different environmental requirements and within the local context of the southern Cape. The Calitzdorp area falls within a biogeographical zone of mixed C_3 and C_4 vegetation, strongly associated with year-round rainfall, receiving approximately 205–239 mm annually and classifying the region as semi-arid (Vogel et al., 1978; Cowling, 1983; Chase and Meadows, 2007; Holzapfel, 2008; Abatzoglou et al., 2018). The coupling of rainfall zones (i.e., SRZ, WRZ, and YRZ) and vegetation within South Africa likely persisted throughout the Quaternary, with minor spatial shifts. While year-round rainfall may have prevailed during the Middle Pleistocene, as suggested by the mixed C_3 and C_4 vegetation signal at the Calitzdorp ichnosite, it was likely low enough to support the formation of pedogenic carbonates in the termitaria.

Although the Calitzdorp and Groenefontein ichnosites are only 12 km apart (Fig. 2.1 B), the fossil termitaria at Calitzdorp have, on average, higher $\delta^{13}C$ values (-0.79 to -0.69‰ vs.-7.19

to -1.56‰) and therefore a stronger C_4 signal than those from Groenefontein (Fig. 4.13; Table 4.3). These differences in isotopic signals, including the distinct signature of fossil termitaria at Groenefontein (Figs. 4.8, 4.13; Table 4.3), may be attributed to:

1) *Timing of carbonate precipitation:* The $\delta^{13}C$ values of carbonates in the fossil termitaria indicate the prevailing vegetation at the time of carbonate precipitation (Meyer et al., 2014; Licht et al., 2014). The overlapping signature of the Calitzdorp fossil termitaria and their host palaeosol may be due to the clustered fossil termitaria and palaeosol carbonate precipitation occurring at the same time, around 320 ka. The more dispersed fossil termitaria at Groenefontein may contain carbonates that precipitated at different times, with CAL GR 2, which coincides with the signatures of fossil termitaria at Calitzdorp potentially containing carbonate that also precipitated ~320 ka (Figs. 2.1, 4.13). Potential climate variation during the Quaternary may have influenced the dominant vegetation types, thereby affecting the groupings of the $\delta^{13}C$ values (Walker, 1990; Talma and Vogel, 1992; Petit et al., 1999; Hewitt, 2000; Chase and Meadows, 2007; Bar-Matthews et al., 2010; Grobler et al., 2020; Mohale et al., 2022). The climate variation is more likely responsible for the variation in vegetation, as minor spatial differences between termitaria within or between the ichnosites (0.05–12 km) would not account for vegetation differences observed at approximately 320 ka.
2) *The porosity of the host palaeosols*: The lower water uptake efficiency of C_3 vegetation compared to C_4 vegetation may explain the distribution of vegetation types at the Groenefontein and Calitzdorp ichnosites (Hura et al., 2007; Leegood, 2013; Cui, 2021). The host palaeosol at Groenefontein, consisting of fine-grained sands and muds, likely had higher water retention than the more coarse, medium-grained sands at Calitzdorp, which may have favoured C_4 vegetation over the C_3-dominated vegetation at Groenefontein (Yu et al., 1993). The coarser sands at the Calitzdorp ichnosite may have retained less water and would have been more suitable for C_4 vegetation, which thrives in water-stressed conditions (Sage et al., 1999; Sharp, 2017). Therefore, the palaeosols' varying water retention capacities could have influenced the vegetation distinction between the Groenefontein and Calitzdorp ichnosites.
3) *Elevation:* The Calitzdorp ichnosite is at ~80 m lower than Groenefontein. The growth of C_3 vegetation is generally favoured at higher altitudes, where cooler temperatures and increased moisture availability create more suitable conditions (Tieszen et al., 1979;

Rundel, 1980; Cowling, 1983; Cavagnaro, 1988; Masrahi et al., 2011). However, the 80 m elevation difference between Groenefontein and the Calitzdorp ichnosite is unlikely to cause significant vegetation changes; factors like soil composition and water availability likely played a more significant role in the dominance of C_3 vegetation at Groenefontein.

Differences in palaeosol porosity and elevation may partially explain the varying $\delta^{13}C$ values between Calitzdorp and Groenefontein. However, the timing of carbonate precipitation must also be considered. Although dating the fossil termitaria is beyond the scope of this project, it is part of ongoing research. If carbonate precipitation occurred at different times, these findings may reflect changes in Quaternary vegetation and climate in the Calitzdorp area.

The $\delta^{18}O$ values of the carbonates are significantly influenced by the $\delta^{18}O$ signature of the soil water from which they precipitate (Talma and Netterberg, 1983; Dworkin et al., 2005; Jolivet and Boulvais, 2021). The carbonates in the fossil termitaria at both sites are largely overlapping and range from 26 to 33‰ (Fig. 4.6; Tables 4.3, 4.4). Given the overlap in $\delta^{18}O$ values between the two ichnosites, it is possible that the groundwater source had similar $\delta^{18}O$ values if the carbonates precipitated during the same period. However, if the carbonates precipitated at different times, the comparable $\delta^{18}O$ values could instead reflect similar environmental conditions during both periods of carbonate formation.

The temperature of the soil water from which the carbonates at both ichnosites precipitated is unknown. This means that the $\delta^{18}O$ values of the carbonates cannot be used directly to estimate their temperature of formation. The temperature of the carbonate formation has been calculated for different water $\delta^{18}O$ values to estimate a reasonable temperature range (+3 to -3‰; Table 5.1; Appendix Table 1). The fractionation factor (α) between dolomite and water was calculated using the $\delta^{18}O$ values of all carbonate samples using the equation $\alpha\ \delta^{18}O\text{-water} = (1000 + \delta^{18}O\text{-carbonate})/(1000 + \delta^{18}O\text{-water})$. The value of α determined for each sample was used to calculate temperature with the following equation:

$$10^3 \ln \alpha_{\text{carbonate-water}} = 0.3140(\pm 0.022) \times \frac{10^6}{T^2} - 3.14(\pm 0.11)$$ (Horita, 2014).

The values of water between -1 and 3‰ generated the highest proportion of plausible temperature estimates, comparable to the modern historical temperature range in Calitzdorp (Abatzoglou et al., 2018; Table 5.1; Appendix Table 1). To encompass the full range of possible temperatures, we considered a slightly broader range of 10–35 °C. The mean temperatures derived from water $\delta^{18}O$ values between -1 and 3‰ spanned 15–34 °C. Water $\delta^{18}O$ values between 0 and +1 yielded the most likely temperature distribution, with ~98% of the data falling within 10–35 °C. Furthermore, water $\delta^{18}O$ values between 1 and 2‰ produced temperature estimates that were consistently warm, with 89–95% of values concentrated between 20–35 °C. The calculated temperatures suggest conditions similar to, or slightly warmer than, the present day, implying a warm climate regime (Abatzoglou et al., 2018). These estimates exceed modern-day groundwater temperatures in the region, inferred from Gamkaberg $\delta^{18}O$ values of -3.4‰ (Diamond and Harris, 2019). The 4–5‰ discrepancy in $\delta^{18}O$ values between fossil termitaria carbonates (~1–2‰) and modern-day groundwater (-3.4‰) can be attributed to various environmental factors. However, evaporation of water from the termitaria before secondary dolomite precipitation provides a plausible explanation, enriching the remaining water in ^{18}O and resulting in relatively higher $\delta^{18}O$ values.

The warm environmental temperature (concentrated between 20-35°C) calculated from the $\delta^{18}O$ values is supported by the contrasting geochemistry between host palaeosol and fossil termitaria (Figs. 4.1, 4.7, 4.12; Tables 4.1, 4.2). Additionally, in the absence of sufficient rainfall, the nutrients will not be leached, and the geochemical contrast between the host palaeosol and fossil termitaria can be preserved over time (Booi, 2011; Francis and Poch, 2019; Francis et al., 2022). This preservation is evident in our study, where the fossil termitaria exhibit different geochemical signatures compared to their host yet are similar to each other (Figs. 4.11, 4.12; Table 4.2). This implies that the study region did not receive large amounts of rainfall, allowing for the preservation of the geochemical gradient between host palaeosol and fossil termitaria. Furthermore, the subterranean position of the fossil termitaria indicates a possible adaptation to unfavourable environmental conditions (i.e., extreme temperature or aridity), despite termite activity predating the calcretisation of the fossil termitaria (Turner et al., 2006). Faunal species which burrow or construct subterranean termitaria are protected from harsh environmental changes (Sankovitz and Purcell, 2021; Parr and Bishop, 2022). Under relatively warm and dry environmental conditions, the ancient termites may have

resorted to the cool and moist conditions provided by their subterranean shelters. These findings collectively suggest that warm, semi-arid conditions, characterised by limited (perennial) precipitation, prevailed in the study area, which possibly extended into the period in which the ancient termites constructed and occupied the fossil termitaria.

The $\delta^{13}C$ and $\delta^{18}O$ values of carbonates in this study overlap primarily with the Heuweltjie carbonates, with $\delta^{13}C$ values between 0 and -10‰ and $\delta^{18}O$ values from approximately 26 to 34‰ (Fig. 5.2; Table 4.3; Potts et al., 2009). There is also some overlap with carbonates that are not linked to termite activity, including speleothem deposits from the Western Cape, Gauteng, and Limpopo, as well as calcretes from the Northern Cape (Talma and Netterberg, 1983; Hopley et al., 2009; Chase et al., 2021). However, unlike other carbonate groups in South Africa, which span a broader range of generally higher $\delta^{13}C$ and lower $\delta^{18}O$ values, our termitaria carbonates do not extend into these isotopic ranges (i.e., $\delta^{13}C$ values of -15 to 12‰ and $\delta^{18}O$ values of 8 to 38‰; Talma and Netterberg, 1983; Ringrose et al., 2009; Frauenstein et al., 2009; Mthembi et al., 2016). This difference suggests that, unlike the other calcretes that may reflect even more arid conditions or speleothems associated with specific hydrological settings, termitaria carbonates form under more localised or biologically influenced conditions that align closely with Heuweltjies, which are reported to have similar biological influence from termite activity. The restricted isotopic range in $\delta^{13}C$ and relatively high $\delta^{18}O$ values in termitaria carbonates underscore the influence of termite-driven processes and localised environmental factors distinct from broader South African carbonate formations. Although these carbonates are all sourced from Southern Africa and serve to contextualise the termitaria carbonates within a broader geographical framework, they originate from different processes. Therefore, no direct inferences or comparisons regarding Quaternary climate can be made due to their varying ages.

Table 5.1 Summary table of the temperatures estimated from $\delta^{18}O$ values of the carbonates in the termitaria at Calitzdorp and Groenefontein. (See Appendix Table 1 for full details).

Sample	$\delta^{18}O$	α 3	Temp. °C	α 2	Temp. °C	α 1	Temp. °C	α 0	Temp. °C	α -1	Temp. °C	α -2	Temp. °C	α -3	Temp. °C
CAL 2.1	30.56	1.0275	31.49	1.0285	26.56	1.0295	21.84	1.0306	17.33	1.0316	13.02	1.0326	8.89	1.0337	4.96
CAL 2.2	29.78	1.0267	35.47	1.0277	30.33	1.0287	25.43	1.0298	20.76	1.0308	16.31	1.0318	12.04	1.0329	7.96
CAL GR 2	28.77	1.0257	40.65	1.0267	35.26	1.0277	30.14	1.0288	25.26	1.0298	20.58	1.0308	16.14	1.0319	11.86
CAL GR 3	30.29	1.0268	33.13	1.0279	28.10	1.0289	23.31	1.0299	18.74	1.0310	14.36	1.0320	10.16	1.0330	6.15
CAL GR 4	30.32	1.0272	32.63	1.0283	27.62	1.0293	22.85	1.0303	18.33	1.0314	13.95	1.0324	9.80	1.0334	5.8
CAL GR 5	31.15	1.0281	28.58	1.0291	23.78	1.0301	19.18	1.0312	14.78	1.0322	10.6	1.0332	6.58	1.0343	2.73
Average:	30.14	1.0270	33.66	1.0280	28.61	1.0291	23.79	1.0301	19.20	1.0311	14.80	1.0322	10.60	1.0332	6.58
Average temp.			**34.4**		**29.3**		**24.4**		**19.8**		**15.4**		**11.2**		**7.1**
% of values with temps. between 10–35 °C			**64%**		**83%**		**97%**		**98%**		**95%**		**51%**		**27%**

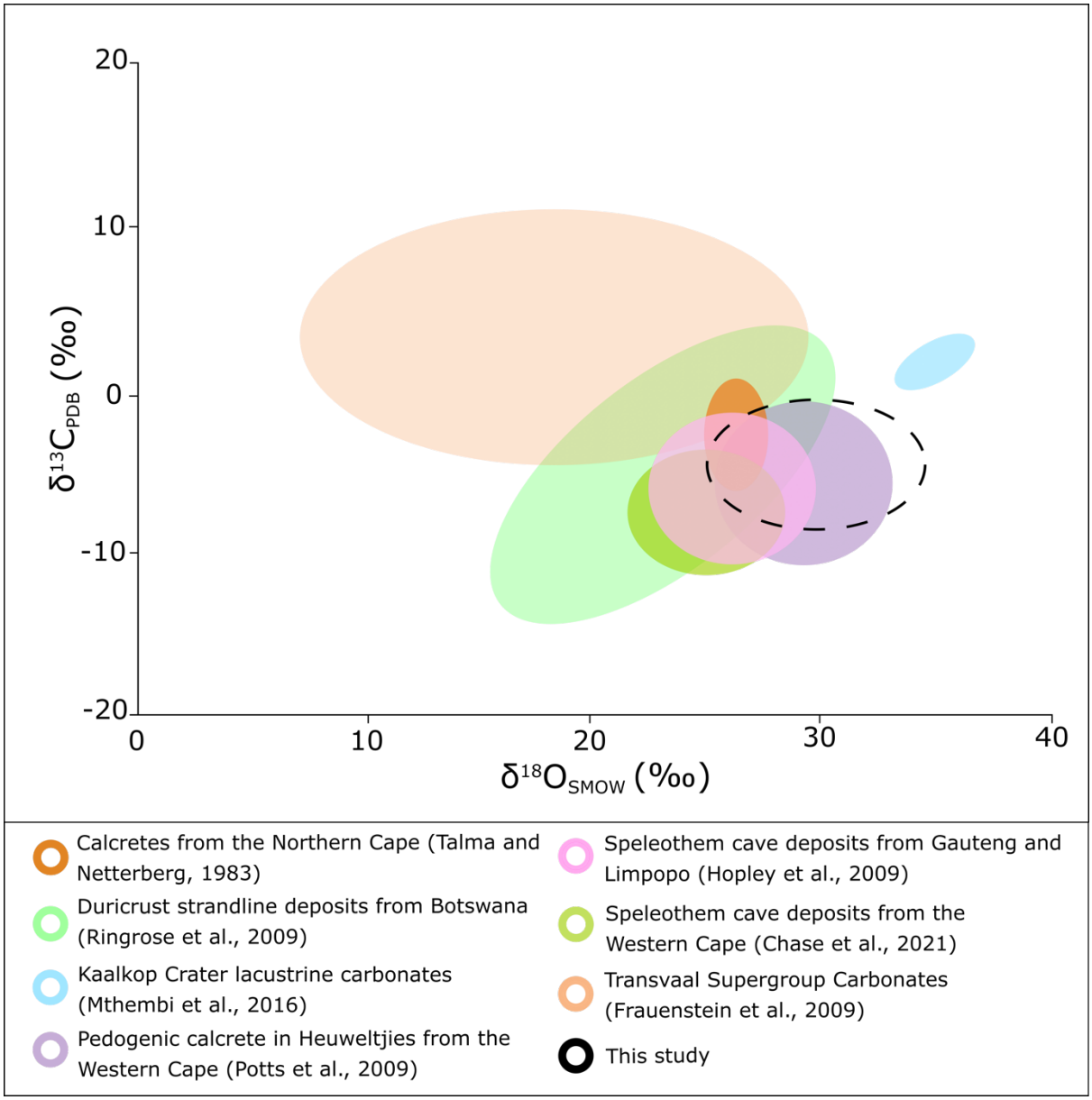

Figure 5.2 The $\delta^{13}C$ vs. $\delta^{18}O$ values of carbonates from across southern Africa relative to the fossil termitaria carbonates from the Calitzdorp and Groenefontein ichnosites in this study.

The palaeoclimate of the southern Cape during the Pleistocene is subject to ongoing debate, with various records presenting contrasting interpretations. While some studies indicate cooler conditions during this period (Bar-Matthews et al., 2010; Eze, 2013; Dupont et al., 2022), others suggest that the middle to late Pleistocene experienced warmer and drier conditions, characterised by the expansion of C_4 grasses and higher interglacial sea levels (Henshilwood, 2008; Quick et al., 2015; Compton, 2016; Braun et al., 2020; Dupont et al., 2022; Strobel et al., 2022). The variability can be attributed to the region's complex climatic dynamics, influenced by contrasting oceanic and atmospheric currents (Rogers, 1988; Walker,

1990; Hare and Sealy, 2013; Strobel et al., 2022). Other palaeoclimate records, which cover a similar period and location relative to the carbonates in this study, are the terrestrial (~263 ka) and offshore sediment cores (~300 ka) from the southern Cape coast (Hahn et al., 2017; Strobel et al., 2022). These records suggest that arid conditions, marked by the cessation of major flood events and reduced rainfall, prevailed during the late Pleistocene. Furthermore, this study's findings of a mixed C_3/C_4 signal are consistent with the speleothem record from Pinnacle Point (~50 km south of Calitzdorp), which also suggests a year-round rainfall regime during the Pleistocene (Braun et al., 2019). These regional palaeoclimate patterns suggest a fluctuating yet warm and dry climate characterised by semi-arid conditions and mixed C_3/C_4 vegetation supported by year-round rainfall. This aligns with the interpretation that Calitzdorp experienced similar conditions during the Pleistocene, with perennial but limited rainfall sustaining both C_3 and C_4 plants. While the literature exhibits variability in its interpretation of the southern Cape's Pleistocene climate, our findings are consistent with much of the evidence indicating warm, dry conditions with limited year-round rainfall during the Quaternary.

Conclusion

The Quaternary fossilised termitaria near Calitzdorp have enhanced our understanding of nutrient enrichment and material selectivity in these fossil termitaria and offered insights into Quaternary palaeoenvironmental conditions in the southern Cape, where climate proxy data is sparse. Based on the geochemical assessment of six fossil termitaria, the following deductions can be made:

1. The fossil termitaria are preferentially calcretised, and where their host palaeosols are calcretised, too, the carbonate content of the termitaria and soil is distinct. Dolomite is only preserved in the fossil termitaria and was likely aided by high initial inputs of magnesium-rich organic matter and frass deposited by the ancient termites.

2. The geochemical signature of the termitaria exhibits a strong influence from termite activity and is distinct from their host palaeosols. Although the two ichnosites have different palaeosols, i.e., one with pedogenic carbonate and one without, the geochemistry between the termitaria relative to their host palaeosols is nearly indistinguishable.

3. At the time of carbonate precipitation, a warm, dry climate with palaeotemperatures ranging from approximately 20 to 35°C persisted. Furthermore, the climate was characterised by consistent but limited year-round rainfall.

This research offers significant contributions to the palaeoenvironmental understanding of the southern Cape during the Quaternary and provides novel geochemical insights into fossil termitaria, furthering our knowledge of termite-driven biogeochemical processes and their implications for palaeoenvironmental reconstructions in South Africa's distinctive biogeographical context. Although these findings are significant and greatly contribute to our understanding, they have also left us with questions that require additional pursuit. Future avenues of research include:

1. Radiometric dating of the Groenefontein termitaria. These termitaria have distinct stable isotope signatures, one of which was similar to the termitaria of Calitzdorp.

Radiometric dates could indicate whether these distinct groupings show climate variability through time.

2. Further investigation into the dolomite content in termitaria. Dolomite is uniquely present in the termitaria; therefore, increasing the sample size of the termitaria analysed can help to validate this observation.

References

Abatzoglou, J.T., Dobrowski, S.Z., Parks, S.A. & Hegewisch, K.C. 2018. TerraClimate, a high-resolution global dataset of monthly climate and climatic water balance from 1958–2015. *Scientific Data*, 5, 170191.

Abe, T., Bignell, D.E. & Higashi, M. 2000. *Termites: Evolution, Sociality, Symbioses, Ecology*. Springer Science & Business Media, 498.

Abe, S.S., Watanabe, Y., Onishi, T., Kotegawa, T. & Wakatsuki, T. 2011. Nutrient storage in termite (*Macrotermes bellicosus*) mounds and the implications for nutrient dynamics in a tropical savanna Ultisol. *Soil Science and Plant Nutrition* 57, 795.

Adeyeye, E. 2005. The composition of the winged termite (*Macrotermes bellicosus*). *Journal of Chemical Society of Nigeria* 30: 145–249.

Al-Aasm, I.S., Taylor, B.E. & South, B. 1990. Stable isotope analysis of multiple carbonate samples using selective acid extraction. *Chemical Geology: Isotope Geoscience Section*, 80, 125.

Almond, J. 2005. Geology of the Gamkaberg-Rooiberg Conservation Area, Little Karoo. Cape Nature, Cape Town, Natura Viva cc, 65. Unpublished report.

Alonso-Zarza, A.M. 2003. Palaeoenvironmental significance of palustrine carbonates and calcretes in the geological record. *Earth-Science Reviews*, 60, 298.

Alonso-Zarza, A.M. & Wright, V.P. 2010. Chapter 5 Calcretes. In: A.M. Alonso-Zarza & L.H. Tanner (Eds.), *Developments in Sedimentology. Carbonates in Continental Settings: Facies, Environments, and Processes*. Elsevier, 267.

Arshad, M.A. 1981. Physical and chemical properties of termite mounds of two species of Macrotermes (*Isoptera, Termitidae*) and the surrounding soils of semiarid Kenya. *Soil Science* 132, 174.

Asawalam, D.O., Osodeke, V.E., Kamalu, O.J. & Ugwa, I.K. 1999. Effects of termites on the physical and chemical properties of the acid sandy soils of southern Nigeria. *Communications in Soil Science and Plant Analysis*, 30, 1696.

Avery, D.M. 2001. The Plio-Pleistocene vegetation and climate of Sterkfontein and Swartkrans, South Africa, based on micromammals. *Journal of Human Evolution*, 41, 132.

Badawy, H.S. 2018. Termite nests, rhizoliths and pedotypes of the Oligocene fluviomarine rock sequence in northern Egypt: Proxies for Tethyan tropical palaeoclimates. *Palaeogeography, Palaeoclimatology, Palaeoecology*, 492, 176.

Backwell, L., Huchet, J.-B., Jashashvili, T., Dirks, P.H.G.M. & Berger, L.R. 2020. Termites and necrophagous insects associated with early Pleistocene (Gelasian) *Australopithecus sediba* at Malapa, South Africa. *Palaeogeography, Palaeoclimatology, Palaeoecology*, 560, 109989.

Baig, M.M., Rout, A., Sinha, A., Pandiaraj, T.P., Sinku, C. & Singh, G. 2018. Evaluation of nutrient status in termite mounds and adjacent soils associated with tasar sericulture ecosystem. *Journal Name or Conference Proceedings,* 6, 210.

Bar-Matthews, M., Marean, C.W., Jacobs, Z., Karkanas, P., Fisher, E.C., Herries, A.I.R., Brown, K., Williams, H.M., Bernatchez, J., Ayalon, A. & Nilssen, P.J. 2010. A high-resolution and continuous isotopic speleothem record of paleoclimate and paleoenvironment from 90 to 53 ka from Pinnacle Point on the south coast of South Africa. *Quaternary Science Reviews*, 29, 2145.

Bennett, K.D. 1997. *Evolution and Ecology: The Pace of Life*. Cambridge University Press, 272.

Bera, D., Bera, S. & Chatterjee, N.D. 2020. Termite mound soil properties in West Bengal, India. *Geoderma Regional*, 22, e00293.

Bezerra, F.I., DeSouza, O., Ribeiro, G.C. & Mendes, M. 2021. A new primitive termite (*Isoptera*) from the Crato Formation, Araripe Basin, Early Cretaceous of South America. *Journal of South American Earth Sciences*, 109, 260.

Black, H.I.J. & Okwakol, M.J.N. 1997. Agricultural intensification, soil biodiversity and agroecosystem function in the tropics: the role of termites. *Applied Soil Ecology*, 6, 37–53.

Booi, N. 2011. Structure and function of heuweltjies across a rainfall gradient in the South-Western Cape. (Unpublished Doctoral dissertation, Stellenbosch: University of Stellenbosch).

Bordy, E.M., Bumby, A.J., Catuneanu, O. & Eriksson, P.G. 2004. Advanced Early Jurassic termite (Insecta*: Isoptera*) nests: Evidence from the Clarens Formation in the Tuli Basin, Southern Africa. *Palaios*, 19, 78.

Bown, T.M. & Laza, J.H. 1990. A Miocene termite nest from southern Argentina and its paleoclimatological implications. *Ichnos: An International Journal for Plant and Animal Traces*, 1, 79.

Brauman, A. 2000. Effect of gut transit and mound deposit on soil organic matter transformations in the soil-feeding termite: A review. *European Journal of Soil Biology,* 36, 125.

Braun, K., Bar-Matthews, M., Matthews, A., Ayalon, A., Cowling, R.M., Karkanas, P., Fisher, E.C., Dyez, K., Zilberman, T. & Marean, C.W. 2019. Late Pleistocene records of speleothem stable isotopic compositions from Pinnacle Point on the South African south coast. *Quaternary Research,* 91, 288.

Braun, K., Bar-Matthews, M., Matthews, A., Ayalon, A., Zilberman, T., Cowling, R.M., Fisher, E.C., Herries, A.I.R., Brink, J.S. & Marean, C.W. 2020. Comparison of climate and environment

on the edge of the Palaeo-Agulhas Plain to the Little Karoo (South Africa) in Marine Isotope Stages 5–3 as indicated by speleothems. *Quaternary Science Reviews*, 235, 105803.

Brossard, M., López-Hernández, D., Lepage, M. & Leprun, J.-C. 2007. Nutrient storage in soils and nests of mound-building *Trinervitermes* termites in Central Burkina Faso. *Biology and Fertility of Soils,* 43, 447.

Bruch, A.A., Sievers, C. & Wadley, L. 2012. Quantification of climate and vegetation from southern African Middle Stone Age sites – an application using Late Pleistocene plant material from Sibudu, South Africa. *Quaternary Science Reviews,* 45, 17.

Brune, A. & Kühl, M. 1996. pH profiles of the extremely alkaline hindguts of soil-feeding termites (*Isoptera: Termitidae*) determined with microelectrodes. *Journal of Insect Physiology*, 42, 1127.

Bustillo, M.A. and Alonso-Zarza, A.M. 2007. Overlapping of pedogenesis and meteoric diagenesis in distal alluvial and shallow lacustrine deposits in the Madrid Miocene Basin, Spain. *Sedimentary Geology*, 198, 271.

Candy, I. & Black, S. 2009. The timing of Quaternary calcrete development in semi-arid southeast Spain: Investigating the role of climate on calcrete genesis. *Sedimentary Geology*, 218, 15.

Castañeda, I.S., Caley, T., Dupont, L., Kim, J.-H., Malaizé, B. & Schouten, S. 2016. Middle to Late Pleistocene vegetation and climate change in subtropical southern East Africa. *Earth and Planetary Science Letters*, 450, 316.

Cavagnaro, J.B. 1988. Distribution of C_3 and C_4 grasses at different altitudes in a temperate arid region of Argentina. *Oecologia*, 76, 277.

Cawthra, H.C. & Bateman, M.D. 2016. Sandy coasts. In: Knight, J. & Grab, S.W. (Eds.), *Quaternary Environmental Change in Southern Africa: Physical and Human Dimensions*. Cambridge University Press, 218.

Cerling, T.E. 1984. The stable isotopic composition of modern soil carbonate and its relationship to climate. *Earth and Planetary Science Letters*, 71, 240.

Cerling, T.E. 1999. Paleorecords of C_4 plants and ecosystems. In: *C_4 Plant Biology*, 469.

Cerling, T.E., Quade, J., Wang, Y. & Bowman, J.R. 1989. Carbon isotopes in soils and palaeosols as ecology and palaeoecology indicators. Nature, 341, 139.

Chase, B., Harris, C., De Wit, M.J., Kramers, J., Doel, S. & Stankiewicz, J. 2021. South African speleothems reveal influence of high- and low-latitude forcing over the past 113.5 k.y. Geology, 49, 1357.

Chase, B.M. & Meadows, M.E. 2007. Late Quaternary dynamics of southern Africa's winter rainfall zone. *Earth-Science Reviews*, 84, 138.

Chen, C., Zou, X., Wu, J., Zhu, X., Jiang, X., Zhang, W., Zeng, H. & Liu, W. 2021. Accumulation and spatial homogeneity of nutrients within *Odontotermes yunnanensis* mounds in the Xishuangbanna region, SW China. *Catena*, 198, 105057.

Coaton, W.G.H. 1981. Fossilised nests of *Hodotermitidae* (*Isoptera*) from the Clanwilliam district, Cape Province. Journal of the Entomological Society of Southern Africa, 44, 79–81.

Compton, J.S. 2016. Quaternary environmental change on the southern African coastal plain. In: Knight, J. & Grab, S.W. (Eds.), *Quaternary Environmental Change in Southern Africa: Physical and Human Dimensions*. Cambridge University Press, 98.

Coope, G.R., Wilkins, A.S., Lawton, J.H. & May, R.M. 1997. The response of insect faunas to glacial-interglacial climatic fluctuations. *Philosophical Transactions of the Royal Society of London, Series B: Biological Sciences*, 344, 26.

Cooper, J.A.G., Green, A.N. & Compton, J.S. 2018. Sea-level change in southern Africa since the Last Glacial Maximum. *Quaternary Science Reviews*, 201, 318.

Cowling, R.M. 1983. The occurrence of C_3 and C_4 grasses in fynbos and allied shrublands in the South Eastern Cape, South Africa. *Oecologia*, 58, 127.

Crossley, R., 2022. Fossil termite mounds associated with stone artefacts in Malawi, Central Africa. In: *Palaeoecology of Africa*, 16, 401. Routledge.

Cui, H. 2021. Challenges and approaches to crop improvement through C_3-to-C_4 engineering. *Frontiers in Plant Science*, 12, 715391.

Dansgaard, W. 1964. Stable isotopes in precipitation. *Tellus*, 16, 468.

De Bruyn, L. & Conacher, A. 1990. The role of termites and ants in soil modification - a review. *Soil Research*, 28, 55.

Deacon, H.J. 1983. Another look at the Pleistocene climates of South Africa. *South African Journal of Science*, 79, 328.

Deer, W.A., Howie, R.A. & Zussman, J., 2009. *An Introduction to the Rock-Forming Minerals. Pearson/Prentice Hall*, Harlow, 696.

deMenocal, P.B. 2004. African climate change and faunal evolution during the Pliocene–Pleistocene. *Earth and Planetary Science Letters*, 220, 24.

deMenocal, P.B. 2011. Climate and human evolution. *Science*, 331, 542.

Detlef, H., Belt, S.T., Sosdian, S.M., Smik, L., Lear, C.H., Hall, I.R., Cabedo-Sanz, P., Husum, K. & Kender, S. 2018. Sea ice dynamics across the Mid-Pleistocene transition in the Bering Sea. *Nature Communications*, 9, 941.

Diamond, R.E. & Harris, C., 2019. Stable isotope constraints on hydrostratigraphy and aquifer connectivity in the Table Mountain Group. *South African Journal of Geology*, 122(2), 330.

Dingle, R. 1973. Mesozoic palaeogeography of the southern Cape, South Africa. *Palaeogeography, Palaeoclimatology, Palaeoecology*, 13, 213.

Dingle, R., Siesser, W.G. & Newton, R. 1983. *Mesozoic and Tertiary Geology of Southern Africa*. Rotterdam, A.A. Balkema, 375.

Dixon, J.C. 2022. Pedogenesis with respect to geomorphology. In: J.F. Shroder (Editor) *Treatise on Geomorphology* (Second Edition). Oxford, Academic Press, 77.

Dupont, L.M., Zhao, X., Charles, C., Faith, J.T. & Braun, D. 2022. Continuous vegetation record of the Greater Cape Floristic Region (South Africa) covering the past 300 000 years (IODP U1479). *Climate of the Past*, 18, 21.

Durand, N., Gunnell, Y., Curmi, P. and Ahmad, S.M. 2006. Pathways of calcrete development on weathered silicate rocks in Tamil Nadu, India: Mineralogy, chemistry and paleoenvironmental implications. *Sedimentary Geology*, 192, 18Duringer, P., Schuster, M., Genise, J.F., Mackaye, H.T., Vignaud, P. & Brunet, M. 2007. New termite trace fossils: Galleries, nests and fungus combs from the Chad basin of Africa (Upper Miocene–Lower Pliocene). *Palaeogeography, Palaeoclimatology, Palaeoecology*, 251, 353.

Duvert, C., Butman, D.E., Marx, A., Ribolzi, O. & Hutley, L.B. 2018. CO2 evasion along streams driven by groundwater inputs and geomorphic controls. *Nature Geoscience*, 11, 818.

Dworkin, S.I., Nordt, L. & Atchley, S. 2005. Determining terrestrial paleotemperatures using the oxygen isotopic composition of pedogenic carbonate. *Earth and Planetary Science Letters*, 237, 68.

Ehlers, J., Gibbard, P.L. & Hughes, P.D. 2018. Quaternary glaciations and chronology. In: J. Menzies & J.J.M. van der Meer (Editors) *Past Glacial Environments* (Second Edition). Elsevier, 101.

Elderfield, H., Ferretti, P., Greaves, M., Crowhurst, S., McCave, I.N., Hodell, D. & Piotrowski, A.M. 2012. Evolution of ocean temperature and ice volume through the mid-Pleistocene climate transition. *Science*, 337, 709.

Elidrissi, S., Daoudi, L. & Fagel, N. 2018. Palygorskite occurrences and genesis in calcisol and groundwater carbonates of the Tensift Al Haouz area, Central Morocco. *Geoderma*, 316, 88.

Elidrissi, S., Omdi, F.E., El Azhari, A., Fagel, N. & Daoudi, L. 2020. New application of GIS and statistical analysis in mapping the distribution of Quaternary calcrete (Tensift Al Haouz area, Central Morocco). *Catena,* 188, 104419.

Eze, P.N., 2013. Reconstruction of environmental and climate dynamics using multi-proxy evidence from palaeosols of the Western Cape, South Africa. Unpublished PhD thesis, University of Cape Town, 8.

Eze, P.N., Kokwe, A. & Eze, J.U. 2020. Advances in nanoscale study of organomineral complexes of termite mounds and associated soils: A systematic review. *Applied and Environmental Soil Science*, 2020, 9.

Faith, J.T., Chase, B.M. & Pargeter, J. 2024. The Last Glacial Maximum climate at Boomplaas Cave, South Africa. *Quaternary Science Reviews*, 329, 108557.

Francis, M.L., Clarke, C.E., van Gend, J., Vermooten, M., Maponya, M., Mashimbye, E., Palcsu, L., Watson, A., van Rooyen, J. & Miller, J.A. 2022. The relationship between Heuweltjies and

saline groundwater along the West Coast of South Africa. *Department of Earth Sciences, Stellenbosch University, Water Research Commission*, 13.

Francis, M.L. & Poch, R.M. 2019. Calcite accumulation in a South African heuweltjie: Role of the termite *Microhodotermes viator* and oribatid mites. *Journal of Arid Environments*, 170, 103981.

Frauenstein, F., Veizer, J., Beukes, N., Van Niekerk, H.S. & Coetzee, L.L. 2009. Transvaal Supergroup carbonates: Implications for Paleoproterozoic $\delta^{18}O$ and $\delta^{13}C$ records. *Precambrian Research*, 175, 160.

Genise, J.F. 1997. A fossil termite nest from the Marplatan stage (late Pliocene) of Argentina: Palaeoclimatic indicator. *Palaeogeography, Palaeoclimatology, Palaeoecology*, 136, 144.

Genise, J.F. 2017. Paleoenvironmental analysis and ichnoentomological synthesis. In: J.F. Genise (Editor) *Ichnoentomology: Insect Traces in Soils and Paleosols*. Cham, Springer International Publishing, 606.

Genise, J.F., Bellosi, E.S., Melchor, R.N. & Cosarinsky, M.I. 2005. Comment: Advanced Early Jurassic termite (Insecta: *Isoptera*) nests: Evidence from the Clarens Formation in the Tuli Basin, Southern Africa (Bordy et al., 2004). *Palaios*, 20, 308.

Genise, J.F., Mángano, M.G., Buatois, L.A., Laza, J.H. & Verde, M. 2000. Insect trace fossil associations in paleosols: The Coprinisphaera ichnofacies. *Palaios*, 15, 64.

Ghosh, P., Bhattacharya, S.K. & Jani, R.A. 1995. Palaeoclimate and palaeovegetation in central India during the Upper Cretaceous based on stable isotope composition of the palaeosol carbonates. *Palaeogeography, Palaeoclimatology, Palaeoecology*, 114, 296.

Gocke, M. & Kuzyakov, Y. 2011. Effect of temperature and rhizosphere processes on pedogenic carbonate recrystallization: Relevance for paleoenvironmental applications. *Geoderma*, 166, 65.

Gocke, M. Pustovoytov, K. & Kuzyakov, Y. 2012. Pedogenic carbonate formation: Recrystallization versus migration—Process rates and periods assessed by ^{14}C labeling. *Global Biogeochemical Cycles*, 26.

Goudie, A. 1973. *Duricrusts in Tropical and Subtropical Landscapes*. Oxford University Press, Oxford, 174.

Goudie, A., Goudie, A. and Pye, K. (eds.), 1983. *Chemical Sediments and Geomorphology: Precipitates and Residua in the Near-Surface Environment*. Academic Press, London, 439.

Gouttefarde, R., Bon, R., Fourcassié, V., Arrufat, P., Haifig, I., Baehr, C. and Jost, C., 2017. Investigating termite nest thermodynamics using a quick-look method and the heat equation. *bioRxiv*, 161075.

Green, P., Duddy, I. and Japsen, P. 2022. Episodic kilometre-scale burial and exhumation and the importance of missing section. *Earth-Science Reviews*, 234, 104226.

Grobler, B.A., Cawthra, H.C., Potts, A.J. and Cowling, R.M. 2020. Plant diversity of Holocene dune landscapes in the Cape Floristic Region: The legacy of Pleistocene sea-level dynamics. *The Palaeo-Agulhas Plain: a lost world and extinct ecosystem*, 235, 106058.

Grube, A. and Rudolph, R. 1995. Termites in arid environments: the water balance of *Psammotermes allocerus* Silvestri. *Mitteilungen der Deutschen Gesellschaft für Allgemeine und Angewandte Entomologie*, 668.

Hadebe, G. 2021. The Geological Context of a Fossil Termite Nest Site in the Gamka Valley (near Calitzdorp, South Africa). BSc (Honours) thesis (unpublished). University of Cape Town, Cape Town, 29.

Hahn, A., Schefuß, E., Andò, S., Cawthra, H.C., Frenzel, P., Kugel, M., Meschner, S., Mollenhauer, G. and Zabel, M. 2017. Southern Hemisphere anticyclonic circulation drives

oceanic and climatic conditions in late Holocene southernmost Africa. *Climate of the Past*, 13, 665.

Hare, V. and Sealy, J. 2013. Middle Pleistocene dynamics of southern Africa's winter rainfall zone from $\delta^{13}C$ and $\delta^{18}O$ values of Hoedjiespunt faunal enamel. *Palaeogeography, Palaeoclimatology, Palaeoecology*, 374, 80.

Hasiotis, S.T. and Dubiel, R.F. 1995. Termite (*Isoptera*) nest ichnofossils from the Upper Triassic Chinle Formation, Petrified Forest National Park, Arizona. *Ichnos: An International Journal of Plant & Animal*, 4, 130.

Henshilwood, C.S. 2008. Winds of change: palaeoenvironments, material culture and human behaviour in the late Pleistocene (~77 ka-48 ka ago) in the Western Cape Province, South Africa. *Goodwin Series*, 10, 51.

Hervé, V., Clerc, M., Cailleau, G., Bueche, M., Junier, T., Verrecchia, E. and Junier, P. 2018. Carbonate Accumulation in the Bark of *Terminalia bellirica*: A New Habitat for the Oxalate-Carbonate Pathway. *Geomicrobiology Journal*, 35, 39.

Hesse, P.R. 1955. A Chemical and Physical Study of the Soils of Termite Mounds in East Africa. *Journal of Ecology*, 43, 461.

Hewitt, G. 2000. The genetic legacy of the Quaternary ice ages. *Nature*, 405, 913.

Holt, J.A. and Lepage, M. 2000. Termites and Soil Properties. In: T. Abe, D.E. Bignell and M. Higashi (Editors) *Termites: Evolution, Sociality, Symbioses, Ecology*. Dordrecht, Springer Netherlands, 407.

Holzapfel, C. 2008. Deserts. In: S.E. Jørgensen and B.D. Fath (Editors) *Encyclopedia of Ecology*. Oxford, Academic Press, 898.

Holzkämper, S., Holmgren, K., Lee-Thorp, J., Talma, S., Mangini, A. and Partridge, T. 2009. Late Pleistocene stalagmite growth in Wolkberg Cave, South Africa. *Earth and Planetary Science Letters*, 282, 221.

Hopkins, D.W., Chudek, J.A., Bignell, D.E., Frouz, J., Webster, E.A. and Lawson, T. 1998. Application of ^{13}C NMR to investigate the transformations and biodegradation of organic materials by wood- and soil-feeding termites, and a coprophagous litter-dwelling dipteran larva. *Biodegradation*, 9, 431.

Hopley, P.J., Marshall, J.D. and Latham, A.G. 2009. Speleothem preservation and diagenesis in South African hominin sites: implications for paleoenvironments and geochronology. *Geoarchaeology*, 24, 547.

Hopley, P.J. and Maslin, M.A. 2010. Climate-averaging of terrestrial faunas: an example from the Plio-Pleistocene of South Africa. *Paleobiology*, 36, 50.

Horita, J. 2014. Oxygen and carbon isotope fractionation in the system dolomite–water–CO2 to elevated temperatures. *Geochimica et Cosmochimica Acta*, 129, 124.

Hura, T., Hura, K., Grzesiak, M. and Rzepka, A. 2007. Effect of long-term drought stress on leaf gas exchange and fluorescence parameters in C_3 and C_4 plants. *Acta Physiologiae Plantarum*, 29, 113.

Irwin, H., Curtis, C. and Coleman, M. 1977. Isotopic evidence for source of diagenetic carbonates formed during burial of organic-rich sediments. *Nature*, 269, 213.

Janzow, M.P. and Judd, T.M. 2015. The termite Reticulitermes flavipes (*Rhinotermitidae: Isoptera*) can acquire micronutrients from soil. *Environmental Entomology*, 44, 820.

Jolivet, M. and Boulvais, P. 2021. Global significance of oxygen and carbon isotope compositions of pedogenic carbonates since the Cretaceous. *Geoscience Frontiers*, 12, 101132.

Jones, J.C. and Oldroyd, B.P. 2006. Nest Thermoregulation in Social Insects. In: S.J. Simpson (Editor) *Advances in Insect Physiology*. Academic Press, 191.

Joseph, G.S., Seymour, C.L., Coetzee, B.W.T., Ndlovu, M., De La Torre, A., Suttle, R., Hicks, N., Oxley, S. and Foord, S.H. 2016. Microclimates mitigate against hot temperatures in dryland ecosystems: termite mounds as an example. *Ecosphere,* 7,e01509.

Jouquet, P., Bottinelli, N., Shanbhag, R., Bourguignon, T., Traoré, S. and Abbasi, S.A. 2016. Termites: The Neglected Soil Engineers of Tropical Soils*. Soil Science*, 181, 165.

Jouquet, P., Tessier, D. and Lepage, M. 2004. The Soil Structural Stability of Termite Nests: Role of Clays in *Macrotermes bellicosus* (Isoptera: *Macrotermitinae*) Mound Soils. *European Journal of Soil Biology*, 40, 29.

Kandasami, Borges and Murthy 2016. Effect of biocementation on the strength and stability of termite mounds*. Environmental Geotechnics,* 3, 113.

Katariya, L., Ramesh, P.B. and Borges, R.M. 2018. Dynamic environments of fungus-farming termite mounds exert growth-modulating effects on fungal crop parasites. *Environmental Microbiology,* 20, 979.

Kearsey, T., Twitchett, R.J. and Newell, A.J. 2011. The origin and significance of pedogenic dolomite from the Upper Permian of the South Urals of Russia. *Geological Magazine*, 149, 307.

King, H., Ocko, S. and Mahadevan, L. 2015. Termite mounds harness diurnal temperature oscillations for ventilation. *Proceedings of the National Academy of Sciences*, 112, 11593.

Koch, P.L. 1998. Isotopic reconstruction of past continental environments*. Annual Review of Earth and Planetary Sciences*, 26, 613.

Koné, F., Dosso, K. and Konaté, S. 2022. Agronomical potentiality of termite mound soils in a transitional zone in central Côte d'Ivoire. *Journal of Soil Science and Plant Nutrition*, 22, 1402.

Korb, J. 2008. Termites. *Current Biology*, 17, 999.

Kuzyakov, Y. 2006. Sources of CO_2 efflux from soil and review of partitioning methods. *Soil Biology and Biochemistry*, 38, 448.

Lee, K.E. and Wood, T.G. 1971. Termites and soils. *London, UK, Academic Press.*

Leegood, R.C. 2013. Photosynthesis. In: Lennarz, W.J. and Lane, M.D. (Eds.) *Encyclopedia of Biological Chemistry* (2nd ed.). *Academic Press,* 496.

Licht, A., Van Cappelle, M., Abels, H.A., Ladant, J.-B., Trabucho-Alexandre, J., France-Lanord, C., Donnadieu, Y., Vandenberghe, J., Rigaudier, T., Lécuyer, C., Terry Jr, D., Adriaens, R., Boura, A., Guo, Z., Soe, A.N., Quade, J., Dupont-Nivet, G. and Jaeger, J.-J. 2014. Asian monsoons in a late Eocene greenhouse world. *Nature*, 513, 506.

Lintern, M.J., Sheard, M.J. and Chivas, A.R. 2006. The source of pedogenic carbonate associated with gold-calcrete anomalies in the western Gawler Craton, South Australia. *Chemical Geology*, 235, 324.

Liu, X., Monger, C. and Whitford, W. 2007. Calcium carbonate in termite galleries - Biomineralization or upward transport? *Biogeochemistry*, 82, 250.

Lock, J.M. 2013. Africa, Ecosystems of. In: Levin, S.A. (Ed.) Encyclopedia of Biodiversity (2nd ed.). *Academic Press*, 57.

Lopez-Hernandez, D., Siegert, G. and Rodriguez, J.V. 1986. Competitive Adsorption of Phosphate with Malate and Oxalate by Tropical Soils. *Soil Science Society of America Journal*, 50, 1462.

Lüscher, M. 1961. Air-conditioned Termite Nests. *Scientific American*, 205, 147.

Machette, M.N. 1985. Calcic soils of the southwestern United States. In: Weide, D.L. (Ed.), Soils and Quaternary Geology of the Southwestern United States. *Geological Society of America Special Paper,* 203, 22.Mack, G.H. and Cole, D.R. 1991. Paleoclimatic Controls on Stable Oxygen and Carbon Isotopes in Caliche of the Abo Formation (Permian), South-Central New Mexico, U.S.A. *SEPM Journal of Sedimentary Research*, 61.Mahaney, W.C., Zippin, J., Milner, M.W., Sanmugadas, K., Hancock, R.G.V., Aufreiter, S., Campbell, S., Huffman, M.A., Wink, M., Malloch, D. and Kalm, V. 1999. Chemistry, mineralogy and microbiology of termite mound soil eaten by the chimpanzees of the Mahale Mountains, Western Tanzania. *Journal of Tropical Ecology*, 15, 588.

Martin, J.W. and Croukamp, L. 2021. Exploration into the potential for a low-enthalpy geothermal power plant in Cape fold belt. *Geothermics*, 89, 101934.

Masrahi, Y., Al-Huqail, A., Al-Turki, T.A. and Sayed, O. 2011. Different altitudinal distribution and diversity of plants with different photosynthetic pathways in arid Saudi Arabia. *Australian Journal of Basic and Applied Sciences*, 5,43.

McAuliffe, J.R., Hoffman, M.T., McFadden, L.D., Bell, W., Jack, S., King, M.P. and Nixon, V. 2019. Landscape patterning created by the southern harvester termite, *Microhodotermes viator*: Spatial dispersion of colonies and alteration of soils. *Journal of Arid Environments*, 162, 34.

McAuliffe, J.R., Hoffman, M.T., McFadden, L.D., Jack, S., Bell, W. and King, M.P. 2019. Whether or not heuweltjies: Context-dependent ecosystem engineering by the southern harvester termite, *Microhodotermes viator*. *Journal of Arid Environments*, 163, 33.

McAuliffe, J.R., Hoffman, M.T., McFadden, L.D. and King, M.P. 2014. Role of aeolian sediment accretion in the formation of heuweltjie earth mounds, western South Africa. *Earth Surface Processes and Landforms*, 39, 1912.

McCrea, J.M. 1950. On the isotopic chemistry of carbonates and a paleotemperature scale. *The Journal of Chemical Physics*, 18, 857.

Mehmood, M., 2018. Dolomite and dolomitization model - a short review. *International Journal of Hydrology*, 2(1), 549.

Meyer, N.A., Breecker, D.O., Young, M.H. and Litvak, M.E. 2014. Simulating the effect of vegetation in formation of pedogenic carbonate. *Soil Science Society of America Journal*, 78, 924.

Midgley, G.F. and Musil, C.F. 1990. Substrate effects of zoogenic soil mounds on vegetation composition in the Worcester–Robertson valley, Cape Province. *South African Journal of Botany*, 56, 166.

Midgley, J., Harris, C., Hesse, H. and Swift, A. 2002. Heuweltjie age and vegetation change based on C-13 and C-14 analyses. *South African Journal of Science*, 98, 202–204.

Mills, A.J., Milewski, A., Fey, M.V., Groengroeft, A. and Petersen, A. 2009. Fungus culturing, nutrient mining and geophagy: A geochemical investigation of *Macrotermes* and *Trinervitermes* mounds in southern Africa. *Journal of Zoology*, 278, 35.

Mills, A.J. and Sirami, C. 2018. Nutrient enrichment of ecosystems by fungus-growing versus non-fungus-growing termites. *Journal of Tropical Ecology*, 34, 389.

Milne, G. 1947. A Soil Reconnaissance Journey Through Parts of Tanganyika Territory December 1935 to February 1936. *Journal of Ecology*, 35, 265.

Mohale, N.E., Codron, D. and Horwitz, L.K. 2022. Stable isotope evidence for mid-Pleistocene paleoenvironmental conditions at the site of Kathu Pan 1 (central interior, South Africa). *Quaternary International*, 614, 49.

Moore, J.M. and Picker, M.D. 1991. Heuweltjies (Earth Mounds) in the Clanwilliam District, Cape Province, South Africa: 4000-Year-Old Termite Nests. *Oecologia*, 86, 432.

Mthembi, P., Roberts, D. and Harris, C. 2016. Chemical stratigraphy of lake deposits from the Kalkkop Impact Crater, South Africa, and its palaeoenvironmental significance. *South African Journal of Geology*, 119, 230.

Muir, R., Abrahams, M. and Hadebe, G. 2022. Geomorphology, sedimentology and preliminary radioisotopic age of Middle Pleistocene termitaria near Calitzdorp, South Africa. *Proceedings of the Palaeontological Society of Southern Africa*, 2022, 37.

Muir, R., Bordy, E.M., Reddenng, J.S.V. and Viljoen, J.H.A. 2017. Lithostratigraphy of the Enon Formation (Uitenhage Group), South Africa. *South African Journal of Geology*, 120, 280.

Mujinya, B.B., Mees, F., Boeckx, P., Bodé, S., Baert, G., Erens, H., Delefortrie, S., Verdoodt, A., Ngongo, M. and Van Ranst, E. 2011. The origin of carbonates in termite mounds of the Lubumbashi area, D.R. Congo. *Geoderma*, 165, 105.

Mujinya, B.B., Mees, F., Erens, H., Dumon, M., Baert, G., Boeckx, P., Ngongo, M. and Van Ranst, E. 2013. Clay composition and properties in termite mounds of the Lubumbashi area, D.R. Congo. *Geoderma*, 192, 315.

Muvengwi, J., Davies, A.B., Parrini, F. and Witkowski, E.T.F. 2018. Geology drives the spatial patterning and structure of termite mounds in an African savanna. *Ecosphere*, 9, e02148.

Muvengwi, J., Ndagurwa, H.G.T., Nyenda, T. and Mbiba, M. 2016. Nutrient dynamics and plant assemblages of *Macrotermes falciger* mounds in a savanna ecosystem. *Acta Oecologica*, 76, 21.

Muwawa, E., Makonde, H., Budambula, N., Osiemo Lagat, Z. and Boga, H. 2014. Chemical properties associated with guts, soil and nest materials of Odontotermes and Macrotermes species from Kenya. Journal of Biodiversity and Environmental Sciences, 4, 263.

Netterberg, F. 1980. Geology of southern African calcretes: 1: Terminology, description, macrofeatures, and classification. South African Journal of Geology, 83, 283.

Ngoy, S., Thieblemont, D., Callec, Y., Kampata, D., Mupande, J.F., Auclerc, A. and Watteau, F. 2023. *Macrotermes falciger* termite mounds as indicators of lithogeochemical anomalies of metals of interest. Journal of Geochemical Exploration, 248, 107197.

Noirot, C. and Darlington, J.P.E.C. 2000. Termite Nests: Architecture, Regulation and Defence. In: Abe, T., Bignell, D.E. and Higashi, M. (Eds.) Termites: Evolution, Sociality, Symbioses, Ecology. Springer Netherlands, 139.

Oberst, S., Lai, J.C.S., Martin, R., Halkon, B.J., Saadatfar, M. and Evans, T.A. 2020. Revisiting stigmergy in light of multi-functional, biogenic, termite structures as communication channel. Computational and Structural Biotechnology Journal, 18, 2534.

Ocko, S.A., King, H., Andreen, D., Bardunias, P., Turner, J.S., Soar, R. and Mahadevan, L. 2017. Solar-powered ventilation of African termite mounds. *Journal of Experimental Biology*, 220, 3269.

Parr, C.L. and Bishop, T.R. 2022. The response of ants to climate change. *Global Change Biology*, 28, 3205.

Partridge, T.C., Avery, D.M., Botha, G.A., Brink, J.S., Deacon, J., Herbert, R.S., Maud, R.R., Scholtz, A., Scott, L. and Vogel, J. 1990. Late Pleistocene and Holocene climatic change in Southern Africa. *South African Journal of Science*, 86, 302.

Peterson, 2006. Subterranean Termites: Their prevention and control in buildings. (No. 64). *USDA Forest Service, Wood Products Insect Research Unit*. 5.

Petit, J.R., Jouzel, J., Raynaud, D., Barkov, N.I., Barnola, J.M., Basile, I., Bender, M., Chappellaz, J., Davis, M., Delaygue, G. and Delmotte, M. 1999. Climate and atmospheric history of the past 420,000 years from the Vostok ice core, Antarctica. *Nature*, 399, 36.

Malvern Panalytical, 2024. Phase Quantification Using XRD. Available at: https://www.malvernpanalytical.com/en/products/measurement-type/phase-quantification. (Accessed: 21 October 2024).

Pickford, M. 2006. A termite tale of climate change. *Quest*, 2, 31.

Pina, C.M., Pimentel, C. and Crespo, Á. 2022. The Dolomite Problem: A Matter of Time. *ACS Earth and Space Chemistry*, 6, 1471.

Pisias, N.G. and Moore, T.C. 1981. The evolution of Pleistocene climate: A time series approach. *Earth and Planetary Science Letters*, 52, 458.

Podwojewski, P., 1995. The occurrence and interpretation of carbonate and sulfate minerals in a sequence of Vertisols in New Caledonia. *Geoderma*, 65, 248.

Pomeroy, D.E. 1983. Some effects of mound-building termites on the soils of a semi-arid area of Kenya. *Journal of Soil Science*, 34, 570.

Potts, A.J., Midgley, J. and Harris, C. 2009. Stable isotope and 14C study of biogenic calcrete in a termite mound, Western Cape, South Africa, and its palaeoenvironmental significance. *Quaternary Research*, 72, 264.

Quade, T.C. 1993. Stable carbon and oxygen isotopes in soil carbonates. Climate change in continental isotopic records. *Geophysical Monograph*, 78, 231.

Quick, L.J., Carr, A.S., Meadows, M.E., Boom, A., Bateman, M.D., Roberts, D.L., Reimer, P.J. and Chase, B.M. 2015. A late Pleistocene–Holocene multi-proxy record of palaeoenvironmental change from Still Bay, southern Cape Coast, South Africa. *Journal of Quaternary Science*, 30, 885.

Retallack, G.J. and Wright, V.P. 1990. Micromorphology of Lithified Paleosols. In: Douglas, L.A. (Ed.) *Soil Micro-Morphology: A Basic and Applied Science*. Elsevier, 652.

Reynolds, S.C. 2007. Mammalian body size changes and Plio-Pleistocene environmental shifts: implications for understanding hominin evolution in eastern and southern Africa. *Journal of Human Evolution*, 53, 548.

Ringrose, S., Harris, C., Huntsman-Mapila, P., Vink, B.W., Diskins, S., Vanderpost, C. and Matheson, W. 2009. Origins of strandline duricrusts around the Makgadikgadi Pans (Botswana Kalahari) as deduced from their chemical and isotope composition. *Sedimentary Geology,* 219, 279.

Roberts, J.A. 2024. The problem with dolomite. *Nature Geoscience*, 17, 716.

Roberts, E.M., Todd, C.N., Aanen, D.K., Nobre, T., Hilbert-Wolf, H.L., O'Connor, P.M., Tapanila, L., Mtelela, C. and Stevens, N.J. 2016. Oligocene Termite Nests with In Situ Fungus Gardens from the Rukwa Rift Basin, Tanzania, Support a Paleogene African Origin for Insect Agriculture. *Plos One*, 11, e0156847.

Potts, A.J., Midgely, J. and Harris, C. 2009. Stable isotope and ^{14}C study of biogenic calcrete in a termite mound, Western Cape, South Africa, and its palaeoenvironmental significance. *Quaternary Research*, 72, 264.

Quade, T.C. 1993. Stable carbon and oxygen isotopes in soil carbonates. Climate change in continental isotopic records. *Geophysical Monograph*, 78, 231.

Quick, L.J., Carr, A.S., Meadows, M.E., Boom, A., Bateman, M.D., Roberts, D.L., Reimer, P.J. and Chase, B.M. 2015. A late Pleistocene–Holocene multi-proxy record of palaeoenvironmental change from Still Bay, southern Cape Coast, South Africa. *Journal of Quaternary Science*, 30, 885.

Retallack, G.J. and Wright, V.P. 1990. Micromorphology of Lithified Paleosols. In: Douglas, L.A. (Ed.), Soil Micro-Morphology: A Basic and Applied Science. *Developments in Soil Science*, 17, 652.

Roberts, S.C. 2007. Mammalian body size changes and Plio-Pleistocene environmental shifts: implications for understanding hominin evolution in eastern and southern Africa. *Journal of Human Evolution*, 53(5), 548.

Ringrose, S., Harris, C., Huntsman-Mapila, P., Vink, B.W., Diskins, S., Vanderpost, C. and Matheson, W. 2009. Origins of strandline duricrusts around the Makgadikgadi Pans (Botswana Kalahari) as deduced from their chemical and isotope composition. Sedimentary Geology, 219(2), 279.

Roberts, J.A. 2024. The problem with dolomite. *Nature Geoscience*, 17, 716.

Roberts, E.M., Todd, C.N., Aanen, D.K., Nobre, T., Hilbert-Wolf, H.L., O'Connor, P.M., Tapanila, L., Mtelela, C. and Stevens, N.J. 2016. Oligocene Termite Nests with In Situ Fungus Gardens from the Rukwa Rift Basin, Tanzania, Support a Paleogene African Origin for Insect Agriculture. *Plos One*, 11(10), e0156847.

Rogers, 1903. The geological history of the Gouritz River system. *Transactions of the South African Philosophical Society*, 14, 384.

Rogers, J.C. 1988. Climatic Change and Variability in Southern Africa, P.D. Tyson (Book Review). *Annals of the Association of American Geographers*, 78(1), 206.

Rohr, D., Boucot, A., Miller, J. and Abbott, M. 1986. Oldest termite nest from the Upper Cretaceous of west Texas (USA). *Geology,* 14(2), 88.

Rundel, P.W. 1980. The ecological distribution of C_4 and C_3 grasses in the Hawaiian Islands. *Oecologia*, 45(2), 359.

Sage, R.F., Ward, D.A. and Kubien, D.S. 1999. C_4 Plant biology. In: Sage, R.F. and Monson, R.K. (Eds.), C_4 Plant Biology. *Elsevier*, 376.

Sako, A., Mills, A.J. and Roychoudhury, A.N. 2009. Rare earth and trace element geochemistry of termite mounds in central and northeastern Namibia: Mechanisms for micro-nutrient accumulation. *Geoderma*, 153(2), 230.

Sankovitz, M. and Purcell, J. 2021. Ant nest architecture is shaped by local adaptation and plastic response to temperature. Scientific Reports, 11, 23053.

Sarcinelli, T.S., Schaefer, C.E.G.R., Lynch, L.D.S., Arato, H.D., Viana, J.H.M., Filho, M.R.D.A. and Gonçalves, T.T. 2009. Chemical, physical and micromorphological properties of termite mounds and adjacent soils along a toposequence in Zona da Mata, Minas Gerais State, Brazil. *Catena,* 76(2), 113.

Seymour, C.L., Milewski, A.V., Mills, A.J., Joseph, G.S., Cumming, G.S., Cumming, D.H.M. and Mahlangu, Z. 2014. Do the large termite mounds of *Macrotermes* concentrate micronutrients in addition to macronutrients in nutrient-poor African savannas? *Soil Biology and Biochemistry*, 68, 105.

Sharma, S.D., Patil, D.J. & Gopalan, K. 2002. Temperature dependence of oxygen isotope fractionation of CO2 from magnesite-phosphoric acid reaction. *Geochimica et Cosmochimica Acta*, 66, 593.

Sharp, Z. 2017. *Principles of Stable Isotope Geochemistry*, 2nd ed. Open Textbooks. 22.

Siddall, M., Hönisch, B., Waelbroeck, C. and Huybers, P. 2010. Changes in deep Pacific temperature during the mid-Pleistocene transition and Quaternary. *Quaternary Science Reviews*, 29, 181.

Singh, S., Chaudhary, A., Handique, S., Singh, S. and Tripathi, J. 2017. Biological weathering and geochemical fractionation by termites: A case study of loessic sediments from Jawaharlal Nehru University, New Delhi, India. *Earth Science Indi*a, 10.

Souza, H.J.D., Delabie, J.H.C. and Sodré, G.A. 2020. Termite participation in the soil-forming processes of '*murundus*' structures in the semi-arid region of Brazil. *Revista Brasileira de Ciência do Solo*, 44, e0190133.

Specht, R.L. 1981. Major vegetation formations in Australia. In: Keast, A. (Ed.), *Ecological Biogeography of Australia*. Dr. W. Junk Publishers, 297.

Srivastava, P., Aruche, M., Arya, A., Pal, D.K. and Singh, L.P. 2016. A micromorphological record of contemporary and relict pedogenic processes in soils of the Indo-Gangetic Plains: implications for mineral weathering, provenance and climatic changes. *Earth Surface Processes and Landforms*, 41(5), 790.

Stevens, R.E. 1980. Insects associated with ponderosa pine in Colorado. *USDA Forest Service, Rocky Mountain Forest and Range Experiment Station.*

Stewart, A., Anand, R. and Balkau, J. 2012. Source of anomalous gold concentrations in termite nests, Moolart Well, Western Australia: Implications for exploration. *Geochemistry: Exploration, Environment, Analysis,* 12(2), 337.

Strobel, P., Bliedtner, M., Carr, A.S., Struck, J., Du Plessis, N., Glaser, B., Meadows, M.E., Quick, L.J., Zech, M., Zech, R. and Haberzettl, T. 2022. Reconstructing Late Quaternary precipitation and its source on the southern Cape coast of South Africa: A multi-proxy paleoenvironmental record from Vankervelsvlei. *Quaternary Science Reviews*, 284, 107467.

Stynder, D.D. and Bishop, L.C. 2023. Mid-Pleistocene of Africa: Large mammals. In: Elias, S.A. & Mock, C.J. (Eds.), Encyclopedia of Quaternary Science (2nd ed.). *Elsevier*, 363.

Su, N. and Puche, H. 2003. Tunneling Activity of Subterranean Termites (Isoptera: Rhinotermitidae) in Sand with Moisture Gradients. *Journal of Economic Entomology*, 96(1), 93.

Sutter, J., Fischer, H., Grosfeld, K., Karlsson, N.B., Kleiner, T., Van Liefferinge, B. and Eisen, O. 2019. Modelling the Antarctic Ice Sheet across the mid-Pleistocene transition – implications for Oldest Ice. *The Cryosphere*, 13(6), 2041.

Talma, A.S. and Netterberg, F. 1983. Stable isotope abundances in calcretes. *Geological Society, London, Special Publications,* 11, 233.

Talma, A.S. and Vogel, J.C. 1992. Late Quaternary Paleotemperatures Derived from a Speleothem from Cango Caves, Cape Province, South Africa. *Quaternary Research*, 37(2), 213.

Tanner, L.H. 2010. Continental Carbonates as Indicators of Paleoclimate. In: Alonso-Zarza, A.M. and Tanner, L.H. (Eds.), Carbonates in Continental Settings: Geochemistry, Diagenesis and Applications. *Developments in Sedimentology,* 62, 214.

Thorne, B.L., Grimaldi, D.A. and Krishna, K. 2000. Early Fossil History of the Termites. In: Abe, T., Bignell, D.E. and Higashi, M. (Eds.), Termites: Evolution, Sociality, Symbioses, Ecology. *Springer Netherlands*, 93.

Tieszen, L.L., Senyimba, M.M., Imbamba, S.K. and Troughton, J.H. 1979. The distribution of C_3 and C_4 grasses and carbon isotope discrimination along an altitudinal and moisture gradient in Kenya. *Oecologia,* 37(2), 350.

Timmermann, A. and Friedrich, T. 2016. Late Pleistocene climate drivers of early human migration. *Nature,* 538(7624), 95.

Tinker, J., de Wit, M. and Brown, R. 2008. Mesozoic exhumation of the southern Cape, South Africa, quantified using apatite fission track thermochronology. *Tectonophysics*, 455(2), 93.

Traoré, S. and Jouquet, P. 2020. Growth Performance and Adaptive Strategy of Early Seedlings of Three Savanna Woody Species in Pots as Feedback to the Soil of *Macrotermes Subhyalinus* Mound. *European Scientific Journal*, 16(14).

Turner, B.C. 2001. On the Mound of *Macrotermes michaelseni* as an Organ of Respiratory Gas Exchange. *Physiological and Biochemical Zoology*, 74(5), 822.

Turner, S., Marais, E., Vinte, M., Mudengi, A. and Park, W. 2006. Termites, water and soils. *Agricola*, 16.

Venter, J.A., Brooke, C.F., Marean, C.W., Fritz, H. and Helm, C.W. 2020. Large mammals of the Palaeo-Agulhas Plain showed resilience to extreme climate change but vulnerability to modern human impacts*. Quaternary Science Reviews*, 235, 106050.

Vogel, J.C., Fuls, A. and Ellis, R.P. 1978. The geographical distribution of Kranz grasses in South Africa. *South African Journal of Science*, 74(5), 215.

Vrba, E.S. 1995. On the connections between paleoclimate and evolution. In: Vrba, E.S., Denton, G.H., Partridge, T.C. and Burckle, L.H. (Eds.), Paleoclimate and Evolution, with Emphasis on Human Origins. Yale University Press, 45.

Walker, N.D. and Shillington, F.A. 1990. The effect of oceanographic variability on South African weather and climate. South African Journal of Science, 86(7), 386.

Wang, C. and Henderson, G. 2013. Clay preference and particle transport behavior of Formosan subterranean termites (Isoptera: *Rhinotermitidae*): A laboratory study. *Insect Science,* 21(3), 265.

Watson, J.P. 1974. Calcium Carbonate in Termite Mounds. *Nature*, 247(5436), 75.

Watson, J.P. 1977. The use of mounds of the termite *Macrotermes falciger* (Gerstäcker) as a soil amendment. *Journal of Soil Science*, 28(4), 672.

Weckmann, U., Ritter, O., Chen, X., Tietze, K. and De Wit, M. 2012. Magnetotelluric image linked to surface geology across the Cape Fold Belt, South Africa. *Terra Nova*, 24(3), 212.

Weir, J.S. 1973. Air flow, evaporation and mineral accumulation in mounds of *Macrotermes subhyalinus* (Rambur). *Journal of Animal Ecology*, 42(3), 520.

Whipkey, C.E., Capo, R.C., Hsieh, J.C.C. and Chadwick, O.A. 2002. Development of magnesian carbonates in Quaternary soils on the island of Hawaii. *Journal of Sedimentary Research,* 72(2), 165.

Whitford, W.G., Ludwig, J.A. and Noble, J.C. 1992. The importance of subterranean termites in semi-arid ecosystems in south-eastern Australia. *Journal of Arid Environments*, 22(1), 91.

Wijas, B.J., Lim, S. and Cornwell, W.K. 2022. Continental-scale shifts in termite diversity and nesting and feeding strategies. *Ecography*, e05902.

Williams, M.A.J. 2023. A century of research reconstructing Quaternary environments in East and North Africa and its global legacy. *Journal of African Earth Sciences*, 208, 105071.

Wilson, E.O., 1995. *The Insect Societies*. Belknap Press, Cambridge, Mass. 548.

Wood, T.G. 1988. Termites and the soil environment. *Biology and Fertility of Soils*, 6(3), 236.

Wright, V.P. and Tucker, M.E. 2009. *Calcretes.* John Wiley & Sons, 363.

Yanes, Y., Tomašových, A., Kowalewski, M., Castillo, C., Aguirre, J., Alonso, M.R. and Ibáñez, M. 2008. Taphonomy and compositional fidelity of Quaternary fossil assemblages of terrestrial gastropods from carbonate-rich environments of the Canary Islands. *Lethaia*, 41(3), 256.

Yu, C., Cheng, J.J., Jones, L.G., Wang, Y.Y., Faillace, E., Loureiro, C. and Chia, Y.P. 1993. *Data Collection Handbook to Support Modeling the Impacts of Radioactive Material in Soil. 22.*

Appendix

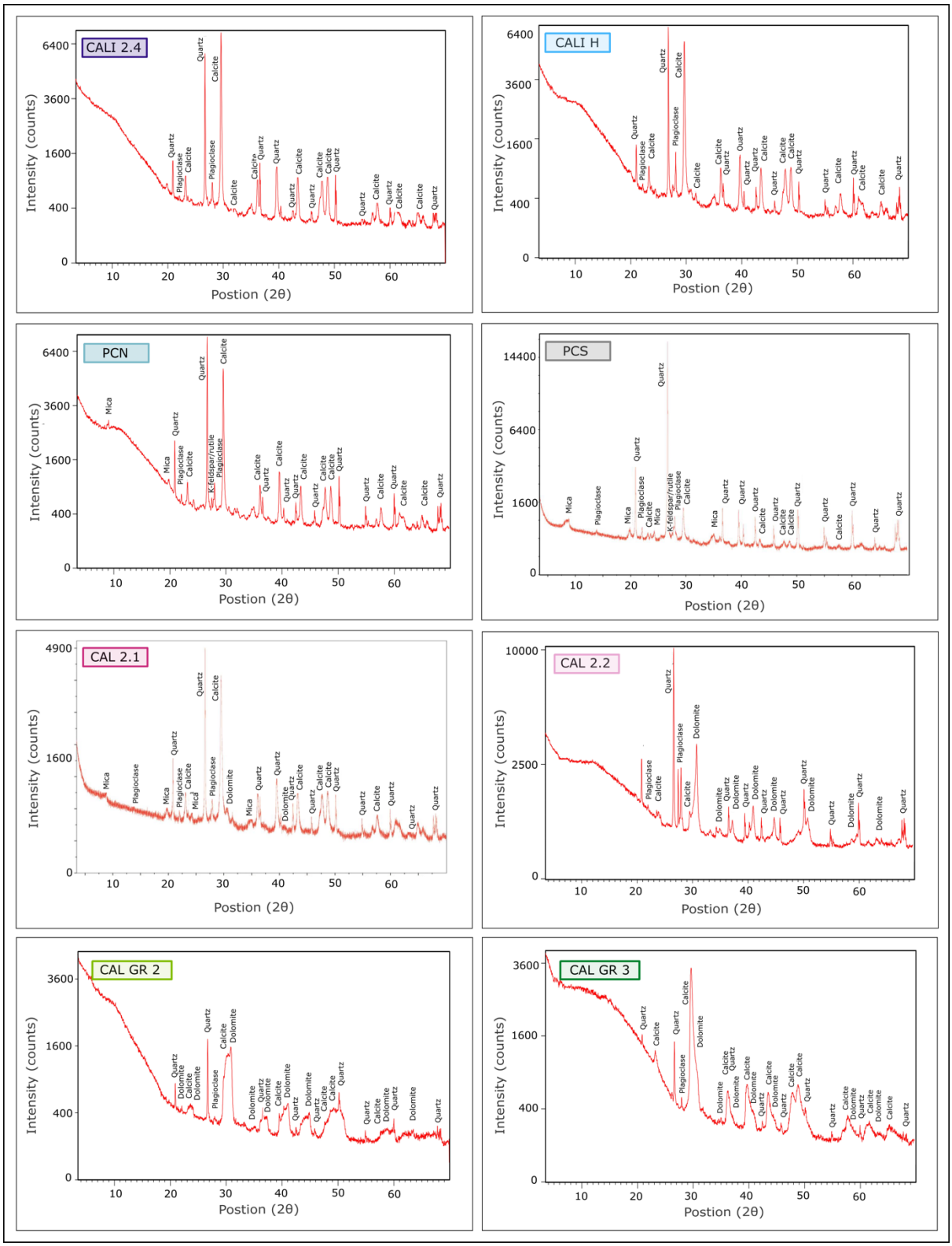
CALI 2.4
CALI H
PCN
PCS
CAL 2.1
CAL 2.2
CAL GR 2
CAL GR 3
Intensity (counts)
Postion (2θ)

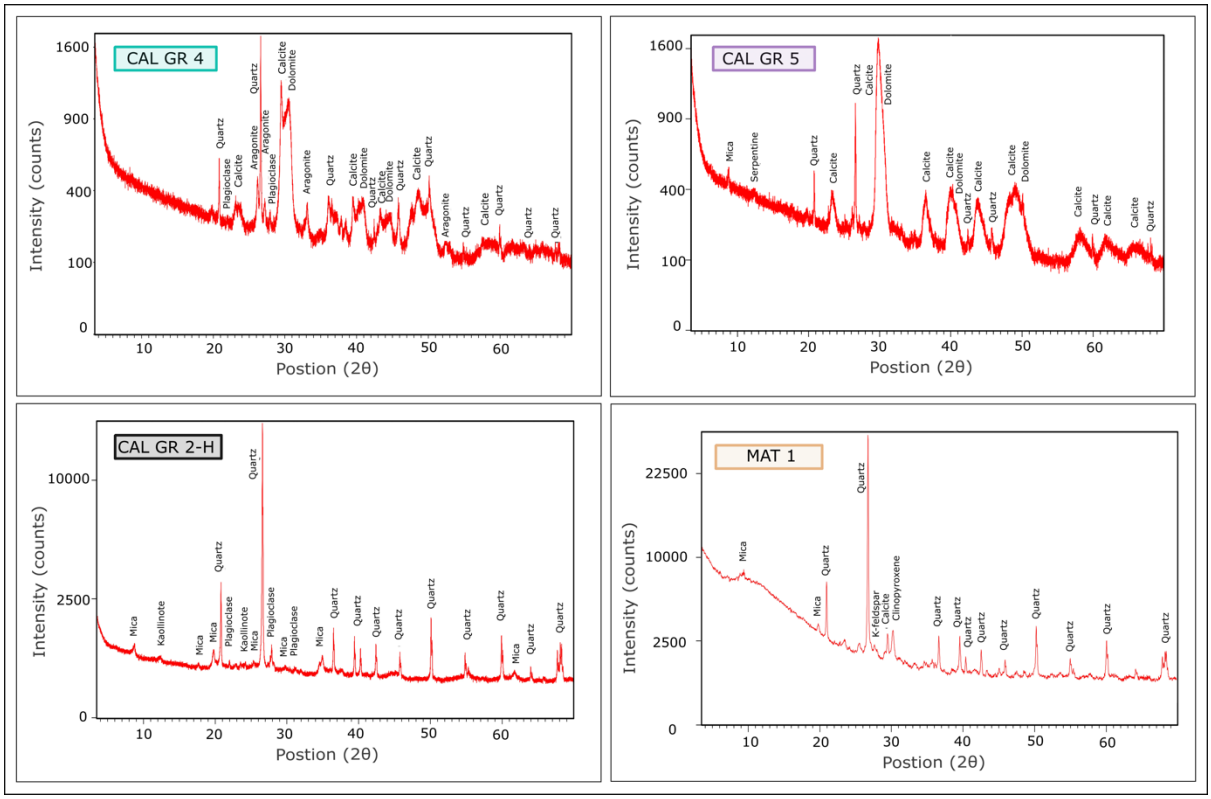

Figure 1: X-ray diffractograms for samples of all the samples from Calitzdorp, Groenefontein and Matjiesrivier. For relative mineral proportions, see in-text Figure 4.1, Table 4.1.

Table 1. Temperatures estimated from $\delta^{18}O$ values of the carbonates in the termitaria at Calitzdorp and Groenefontein. Values below α are represent the different assumed $\delta^{18}O$ water values.

Sample CAL 2.1	$\delta^{18}O$	α +4	T. °C	α +3	T. °C	α +2	T. °C	α +1	T. °C	α 0	T. °C	α -1	T. °C	α -2	T. °C	α -3	T. °C	α -4	T. °C
1	30.56	1.0265	36.60	1.0275	**31.40**	1.0285	**26.50**	1.0295	**21.80**	1.0306	**17.30**	1.0316	**13.00**	1.0326	8.90	1.0337	4.90	1.0347	1.10
2	29.70	1.0256	41.10	1.0266	35.70	1.0276	**30.60**	1.0287	**25.70**	1.0297	**21.00**	1.0307	**16.50**	1.0318	**12.30**	1.0328	8.20	1.0338	4.20
3	29.12	1.0250	44.40	1.0260	38.80	1.0271	**33.50**	1.0281	**28.40**	1.0291	**23.60**	1.0301	**19.10**	1.0312	**14.70**	1.0322	**10.50**	1.0333	6.40
4	31.10	1.0270	**33.90**	1.0280	**28.80**	1.0290	**24.00**	1.0301	**19.40**	1.0311	**15.00**	1.0321	**10.80**	1.0332	6.80	1.0342	2.90	1.0352	-0.80
5	30.67	1.0266	36.00	1.0276	**30.90**	1.0286	**26.00**	1.0296	**21.30**	1.0307	**16.80**	1.0317	**12.50**	1.0327	8.40	1.0338	4.50	1.0348	0.70
6	30.59	1.0265	36.50	1.0275	**31.30**	1.0285	**26.40**	1.0296	**21.70**	1.0306	**17.20**	1.0316	**12.90**	1.0327	8.70	1.0337	4.80	1.0347	1.00
7	31.27	1.0272	**33.00**	1.0282	**28.00**	1.0292	**23.20**	1.0302	**18.60**	1.0313	**14.30**	1.0323	**10.10**	1.0333	6.10	1.0344	2.30	1.0354	-1.40
8	30.66	1.0266	36.10	1.0276	**30.90**	1.0286	**26.00**	1.0296	**21.30**	1.0307	**16.80**	1.0317	**12.50**	1.0327	8.40	1.0338	4.50	1.0348	0.70
9	30.76	1.0267	35.60	1.0277	**30.40**	1.0287	**25.60**	1.0297	**20.90**	1.0308	**16.40**	1.0318	**12.20**	1.0328	8.10	1.0339	4.20	1.0349	0.40
10	30.67	1.0266	36.00	1.0276	**30.90**	1.0286	**26.00**	1.0296	**21.30**	1.0307	**16.80**	1.0317	**12.50**	1.0327	8.40	1.0338	4.50	1.0348	0.70
11	31.93	1.0278	**29.70**	1.0288	**24.90**	1.0299	**20.30**	1.0309	**15.80**	1.0319	**11.60**	1.0330	7.50	1.0340	3.60	1.0350	-0.10	1.0361	-3.70
12	30.68	1.0266	36.00	1.0276	**30.90**	1.0286	**25.90**	1.0296	**21.30**	1.0307	**16.80**	1.0317	**12.50**	1.0327	8.40	1.0338	4.50	1.0348	0.70
13	30.92	1.0268	**34.80**	1.0278	**29.70**	1.0289	**24.80**	1.0299	**20.20**	1.0309	**15.70**	1.0320	**11.50**	1.0330	7.40	1.0340	3.60	1.0351	-0.20
14	29.09	1.0250	44.50	1.0260	38.90	1.0270	**33.60**	1.0281	**28.60**	1.0291	**23.80**	1.0301	**19.20**	1.0312	**14.80**	1.0322	**10.60**	1.0332	6.50
15	30.67	1.0266	36.00	1.0276	**30.90**	1.0286	**26.00**	1.0296	**21.30**	1.0307	**16.80**	1.0317	**12.50**	1.0327	8.40	1.0338	4.50	1.0348	0.70
CAL 2.2																			
1	30.60	1.0265	36.40	1.0275	**31.20**	1.0285	**26.30**	1.0296	**21.60**	1.0306	**17.10**	1.0316	**12.80**	1.0327	8.70	1.0337	4.70	1.0347	1.00
2	30.05	1.0259	39.30	1.0270	**34.00**	1.0280	**28.90**	1.0290	**24.10**	1.0300	**19.50**	1.0311	**15.10**	1.0321	**10.90**	1.0331	6.80	1.0342	3.00
3	29.37	1.0253	43.00	1.0263	37.50	1.0273	**32.20**	1.0283	**27.30**	1.0294	**22.50**	1.0304	**18.00**	1.0314	**13.60**	1.0325	9.50	1.0335	5.50
4	28.67	1.0246	46.90	1.0256	41.20	1.0266	35.80	1.0276	**30.60**	1.0287	**25.70**	1.0297	**21.00**	1.0307	**16.50**	1.0318	**12.30**	1.0328	8.20
5	30.23	1.0261	38.40	1.0271	**33.10**	1.0282	**28.10**	1.0292	**23.30**	1.0302	**18.70**	1.0313	**14.30**	1.0323	**10.20**	1.0333	6.20	1.0344	2.30
6	30.41	1.0263	37.40	1.0273	**32.20**	1.0284	**27.20**	1.0294	**22.50**	1.0304	**17.90**	1.0314	**13.60**	1.0325	9.40	1.0335	5.50	1.0345	1.70
7	30.66	1.0266	36.10	1.0276	**31.00**	1.0286	**26.00**	1.0296	**21.30**	1.0307	**16.90**	1.0317	**12.60**	1.0327	8.50	1.0338	4.50	1.0348	0.80
8	29.27	1.0252	43.50	1.0262	38.00	1.0272	**32.70**	1.0282	**27.70**	1.0293	**22.90**	1.0303	**18.40**	1.0313	**14.00**	1.0324	9.90	1.0334	5.90
9	30.39	1.0263	37.50	1.0273	**32.20**	1.0283	**27.30**	1.0294	**22.50**	1.0304	**18.00**	1.0314	**13.70**	1.0325	9.50	1.0335	5.50	1.0345	1.70

10	30.22	1.0261	38.40	1.0271	**33.10**	1.0282	**28.10**	1.0292	**23.30**	1.0302	**18.70**	1.0313	**14.40**	1.0323	**10.20**	1.0333	6.20	1.0344	2.30
11	29.59	1.0255	41.80	1.0265	36.30	1.0275	**31.20**	1.0286	**26.20**	1.0296	**21.50**	1.0306	**17.00**	1.0317	**12.70**	1.0327	8.60	1.0337	4.70
12	29.47	1.0254	42.40	1.0264	36.90	1.0274	**31.70**	1.0284	**26.80**	1.0295	**22.00**	1.0305	**17.50**	1.0315	**13.20**	1.0326	9.10	1.0336	5.10
13	30.32	1.0262	37.80	1.0272	**32.60**	1.0283	**27.60**	1.0293	**22.80**	1.0303	**18.30**	1.0314	**13.90**	1.0324	9.80	1.0334	5.80	1.0345	2.00
14	30.84	1.0267	35.20	1.0278	**30.10**	1.0288	**25.20**	1.0298	**20.50**	1.0308	**16.10**	1.0319	**11.90**	1.0329	7.80	1.0339	3.90	1.0350	0.10
15	29.44	1.0253	42.60	1.0264	37.10	1.0274	**31.90**	1.0284	**26.90**	1.0294	**22.20**	1.0305	**17.60**	1.0315	**13.30**	1.0325	9.20	1.0336	5.20
16	30.74	1.0266	35.70	1.0277	**30.60**	1.0287	**25.70**	1.0297	**21.00**	1.0307	**16.50**	1.0318	**12.30**	1.0328	8.20	1.0338	4.20	1.0349	0.50
17	28.62	1.0245	47.20	1.0255	41.40	1.0266	36.00	1.0276	**30.80**	1.0286	**25.90**	1.0297	**21.30**	1.0307	**16.80**	1.0317	**12.60**	1.0328	8.40
18	27.10	1.0230	56.30	1.0240	50.00	1.0251	**44.20**	1.0261	**38.60**	1.0271	**33.30**	1.0281	**28.20**	1.0292	**23.40**	1.0302	**18.80**	1.0312	**14.50**
CAL GR 2																			
1	28.72	1.0246	46.60	1.0256	40.90	1.0267	35.50	1.0277	**30.40**	1.0287	**25.50**	1.0297	**20.80**	1.0308	**16.30**	1.0318	**12.10**	1.0328	8.00
2	28.62	1.0245	47.20	1.0255	41.50	1.0266	36.00	1.0276	**30.90**	1.0286	**26.00**	1.0296	**21.30**	1.0307	**16.80**	1.0317	**12.50**	1.0327	8.40
3	28.90	1.0248	45.60	1.0258	39.90	1.0269	**34.60**	1.0279	**29.50**	1.0289	**24.60**	1.0299	**20.00**	1.0310	**15.60**	1.0320	**11.30**	1.0330	7.30
5	28.12	1.0240	50.10	1.0250	44.20	1.0261	38.70	1.0271	**33.40**	1.0281	**28.30**	1.0291	**23.50**	1.0302	**18.90**	1.0312	**14.50**	1.0322	10.40
6	29.85	1.0257	40.40	1.0268	**35.00**	1.0278	**29.90**	1.0288	**25.00**	1.0298	**20.40**	1.0309	**15.90**	1.0319	**11.70**	1.0329	7.60	1.0340	3.70
7	28.79	1.0247	46.20	1.0257	40.60	1.0267	35.20	1.0278	**30.00**	1.0288	**25.20**	1.0298	**20.50**	1.0309	**16.00**	1.0319	**11.80**	1.0329	7.70
8	28.98	1.0249	45.20	1.0259	39.50	1.0269	**34.20**	1.0279	**29.10**	1.0290	**24.30**	1.0300	**19.70**	1.0310	**15.30**	1.0321	**11.00**	1.0331	7.00
9	28.73	1.0246	46.50	1.0257	40.80	1.0267	35.40	1.0277	**30.30**	1.0287	**25.40**	1.0298	**20.70**	1.0308	**16.30**	1.0318	**12.00**	1.0329	7.90
10	28.47	1.0244	48.10	1.0254	42.30	1.0264	36.80	1.0274	**31.60**	1.0285	**26.60**	1.0295	**21.90**	1.0305	**17.40**	1.0316	**13.10**	1.0326	8.90
11	29.12	1.0250	44.40	1.0260	38.80	1.0271	**33.50**	1.0281	**28.50**	1.0291	**23.70**	1.0301	**19.10**	1.0312	**14.70**	1.0322	**10.50**	1.0332	6.50
13	28.27	1.0242	49.20	1.0252	43.40	1.0262	37.80	1.0272	**32.60**	1.0283	**27.60**	1.0293	**22.80**	1.0303	**18.30**	1.0314	**13.90**	1.0324	9.70
14	28.87	1.0248	45.70	1.0258	40.10	1.0268	**34.70**	1.0278	**29.60**	1.0289	**24.80**	1.0299	**20.10**	1.0309	**15.70**	1.0320	**11.40**	1.0330	7.40
15	28.60	1.0245	47.30	1.0255	41.50	1.0266	36.10	1.0276	**30.90**	1.0286	**26.00**	1.0296	**21.30**	1.0307	**16.80**	1.0317	**12.50**	1.0327	8.40
CAL GR 3																			
1	30.37	1.0263	37.60	1.0273	**32.40**	1.0283	**27.40**	1.0293	**22.60**	1.0304	**18.10**	1.0314	**13.80**	1.0324	9.60	1.0335	5.60	1.0345	1.80
2	33.50	1.0294	**22.40**	1.0304	**17.90**	1.0314	**13.60**	1.0325	9.50	1.0335	5.50	1.0345	1.70	1.0356	-2.00	1.0366	-5.50	1.0377	-8.90
3	29.88	1.0258	40.20	1.0268	**34.80**	1.0278	**29.70**	1.0289	**24.90**	1.0299	**20.20**	1.0309	**15.80**	1.0319	**11.50**	1.0330	7.50	1.0340	3.60
4	30.14	1.0260	38.80	1.0271	**33.50**	1.0281	**28.50**	1.0291	**23.70**	1.0301	**19.10**	1.0312	**14.70**	1.0322	**10.50**	1.0332	6.50	1.0343	2.60
5	26.24	1.0222	61.80	1.0232	55.30	1.0242	49.10	1.0252	43.30	1.0262	37.70	1.0273	**32.50**	1.0283	**27.50**	1.0293	**22.70**	1.0304	**18.10**

6	30.74	1.0266	35.70	1.0277	**30.50**	1.0287	**25.60**	1.0297	**21.00**	1.0307	**16.50**	1.0318	**12.20**	1.0328	8.20	1.0338	4.20	1.0349	0.50
7	30.08	1.0260	39.10	1.0270	**33.80**	1.0280	**28.80**	1.0291	**23.90**	1.0301	**19.40**	1.0311	**15.00**	1.0321	**10.70**	1.0332	6.70	1.0342	2.80
8	30.75	1.0266	35.60	1.0277	**30.50**	1.0287	**25.60**	1.0297	**20.90**	1.0308	**16.50**	1.0318	**12.20**	1.0328	8.10	1.0339	4.20	1.0349	0.40
9	30.75	1.0266	35.60	1.0277	**30.50**	1.0287	**25.60**	1.0297	**20.90**	1.0308	**16.50**	1.0318	**12.20**	1.0328	8.10	1.0339	4.20	1.0349	0.40
10	30.42	1.0263	37.30	1.0273	**32.10**	1.0284	**27.10**	1.0294	**22.40**	1.0304	**17.90**	1.0315	**13.50**	1.0325	9.40	1.0335	5.40	1.0346	1.60
CAL GR 4																			
1	30.91	1.0268	**34.80**	1.0278	**29.70**	1.0289	**24.90**	1.0299	**20.20**	1.0309	**15.80**	1.0319	**11.60**	1.0330	7.50	1.0340	3.60	1.0350	-0.10
2	30.42	1.0263	37.30	1.0273	**32.10**	1.0284	**27.10**	1.0294	**22.40**	1.0304	**17.90**	1.0315	**13.50**	1.0325	9.40	1.0335	5.40	1.0346	1.60
3	30.01	1.0259	39.50	1.0269	**34.20**	1.0280	**29.10**	1.0290	**24.30**	1.0300	**19.70**	1.0310	**15.20**	1.0321	**11.00**	1.0331	7.00	1.0341	3.10
4	29.75	1.0257	40.90	1.0267	35.50	1.0277	**30.30**	1.0287	**25.40**	1.0298	**20.80**	1.0308	**16.30**	1.0318	**12.10**	1.0329	8.00	1.0339	4.00
5	30.98	1.0269	**34.50**	1.0279	**29.40**	1.0289	**24.50**	1.0300	**19.90**	1.0310	**15.50**	1.0320	**11.30**	1.0330	7.20	1.0341	3.30	1.0351	-0.40
6	29.87	1.0258	40.20	1.0268	**34.90**	1.0278	**29.80**	1.0288	**24.90**	1.0299	**20.30**	1.0309	**15.80**	1.0319	**11.60**	1.0330	7.50	1.0340	3.60
CAL GR 5																			
1	30.76	1.0267	35.60	1.0277	**30.50**	1.0287	**25.60**	1.0297	**20.90**	1.0308	**16.40**	1.0318	**12.20**	1.0328	8.10	1.0339	4.20	1.0349	0.40
2	31.53	1.0274	**31.70**	1.0284	**26.80**	1.0295	**22.10**	1.0305	**17.60**	1.0315	**13.20**	1.0326	9.10	1.0336	5.20	1.0346	1.40	1.0357	-2.30
3	31.12	1.0270	**33.80**	1.0280	**28.70**	1.0291	**23.90**	1.0301	**19.30**	1.0311	**14.90**	1.0321	**10.70**	1.0332	6.70	1.0342	2.80	1.0353	-0.90
4	30.93	1.0268	**34.70**	1.0278	**29.60**	1.0289	**24.80**	1.0299	**20.10**	1.0309	**15.70**	1.0320	**11.50**	1.0330	7.40	1.0340	3.50	1.0351	-0.20
5	30.94	1.0268	**34.70**	1.0279	**29.60**	1.0289	**24.70**	1.0299	**20.10**	1.0309	**15.70**	1.0320	**11.40**	1.0330	7.40	1.0340	3.50	1.0351	-0.20
6	31.64	1.0275	**31.20**	1.0286	**26.30**	1.0296	**21.60**	1.0306	**17.10**	1.0316	**12.80**	1.0327	8.70	1.0337	4.70	1.0347	1.00	1.0358	-2.70
Average temp.			**39.7**		**34.4**		**29.3**		**24.4**		**19.8**		**15.4**		11.2		7.1		3.2
% of values with temps. between 10–35 °C			18%		**64%**		**83%**		**97%**		**98%**		**95%**		51%		27%		4%

Note: Abbreviations– T. – temperature. Temperature estimates of carbonate precipitation are in bold, constrained between 10–35°C.

Table 2. Calculation of major oxide values (wt.%) calculated from XRD proportions vs. the actual XRF major oxide proportions of the fossil termitarium CAL 2.1. These calculations assume the sample is ~100 g. Standard mineral proportions obtained from (Deer et al., 2009).

Major oxide	**Quartz**	**Quartz*X**	**Dolomite**	**Dolomite*X**	**Calcite**	**Calcite*X**	**Muscovite**	**Muscovite*X**	**Plagioclase**	**Plagioclase*X**	**% From XRD values**	**Actual % from XRF**
SiO_2	100.00	41.00	0.00	0.00	0.00	0.00	48.42	11.62	67.84	6.11	58.73	28.58
TiO_2	0.00	0.00	0.00	0.00	0.00	0.00	0.87	0.21	0.00	0.00	0.21	0.17
Al_2O_3	0.00	0.00	0.00	0.00	0.00	0.00	27.16	6.52	19.65	1.77	8.29	3.35
Fe_2O_3	0.00	0.00	0.00	0.00	0.00	0.00	6.57	1.58	0.03	0.00	1.58	1.12
MgO	0.00	0.00	21.12	5.28	0.04	0.01	0.00	0.00	0.04	0.00	0.22	10.03
MnO	0.00	0.00	0.00	0.00	0.00	0.00	0.00	0.00	0.00	0.00	0.00	0.02
CaO	0.00	0.00	31.27	7.82	55.92	13.98	0.00	0.00	0.00	0.00	14.29	22.82
Na_2O	0.00	0.00	0.00	0.00	0.00	0.00	0.35	0.08	11.07	1.00	1.08	0.49
K_2O	0.00	0.00	0.00	0.00	0.00	0.00	11.23	2.70	0.29	0.03	2.72	0.85
P_2O_5	0.00	0.00	0.00	0.00	0.00	0.00	0.00	0.00	0.00	0.00	0.00	0.30
CO_2+H_2O	0.00	0.00	47.22	11.81	43.95	10.99	4.50	1.08	0.86	0.08	12.62	30.60
Total	100.00	41.00	99.61	1.00	99.91	24.98	99.10	23.78	99.78	8.98	99.74	98.32
XRD Proportion (X)	**41%**		**1%**		**25%**		**24%**		**9%**			